

“Success consists of going from failure to failure without loss of enthusiasm.”

Winston Churchill

Preface

This thesis completes the Master of Science in Telecommunication. The project is the result of a collaboration between Technical University of Denmark, University of Padua, the National University Hospital Rigshospitalet and the company Hypo-Safe A/S. The study has been carried out from January 4th 2010 to August 6th 2010 and corresponds to an assigned workload of 35 ECTS.

I wish to give my best thanks to my supervisors for their excellent guidance and encouraging spirit throughout the entire study.

A special thanks goes to Federica Bianchi, whose moral support has been invaluable during the whole thesis.

*Andrea Mazzaretto
University of Padua, August 2010*

Abstract

Background: Absence seizures, which are also known as petit mal seizures, are the most common type of seizures in pediatric epilepsy. They appear in several types of epilepsy and are characterized by impaired consciousness and 3-Hz spike-and-slow-wave complexes in the electroencephalogram (EEG). The treatment with anti-epileptic drugs (AEDs) is the result of a very delicate weighting, which leads to a trade-off between the side effects the drugs are causing and the disappearance of the seizures. The company *Hypo-Safe A/S* is currently developing a device, which hopefully will permit to reduce the number of EEG examinations needed to achieve the optimal medication.

Objective: The project has two biomedical signal processing objectives: seizure onset detection and automatic topographic seizure distribution description by means of statistical measures. Seizure onset detection is directly relevant for the user of the subcutaneously implanted *Hypo-Safe* EEG apparatus and for medical monitoring purposes. Automatic topographic distribution description by means of statistical measures is relevant for decision concerning placement of the apparatus.

Methods: An absence seizure detection algorithm based on fractal dimension estimation was designed, implemented and tested together with a topographic evaluation of absence seizure patterns.

Results: Excluding patients with symptomatic epilepsy it was possible to achieve a SE of 97% and a FDR of 0.15 FP/h on channel F4-F8. Similar performance could also be achieved in a few neighboring channels. Therefore for the other patients this area represents a very good location for placing the *Hypo-Safe* subcutaneous electrode. In patients with symptomatic epilepsy it is still possible to find a good location, but they must be assessed individually and the optimal position will change from patient to patient.

Significance: This is the first study which evaluates the topographic distribution of absence seizure patterns using an appositely designed seizure detection algorithm.

Contents

Preface	iii
Abstract	v
List of Figures	ix
List of Tables	xi
Abbreviations	xiii
1 Introduction	1
2 Epilepsy and Absence Seizures	5
2.1 Definition	5
2.2 Seizure Types	6
2.2.1 Generalised Seizures	6
2.2.2 Partial Seizures	7
2.3 Absence Seizures	7
2.3.1 Treatment	8
3 Normal and Ictal EEG Activity	11
3.1 Electrical Activity in the Brain	11
3.2 Definition of EEG	11
3.3 Method and Montages	13
3.4 The International 10-20 System	13
3.5 EEG activity	16
3.5.1 Normal EEG activity	16
3.5.2 The Spike and Wave Complex	17
3.5.3 Artifacts	18
4 State of the art Seizure Detection	19
4.1 Definition of Seizure Detection	19
4.2 Performance Evaluation	20
4.3 Overview of the Main Articles	20
4.4 Choice of a Reference Method	25
5 Fractal Dimension	27

5.1	Intuitive Explanation	27
5.2	Formal Definition	28
5.3	Examples	28
5.3.1	Weierstrass Cosine Function (WCF)	28
5.3.2	Weierstrass Mendelbrot Cosine Function (WMCF)	28
5.3.3	Takagi Function (TF)	29
5.3.4	Fractional Brownian motion (FBM)	29
5.4	Fractal Dimension of Biomedical Waveforms	29
5.4.1	Katz's Method	31
5.4.2	Higuchi's Method	31
5.4.3	Comparison	32
6	Absence Seizures Database	35
6.1	Collection and Classification of Data	35
6.2	Patients Selection and Database Description	35
7	Implementation of an Absence Seizure Onset Detection Algorithm	39
7.1	Overview	39
7.2	Algorithm Input and Channel Constraint	40
7.3	Epoching	40
7.4	Fractal Dimension Estimation	40
7.4.1	Parameter Selection	42
7.5	Binary classification	42
7.6	Matlab Implementation	44
7.7	Deviation from Georgia E. Polchronaki et al.	44
7.8	Summary of algorithm parameters	44
8	Results and Discussion	47
8.1	Visualization Method	47
8.2	Overall Performance	47
8.3	Performance by type of Epilepsy	49
8.3.1	Performance in Patients with CAE	50
8.3.2	Performance in Patients with JAE	51
8.3.3	Performance in Patients with JME	52
8.3.4	Performance in patients with Symptomatic Epilepsy	53
8.4	Performance Excluding Patients with Symptomatic Epilepsy	54
8.5	Performance Excluding Patients with Symptomatic Epilepsy and JME	54
8.6	Discussion and Positioning of <i>Hypo-Safe</i> Device Electrode	54
9	Conclusion	59
	Bibliography	61
A	Algorithm Results across all the Patients	65
B	Matlab Code	85

List of Figures

1.1	Sketch of the <i>Hypo-Safe A/S</i> device	2
2.1	Seizure Classification	6
3.1	A cortical pyramidal neuron	12
3.2	An EEG channel	13
3.3	The international 10-20 system (left and above)	14
3.4	The extended international 10-20 system	15
3.5	The most common EEG waves	16
3.6	EEG and level of consciousness	17
3.7	Spike and wave complex	17
4.1	Example of seizure onset detection	19
5.1	Synthetic fractal waveforms	29
5.2	Fractional Brownian motion	30
5.3	Estimation of fractal dimension	33
5.4	Dependence of the estimation of FD on the amplitude	34
5.5	Dependence of the estimation of FD on the sampling frequency	34
6.1	Transversal montage	36
6.2	EEG recording in EDF format	37
7.1	Architecture of seizure detection algorithm	39
7.2	FD estimator and binary classifier	41
7.3	Leave-one-out cross validation	43
8.1	Average performance across all patients	48
8.2	Average performance across patients with CAE	50
8.3	Average performance across patients with JAE	51
8.4	Average performance across patients with JME	52
8.5	Average performance across patients with symptomatic epilepsy	53
8.6	Average performance excluding patients with symptomatic epilepsy.	55
8.7	Average performance excluding patients with symptomatic epilepsy and JME	56
A.0	Sample Visualization	66
A.1	Performance on patient n. 13	67
A.2	Performance on patient n. 16	68
A.3	Performance on patient n. 17	69

A.4 Performance on patient n. 18	70
A.5 Performance on patient n. 19	71
A.6 Performance on patient n. 23	72
A.7 Performance on patient n. 25	73
A.8 Performance on patient n. 42	74
A.9 Performance on patient n. 11	75
A.10 Performance on patient n. 14	76
A.11 Performance on patient n. 51	77
A.12 Performance on patient n. 36	78
A.13 Performance on patient n. 43	79
A.14 Performance on patient n. 46	80
A.15 Performance on patient n. 8	81
A.16 Performance on patient n. 9	82
A.17 Performance on patient n. 20	83

List of Tables

2.1	Typical and atypical absence seizures	7
2.2	Features of absence and complex partial seizures	8
3.1	Comparison of sEEG and iEEG	13
3.2	Most common montages in EEG	14
3.3	Lobe notation in the 10-20 System	15
3.4	EEG frequency bands	16
4.1	Overview of the state of the art methods for seizure detection	24
6.1	Absence seizures database	36
7.1	Summary of algorithm parameters	45
8.1	Average performance across all patients	48
8.2	Average performance across patients with CAE	50
8.3	Average performance across patients with JAE	51
8.4	Average performance across patient with JME	52
8.5	Average performance across patients with symptomatic epilepsy.	53
8.6	Average performance excluding patients with symptomatic epilepsy	55
8.7	Average performance excluding patients with symptomatic epilepsy and JME	56
A.1	Performance on patient n. 13	67
A.2	Performance on patient n. 16	68
A.3	Performance on patient n. 17	69
A.4	Performance on patient n. 18	70
A.5	Performance on patient n. 19	71
A.6	Performance on patient n. 23	72
A.7	Performance on patient n. 25	73
A.8	Performance on patient n. 42	74
A.9	Performance on patient n. 11	75
A.10	Performance on patient n. 14	76
A.11	Performance on patient n. 51	77
A.12	Performance on patient n. 36	78
A.13	Performance on patient n. 43	79
A.14	Performance on patient n. 46	80
A.15	Performance on patient n. 8	81
A.16	Performance on patient n. 9	82

A.17 Performance on patient n. 20 83

Abbreviations

AED	Antiepileptic drug
CAE	Childhood Absence Epilepsy
ECG	Electrocardiogram
ECoG	Electrocorticography
EEG	Electroencephalogram
iEEG	Intracranial EEG
sEEG	Scalp EEG
EMG	Electromyography
FBM	Fractional Brownian motion
FD	Fractal Dimension
FN	False negative
FPR	False Positive Rate
GTCS	Generalized Tonic-Clonic Seizure
ILAE	The International League Against Epilepsy
IBE	International Bureau for Epilepsy
ICA	Independent Component Analysis
JAE	Juvenile Absence Epilepsy
JME	Juvenile Myoclonic Epilepsy
MCN	Modified Combinatorial Nomenclature
MD	Medical Doctor
fMRI	functional Magnetic Resonance Imaging
MTLE	Medial temporal lobe epilepsy
PET	Positron emission tomography
SE	Sensitivity
SNR	Signal to Noise Ratio
TF	Takagi Function
TLE	Temporal lobe epilepsy
TP	True positive
WCF	Weierstrass Cosine Function
WMCF	Weierstrass Mendelbrot Cosine Function

Chapter 1

Introduction

Background

The term epilepsy is derived from the ancient Greek *epilēpsía*, which literally means "to seize". It is a very common neurological disorder which affects about 50 million people worldwide and as the origin of the word suggests, the disease is characterized by recurrent seizure strikes [1]. Although 30% of the epileptic patients cannot be treated effectively with current medications, the remaining 70% can live a normal seizure-free life if treated properly [2].

Motivation

Absence seizures, which are also known as petit mal seizures, are the most common type of seizures in pediatric epilepsy. They appear in several types of epilepsy and are characterized by impaired consciousness and 3-Hz spike-and-slow-wave complexes [3] in the electroencephalogram (EEG). The EEG is a simultaneous electrical recording from several electrodes located across the skull. The treatment with anti-epileptic drugs (AEDs) is the result of a very delicate weighting, which leads to a trade-off between the side effects the drugs are causing and the disappearance of the seizures. This optimization process is very ponderous for both the family and the patient due to the frequent visits to the hospital and subsequent EEG examinations. In order to partly relieve the patients from this exhaustive process, the company *Hypo-Safe A/S* is currently developing a device, which hopefully will permit to reduce the number of EEG examinations at the hospital significantly. The device is going to be placed on the back of the ear and has a subcutaneously implanted electrode to monitor the EEG activity. When an EEG examination is requested, the patient wears the device wear for a given period of time. A report with the number of automatically detected seizures is then sent to the doctor, who can consequently instruct the patient on the potential changes in the medication. A sketch of the device is shown in figure 1.1.

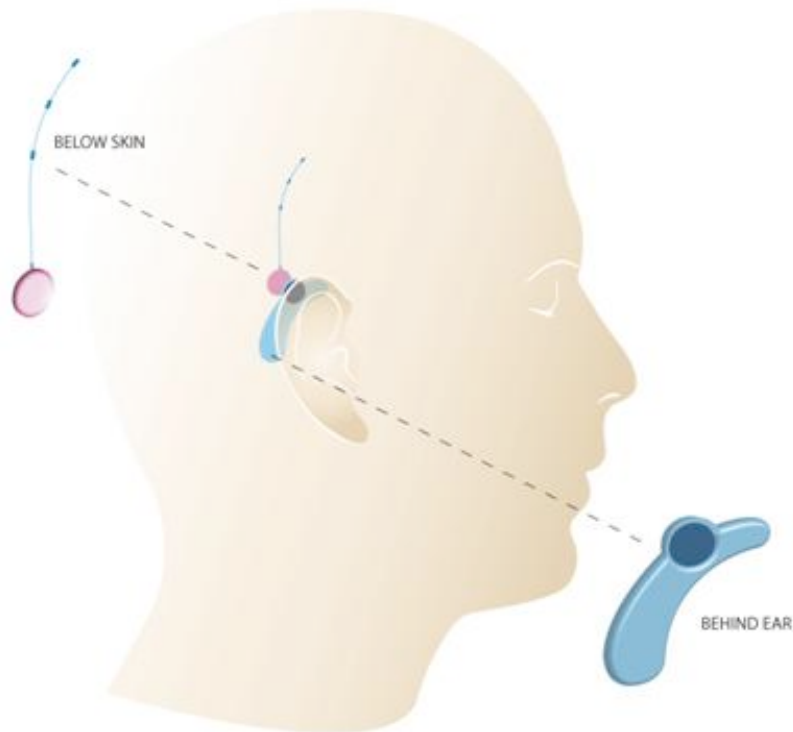


FIGURE 1.1: Sketch of the *Hypo-Safe A/S* device for seizure detection

Objective

This project has 2 biomedical signal processing objectives:

- First of all an algorithm to perform absence seizure onset detection is developed, implemented and tested on scalp EEG data (sEEG), since these are data similar to the ones the device is going to operate with. Different factors are taken into account when evaluating the algorithm. The most important ones are a high sensitivity (SE) and a low false positive rate (FPR).
- The second objective is automatic topographic distribution description by means of statistical measures. The algorithm developed is tested on each of the 19 channel of the sEEG data available for each patient. The results are then compared and analyzed in order to find the optimal location of the electrode of the *Hypo-Safe A/S* device.

Strategy

These goals are going to be reached starting with an exhaustive state of the art literature study. The most promising algorithm will then be selected and used as a starting point for a novel seizure detection approach. Once the implementation is completed a testing

database of patients with known absences is extracted from the Copenhagen University Hospital clinical NF database. Seizures and seizures onsets are identified in collaboration with MD Troels Kjær. The performance is then evaluated both from an overall and a topographic point of view. This is the first time a topographic study has been conducted on EEG of epileptic patients with absence seizures. A novel visualization method is introduced in order to illustrate such an analysis.

Structure

The following two chapters are a mandatory theory introduction to the project, where EEG and Epilepsy are described in detail to give to the reader the basics required to comprehend the study. In the fourth chapter the literature study is presented and discussed. In the fifth chapter the chosen method is analyzed and the modifications made are illustrated in the subsequent chapter. In the sixth chapter the database created for this study is described and commented. The results and discussion are presented in the last chapters followed by conclusion.

Chapter 2

Epilepsy and Absence Seizures

In the beginning of the chapter a definition and a general introduction to epilepsy and epileptic seizures are given. Different types of seizures are introduced and their impact on the patient is described. Later on the focus is moved to absence seizures, in order to give a better understanding on the physiological process the *Hypo-Safe A/S* device is operating with.

2.1 Definition

Giving an exact definition of epilepsy is controversial because the disease cannot be identified as one condition but rather as a syndrome, where many different symptoms are present. In [4] and in [1] an early definition of epilepsy and epileptic seizure was given. In 2005 this was further expanded when the *International League Against Epilepsy* (ILAE) and the *International Bureau for Epilepsy* (IBE) reached an agreement on the definition of these terms [5]:

Epileptic seizure: transient occurrence of signs and/or symptoms due to abnormal excessive or synchronous neuronal activity in the brain [5].

Epilepsy: disorder of the brain characterized by an enduring predisposition to generate epileptic seizures and by the neurobiologic, cognitive, psychological, and social consequences of this condition. The definition of epilepsy requires the occurrence of at least one epileptic seizure [5].

There are over 40 different types of epilepsy. Each one of them is characterized by its own specific combination of seizure type, EEG characteristics, typical age of onset and treatment. It is a very wide topic and analyzing all the types of epilepsy is not in the scope of this project. In the following section the seizure types are classified in an internationally recognized scheme and the type of epilepsies related to absence seizures are described in the subsequent section.

2.2 Seizure Types

In 1981 ILAE proposed a classification scheme of epileptic seizures [6] that, although under revision [7], it is still the de facto standard for seizure classification. The scheme, which is shown in figure 2.1, is based on clinical manifestations and on the EEG rather than pathophysiology or anatomy. It involves a first main classification between generalised and partial seizures, which are better described in the following subsections.

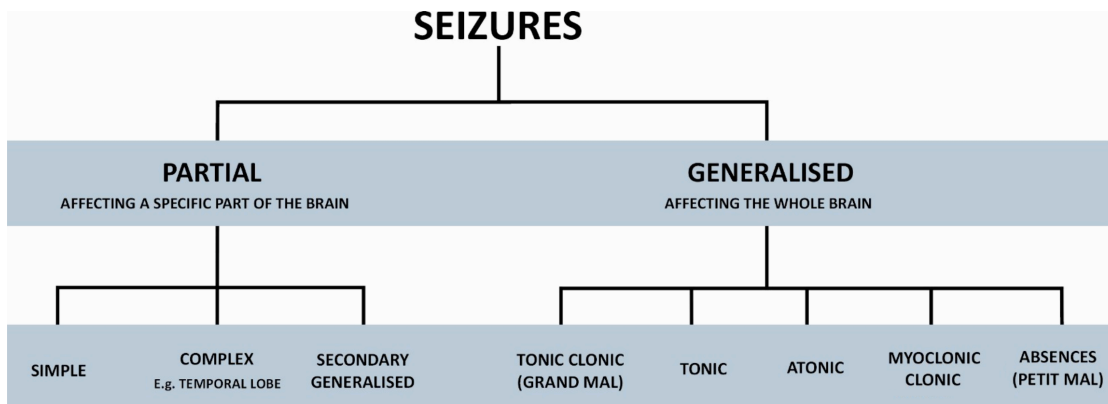


FIGURE 2.1: Seizure classification according to ILAE [6]. The main division is between generalised seizures, which affects the whole brain, and partial seizures, which affects only a part of the brain.

2.2.1 Generalised Seizures

When the onset is recorded simultaneously in both cerebral hemispheres the seizure is classified as generalised. Generalised seizures are further classified into :

- **Tonic clonic:** They are also known as *grand mal* seizures and they are characterized by generalized tonic extension of the extremities followed by jerking of the face. The only difference with secondary generalised seizures is the lacking of an *aura*.
- **Tonic:** They consist of tonic extension of the head, trunk and extremities. They typically occur before falling asleep or just after waking up. In the EEG they are characterized by a high-frequency electrographic discharge in the beta frequency.
- **Atonic:** A seizure with a sudden loss of muscle tone, often resulting in falls and injuries. They are also known as drop seizures.
- **Myoclonic and Clonic:** Myoclonic seizures are characterized by brief, arrhythmic, jerking movements that last less than a second and often cluster within a few minutes. If they evolve into rhythmic, jerking movements they are classified as a clonic seizures.
- **Absences:** They consists of episodes of impaired consciousness that usually lasts less then 20 seconds. Being the main focus of our project, they are better analyzed in the next section.

2.2.2 Partial Seizures

Partial seizures occurs when the onset begin in a focal area of the cerebral cortex. They are further classified in:

- **Simple:** The consciousness of the patient is preserved. A simple partial seizures include sensory, motor, autonomic, and psychic types, which are alle characterized by focal EEG changes.
- **Complex:** During a complex partial seizure the consciousness of the patient is impaired. They are often preceded by a so called *aura*, which is just a simple partial seizure. They typically lasts between 30 and 90 seconds, start with behavioral arrest and end with staring, automatisms, and postictal confusion.
- **Secondary Generalised:** It occurs when a simple or complex partial seizures evolves into a generalised seizure.

2.3 Absence Seizures

This type of seizures were first observed by Poupart in 1705 and defined as *petite access* by Tissot in 1770. The term *absence* was coined and used for the first time by Calmell in 1824 [8]. As alluded in the introduction they are the most common type of pediatric seizures, characterized by 3-Hz spike-and-slow-wave complexes in the EEG (see figure 3.7).The classification of absence seizures has been recently revised and simplified by ILAE [12]. The main division is now simply between *typical* and *atypical* absences. The different characteristics of each of these two types of absence seizures can be observed in table 2.1.

TABLE 2.1: Typical and Atypical absence seizures. Clinical and EEG differences. Information from [12].

Type of Clinical Seizure	EEG Findings
Typical absence <ul style="list-style-type: none"> - Impairment of consciousness only - Mild clonic components - Atonic components - Tonic component - Automatisms - Autonomic components 	Usually regular and symmetrical 3 Hz, possible 2- to 4-Hz spike-and-slow-wave complexes, and possible multiple spike-and-slow-wave complexes
Atypical absence <ul style="list-style-type: none"> - Changes in tone more pronounced than those of typical absence seizure - Nonabrupt onset or cessation abrupt 	EEG more heterogeneous than in typical absence; may include irregular spike-and-slow-wave complexes, fast activity, or other paroxysmal activity; abnormalities bilateral but often irregular and asymmetric

Long absence seizures can be confused with complex partial seizures, especially when automatisms are presents. In the case of absences, the longer the seizure, the higher is

TABLE 2.2: Features of absence and complex partial seizures. Information from [14].

Feature	Complex Partial Seizure	Absence Seizure
Onset	May have simple partial onset	Abrupt
Duration	Usually >30 s	Usually <30 s
Automatisms	Present	Duration dependent
Awareness	No	No
Ending	Gradual postictal	Abrupt

the probability of finding automatisms [14]. In table 2.2 the salient features of absence and complex partial seizures are compared.

Generalized epilepsies can be classified into idiopathic epilepsies, when the causes are genetic and into symptomatic epilepsies, when the causes are unknown. Absence seizures can occur both in idiopathic and symptomatic epilepsies. In the case of idiopathic epilepsy absence seizures are present in:

- **Childhood Absence Epilepsy (CAE)**: characterized by short and frequent seizures usually between 4 and 20 seconds. In some cases more than one hundred seizures can be registered per day. The typical age of onset is between 4 and 8 years, with peaks in the 6-7 years range. [9] [10, pages 106-120].
- **Juvenile Absence Epilepsy (JAE)**: the age of onset is typically between 10 and 17 years with a peak between 10 and 12 years. The semiology of the absences in this syndrome are very similar to the one in CAE, just the first onset occurs later and they are much more sporadic. [10, pages 307-312]
- **Juvenile Myoclonic Epilepsy (JME)**: characterized by generalized tonic-clonic seizures (GTCs), myoclonic jerks and sometimes by absence seizures. The age of onset is very wide (8-26 years), but 79% of the cases occur between 12 and 18 years of age [10, pages 247-258].

In the case of symptomatic generalized epilepsies some differences are present in the absence seizures. They are often characterized by slow spike-wave complexes of 1.5-2.5 Hz, which are also known as sharp-and-slow-wave complexes. Seizure of this type are referred to as atypical absence seizures [11].

2.3.1 Treatment

Absence seizures are treated with antiepileptic drugs (AEDs). After the necessary EEG examinations and subsequent diagnosis, proper medications and dosages are selected. The objective is to suppress all epileptiform activity and this is rarely achieved the first time the drugs are prescribed [13]. Since AEDs are relatively toxic and cause several side effects, reaching the optimal dosage must be achieved in the shortest period of time as possible. The algorithm presented in the following chapters of this thesis, is designed for the *Hypo-Safe A/S* device, which permits to monitor the patient more efficiently.

Consequently the number of EEG examinations required and the trials before finding the best dosage can be significantly reduced.

Chapter 3

Normal and Ictal EEG Activity

All data used in this project consists of electroencephalogram (EEG) recordings of epileptic patients. In order to understand what the implemented algorithm is operating with, a background on electroencephalography must be given. In this chapter the principle behind EEG recordings is described and the different measuring techniques are analyzed. Normal EEG activity is then presented and compared to the EEG activity of an epileptic patient during an absence seizure (ictal EEG).

3.1 Electrical Activity in the Brain

There is an estimated number of 10^{11} neurons in the brain, each one interconnected with 1000-100000 synapses to the others. [15]. In the cortical gray matter these cells are called pyramidal neurons. They are electrically active and generate discrete electrical signals (*action potentials*) that passes through the axon and activate a neurotransmitter in the corresponding synapse. The neurotransmitter travels to the designated neuron (*post synaptic neuron*) on the other side of the synapse and interacts with the receptor in the dendrite of that neuron. This interaction generates an electrical current in the post synaptic neuron. When enough interactions takes place, an action potential is generated and the process just described repeats itself. In particular, the excitatory and inhibitory postsynaptic potentials rather than the action potentials are responsible for the recorded EEG activity. A diagram of a pyramidal neuron is shown in figure 3.1.

3.2 Definition of EEG

Activity of a single neuron cannot be revealed by any existing method. What can be picked up is the synchronous activity of millions of neurons with similar orientation [15]. EEG is defined as the recording of this electrical activity. This is achieved through a series of electrodes placed on the surface of the scalp (*scalp EEG* or sEEG) or under the skull (*intracranial EEG* or iEEG). While sEEG is a very common medical procedure, e.g to diagnose epilepsy, iEEG is only performed in patients with untreatable focal epilepsy in

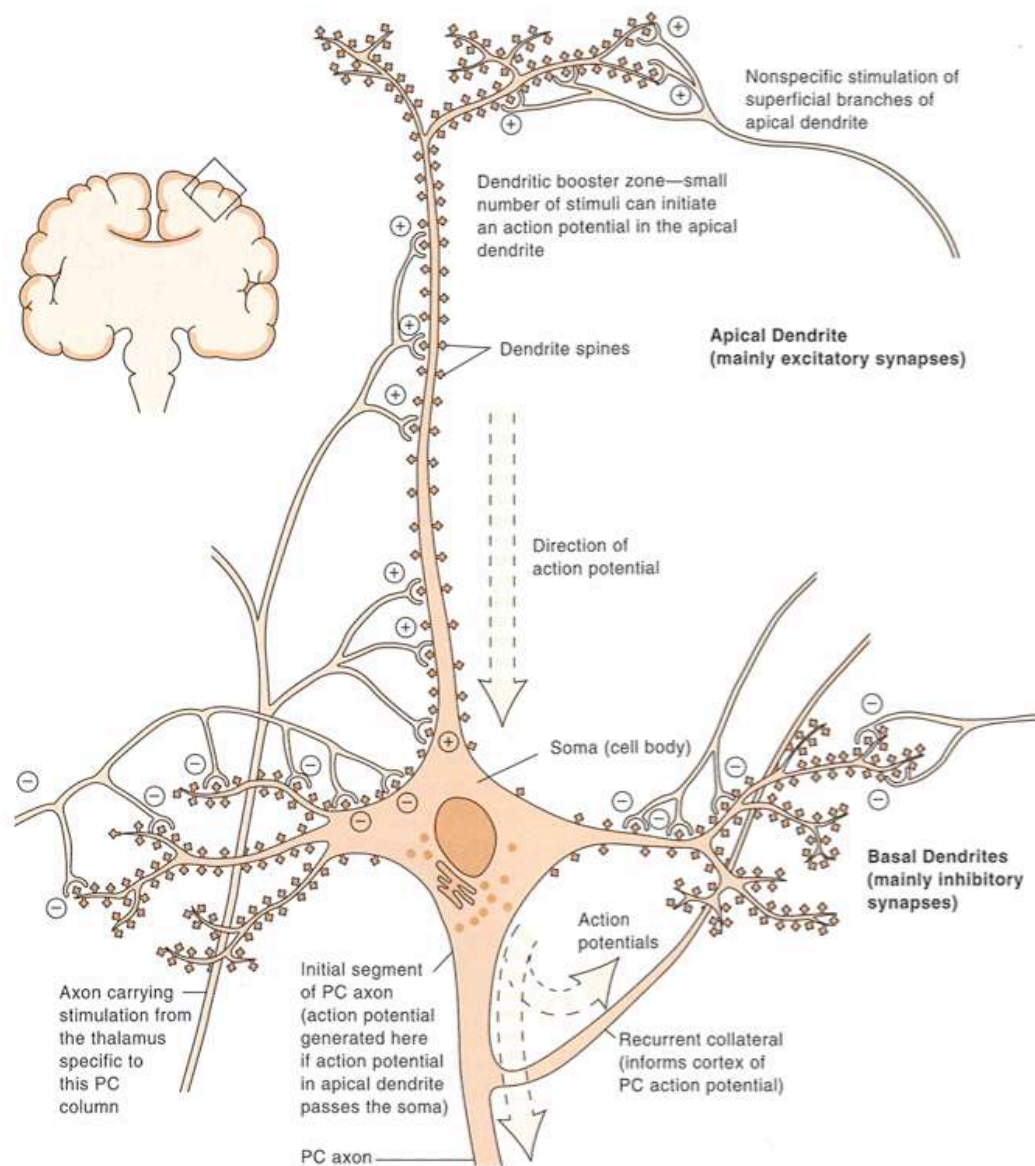


FIGURE 3.1: A cortical pyramidal neuron as it exist in the cerebral cortex. The integration of inhibitory and exhibitory potentials decides whether an action potential will be generated. From [17].

order to determine the exact focus before the surgery [16]. A comparison between the two types of EEG is carried out in table 3.1. In intracranial recordings both a high spatial and temporal resolution are obtained, together with a large SNR, but the procedure is very invasive. *Hypo-Safe A/S* device uses a subcutaneously implanted electrode, therefore it operates with data very similar to sEEG. That is the reason why our analysis from now on will be limited to sEEG. Most of the concepts are anyway applicable also to iEEG.

TABLE 3.1: Comparison of sEEG and iEEG characteristics. Information from [18].

	sEEG	iEEG
Spatial resolution	Low	High
Time resolution	High	High
Susceptibility to artifacts	Medium-high	Low
SNR	Small	Large
Type of procedure	Noninvasive	Invasive
Accessibility	High	low

3.3 Method and Montages

In most applications 19 electrodes are employed to record clinical EEG, however up to 256 electrodes, mounted on a cap or a net, can be used. In order to reduce impedance and improve the quality of the recording a conductive gel is applied on the electrodes before the placement on the scalp. The placement usually follows the 10-20 international standard [19], which is described in the next section.

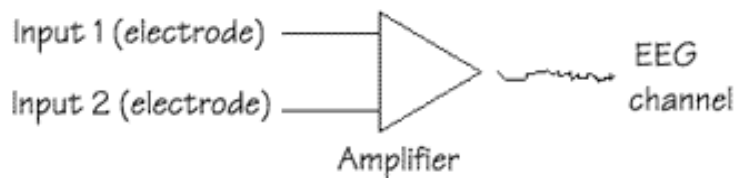


FIGURE 3.2: An EEG channel is the output of a differential amplifier, whose input is the signal registered by two EEG electrodes. From [22].

The result of an EEG examination is a certain number of *EEG channels*, which are not the result of unipolar measurements from the single electrodes. An EEG channel is the output of a differential amplifier connected to 2 different electrodes, as it can be observed from figure 3.2. Therefore there are several ways to display the results of an EEG examination. Each one of them is referred to as a *montage*. The most commonly used ones are shown in table 3.2.

The amplitude of a typical scalp EEG is between $10 \mu V$ and $100 \mu V$, while in the case of an iEEG the voltage obtained is between $20 mV$ and $40 mV$ [20].

3.4 The International 10-20 System

An international standard, which establishes the placement of the electrodes in the EEG, is needed to compare examinations of different subjects to each other. The international 10-20 system was designed for this purpose and it is one of the most widely used method for electrodes positioning in spontaneous clinical EEG. Other standards exist, e.g. the *Queen Square* is used to record the pattern of evoked potential in clinical testings [23].

In the 10-20 system the nasion and the inion are taken as reference to measure the skull perimeters from front to back and from right to left. These perimeters are then divided

TABLE 3.2: Most common montages in EEG. Information from [21].

Montage	Description
Bipolar	Each channel represents the difference between an electrode and one of its neighbours. Different configurations are possible depending on the pairs of electrodes chosen. Two very common ones are the <i>Transversal</i> montage and the <i>Banana</i> montage.
Referential	An electrode is chosen as reference and each channel is the difference between this electrode and designated electrode. The reference can be chose arbitrarily. Common choices are positions between the recording electrodes or an average of the electrodes positioned on the earlobes.
Average	A special case of <i>Referential</i> montage where the reference is an average of all the available channels.
Laplacian	Another special case of <i>Referential</i> montage. This time the reference is a weighted average of the neighbouring electrodes.

in 10% and 20% intervals in order to determine the positioning of the electrodes. This is shown in figure 3.3. Each electrode position is then represented by a letter identifying the lobe and a number identifying the hemisphere (Odd numbers refers to the left emisphere, while even numbers refers to the right emisphere). The letter notation is presented in table 3.3.

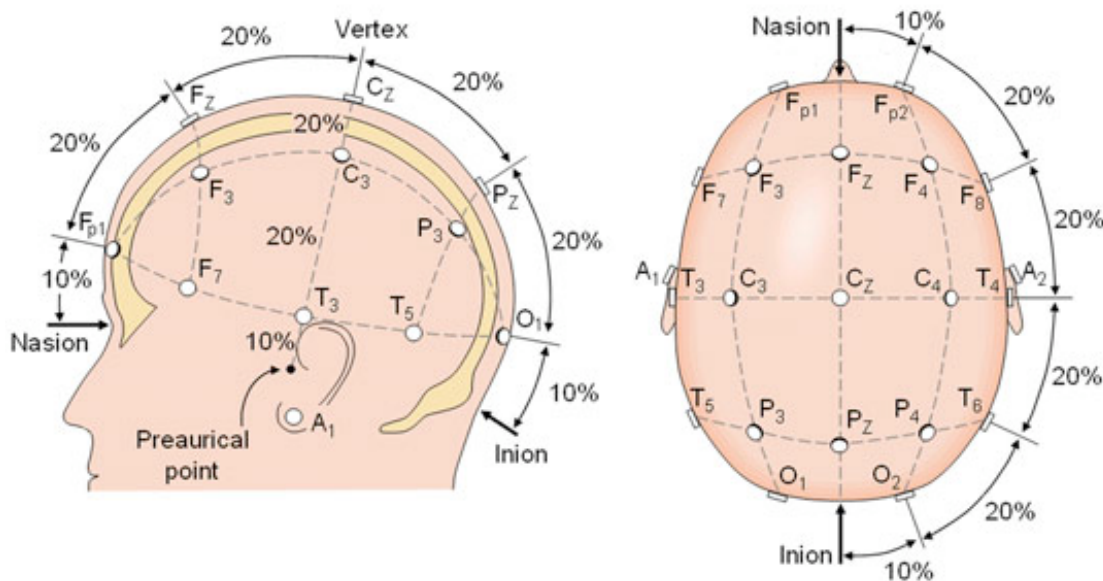


FIGURE 3.3: The international 10-20 system seen from left and above the head. Nasion, Inion and 10% and 20% intervals are visible. From [24].

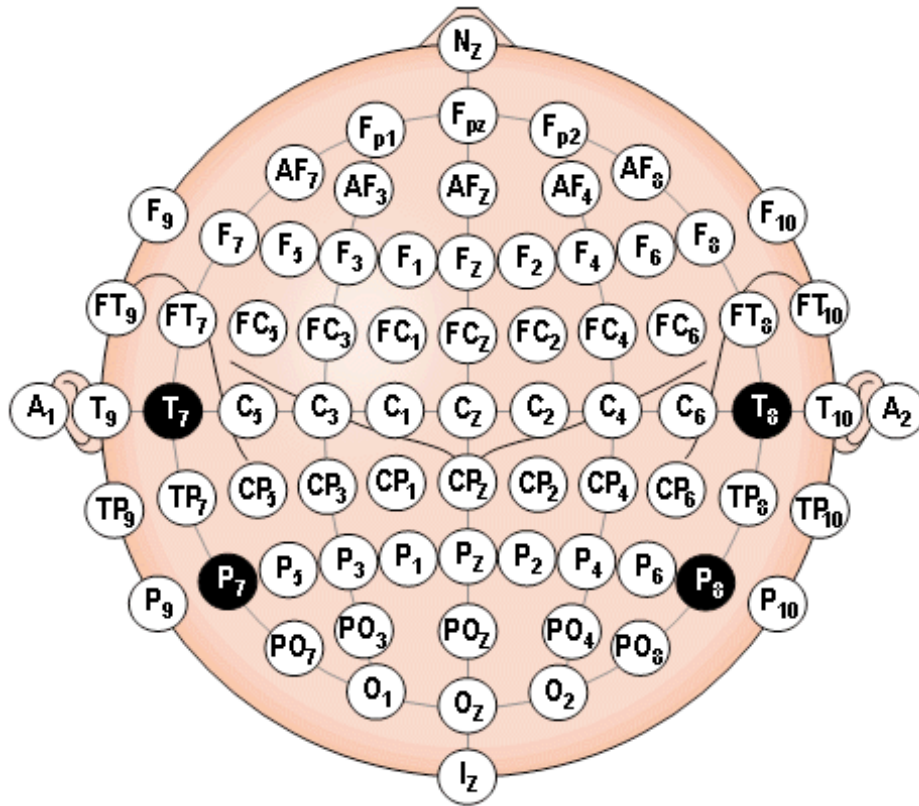


FIGURE 3.4: The extended international 10-20 system. Standardization by the American Electroencephalographic Society. From [24].

TABLE 3.3: Lobe notation in the 10-20 System. Information from [24].

Letter	Lobe
A	Ear lobe
C	Central
Pg	Nasopharyngeal
P	Parietal
F	Frontal
Fp	Frontal polar
O	Occipital
T	Temporal

When an EEG examination with higher spatial resolution is required new electrodes are placed in between the original 10-20 system electrodes. This gives birth to an extended version of the 10-20 system, where the naming of the new electrodes sites is regulated by the Modified Combinatorial Nomenclature (MCN). A complete overview of this system can be observed in figure 3.4.

3.5 EEG activity

3.5.1 Normal EEG activity

Normal EEG activity shows *periodic* or *rhythmic* activity, which is usually classified according to the frequency bands defined in table 3.4. In figure 3.5 an example of activity for each one of these bands is shown.

EEG is strongly dependent on the level of consciousness of the subject examined and in order to better illustrate this fact the EEG associated with various sleep stages is shown in figure 3.6. *Alpha* waves usually appears in an awake subject, while *theta* and *delta* waves appear with light and deep sleep respectively. Strong *alpha* waves instead are present during auditory and mental arithmetic tasks and *Beta* waves appears as background activity during intense mental tasks [26].

TABLE 3.4: EEG frequency bands. Information from [26].

EEG band	Frequency Range [Hz]
Delta (δ)	0.5 - 4
Theta (θ)	4 - 8
Alpha (α)	8 - 13
Beta (β)	13 - 30

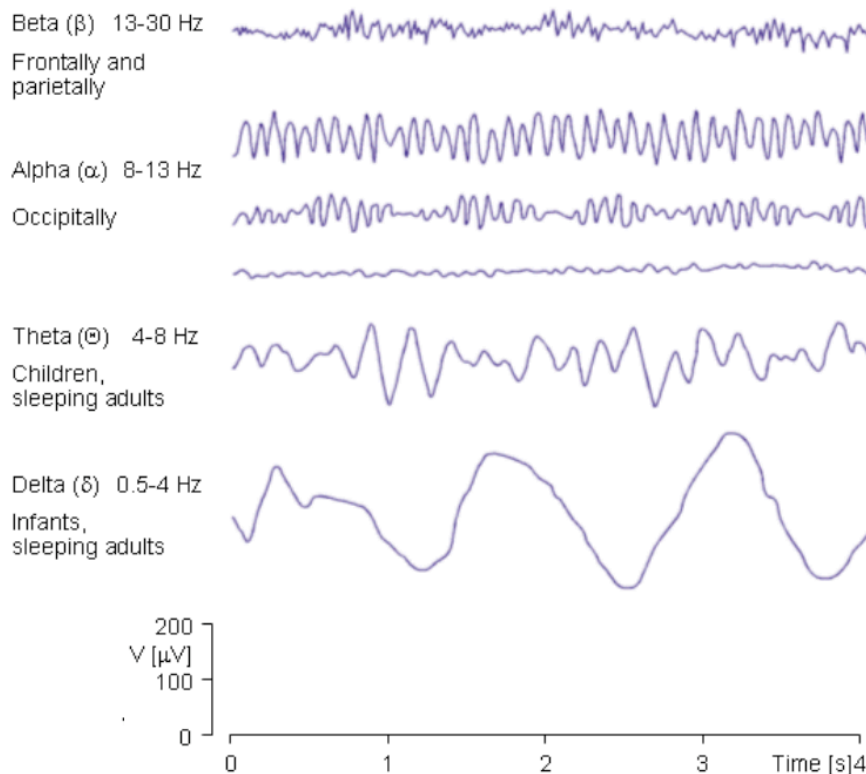


FIGURE 3.5: The most common EEG waves. From [25].

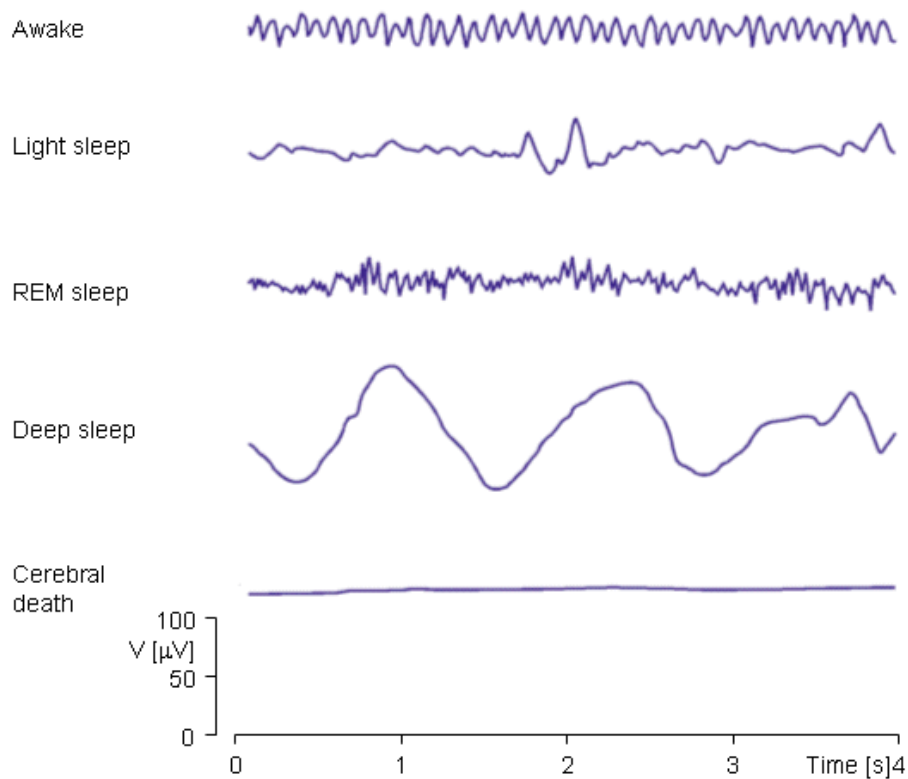


FIGURE 3.6: Dependence of the EEG signal on the level of consciousness of the subject. .From [25].

3.5.2 The Spike and Wave Complex

In an EEG recording also spikes, transients and other type of waves can be present. Each one of them is usually associated with a nervous disorders. In these project our attention is focused on patients with absence seizures, whose main characteristic in the EEG is the spike and slow wave complex, as already discussed in the second chapter.

In these patients usually burst of these complexes are observed, as it can be seen from the single EEG channel shown in figure 3.7.

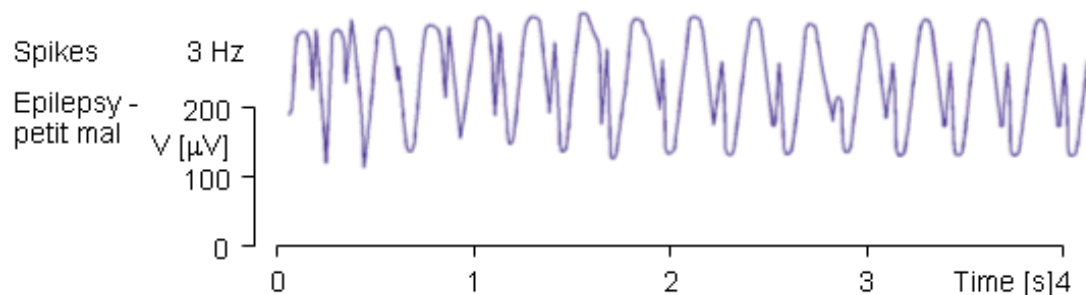


FIGURE 3.7: The spike and wave complexes in a patient with absence seizures. From [25].

3.5.3 Artifacts

Signals recorded by the EEG that are not of cerebral origin are called *artifacts*. Every EEG signal is inevitably corrupted by these *artifacts*, which are the main reason why a trained physician or a neurologist are required to correctly interpret an EEG. The most common ones include [26]:

- Eye-induced artifacts: includes artifacts cause by eye blinking and eye movement.
- ECG artifacts: The high amplitude QRS complex in the ECG can easily contaminate the EEG. That is the reason why in most of the EEG recordings one channel usually is the ECG signal itself.
- EMG-induced artifacts: artifact caused by the electrical activity produced by the activation of skeletal muscles.
- Power system interference artifacts : When the electrodes are not properly grounded a 50 or 60 Hz (depending on the power supply characteristics) noise is introduced in the EEG.

Artifact removal can be achieved through Independent Component Analysis (ICA). The signal is separated into source component and the unwanted components generating the artifacts are removed. However it is a very lengthy procedure and the components to remove must still be chosen manually [27].

Chapter 4

State of the art Seizure Detection

In order to achieve the main objective of this thesis, which is topographic seizure distribution, a seizure onset detection algorithm must be developed. In this chapter a definition of seizure detection is presented together with a state of the art literature study. This has permitted to identify the most promising method for our purposes, which will be the starting point for our automatic seizure detection algorithm.

4.1 Definition of Seizure Detection

As described in the previous chapters the manifestation of epileptic seizures occurs in EEG. An automated seizure detection algorithm must discriminate between seizure and non-seizure activity on the basis of the EEG characteristics and for each detected seizure an *onset* is determined. In figure 4.1 an absence seizure is shown together with the estimated onset. In order to be able to use an algorithm in a clinical setting the algorithm should provide a high detection rate, together with a low false positive rate.



FIGURE 4.1: Example of seizure onset detection. The red line represents the estimated onset. Signal (in blue) is a one channel EEG signal of a transversal montage representing a slow spike and wave complex. EEG recording is taken from the data collected for this thesis.

4.2 Performance Evaluation

Evaluation of the various methods is carried out by comparing the results of the corresponding algorithm with the seizures marked by a neurologist or a trained physician. Quantitative analysis is performed using several performance measures. The most common used ones are:

- **Sensitivity (SE)**: ratio between the number of detected seizures and the number of total seizures. It is usually expressed in percentage.
- **False Positive Rate (FPR)**: number of false positive (FP) detection declared by the algorithm. Usually measured in FP/h.
- **Median Detection Delay**: Median delay in seconds between the automatically detected seizure onset and the one marked by the neurologist.

4.3 Overview of the Main Articles

During the project a very careful literature study has been conducted. Several articles concerning seizure detection were read and analyzed and in this section the five most promising methods are described. While selecting these articles two important constraints were taken into account. A selected algorithm must:

- **Operate on-line**: Our algorithm is going to be designed for a device which has to operate in real time. On-line detection algorithms have some extra limitations on the signal processing techniques. The classification processes must be computationally efficient, use short time windows for analysis and may only use data occurred before the considered point (*causal* analysis).
- **Be optimized for sEEG data**: The *Hypo-Safe A/S* device is going to operate with data from a subcutaneously implanted electrode, therefore an algorithm already optimized for scalp EEG is clearly an advantage. The ideal algorithm should also have been tested on long term EEG on a fair number of patients because that gives a realistic simulation of the environment where the device will be employed.

For each one of the algorithms a general overview is given by outlining the method, the complexity, the performance and the dataset used for testing. Some considerations on the overall strategy are pointed out at the end of each article. In table 4.1 the algorithms are summarized to facilitate a comparison between them.

A Patient-Specific Algorithm for the Detection of Seizure Onset in Long-Term EEG Monitoring: Possible Use as a Warning Device [28]

Authors: Hao Qu and Jean Gotman

Published: IEEE transactions on biomedical engineering, vol. 44, no. 2, February 1997, manuscript received March 31, 1995; revised September 19, 1996.

Method: A patient specific algorithm to perform seizure onset detection. A modified nearest neighbour classifier is trained with a seizure EEG and with some non seizure EEG. Extreme attention has been put in achieving low false detection rates.

Complexity: medium, a modified nearest neighbour classifier is trained on combinations of features extracted from the EEG.

Specific/Generic: The method is patient specific. It has to be trained with one seizure from a patient and then detect all similar seizures.

Performance:

Sensitivity: 100%

FP/h: 0.02

Median detection delay: 9.35

Data set: scalp EEG recordings including 47 seizures in 12 patients. Type of seizures is not specified.

Considerations: The data set is very small and consist only of 12 patients, so more extensive testing is required to understand the real capabilities of this method. Moreover it has an important limitation: it only detects seizures similar to the template. In epilepsy monitoring, one wants to explore as many kinds of seizures as possible. Therefore their method cannot replace traditional unbiased seizure detection which aims at recording all types of seizures.

Patient-Specific Seizure Onset Detection [29]

Authors: Ali Shoeb, Herman Edwards , Jack Connolly , Blaise Bourgeois , Ted Treves and John Guttag

Published: Proceedings of the 26th Annual International Conference of the IEEE EMBS San Francisco, CA, USA September 1-5, 2004

Method: The method uses a wavelet decomposition to construct a feature vector that captures the morphology and spatial distribution of an EEG epoch, and then determines whether that vector is representative of a patient's seizure or non-seizure EEG using the support-vector machine classification algorithm.

Complexity: medium-high, a SVM classifier is trained on combinations of features extracted from the EEG.

Specific/Generic: patient specific approach in order to exploit the consistency of an individual patient's seizure or non seizure EEG.

Performance:

Sensitivity: 94%,

FP/h: 0.22

Median detection delay: 8.0 ± 3.2 s

Data set: 60 h of scalp EEG, including 139 seizures in 36 patients (leave one out cross validation). Contain focal, lateral, and generalized seizures.

Considerations: No constraints regarding the types of seizure onsets was imposed; the dataset contains focal, lateral, and generalized seizure onsets. Furthermore, the recordings were made in a routine clinical environment, so non-seizure activity and artifacts such as head/body movement, chewing, blinking, early stages of sleep, and electrode pops/movement were present. The recordings lasted 35 minutes on average for 30 patients, so the algorithm has not been tested on long term EEG monitoring. Patient specificity permits to improve sensitivity but requires a labeled training set of seizure and non seizure EEG for each patient

A system to detect the onset of epileptic seizures in scalp EEG [30]

Authors: M.E. Saab, J. Gotman

Published: Clinical Neurophysiology 116 (2005) 427–442, accepted 4 August 2004, available online 18 September 2004

Method: The system is based on determining the seizure probability of a section of EEG. Wavelet decomposition, feature extraction and data segmentation were employed to compute the a priori probabilities required for the Bayesian formulation used in training, testing and operation.

Complexity: medium-high, a bayesian classifier is trained on combinations of features extracted from the EEG.

Specific/Generic: The system is not patient specific and some patients might have higher false detection rates than others. In order to reduce those a tunable threshold is available to manage the trade off between high false detections rates and seizure detection.

Performance: (before/after tuning)

Sensitivity: 77.9% / 76.0%,

FP/h: 0.86 / 0.34

Median detection delay: 9.8 s / 10.0 s

Data set: 652 h of scalp EEG, including 126 seizures in 28 patients for training, 360 h of scalp EEG, including 69 seizures in 16 patients for testing. Type of seizures used for training and testing is not specified precisely.

Considerations: The data set includes patients with different types of epilepsy and seizures. The algorithm is tested on data independent from the training one, that makes the sensitivity measured accurate and reliable.

Comparison of Fractal Dimension Estimation Algorithms for Epileptic Seizure Onset Detection [31]

Authors: Georgia E. Polchronaki , Student Member IEEE, Periklis Ktonas Senior Member, IEEE, Stylianos Gatzonis, Pantelis A. Asvestas Eirini Spanou, Anna Siatouni, Hara Tsekou, Damianos Sakas and Konstantina S. Nikita, Senior Member, IEEE

Published: IEEE transaction, manuscript received July 5, 2008.

Method: Seizure onset detection is attempted by using two methodologies based on fractal dimension (FD), which is a natural measure of irregularity of curves.

Complexity: low, it is a direct feature-based detector.

Specific/Generic: The method is not patient specific, anyway a threshold value has to be employed to run the algorithm. A default threshold value can be used or the optimum one can be calculated for each patient.

Performance:

Sensitivity: 100% (with optimum threshold)

FP/h: 0.85

Median detection delay: 6.5s

Data set: 244.9 h of scalp EEG recording, 16 seizures in 3 patients. Only patients with refractory mesial temporal lobe epilepsy.

Considerations: The data set is very small and has only patients with refractory mesial temporal lobe epilepsy, so the results are not directly comparable with other studies, a more extensive testing is needed. In order to tune the threshold a training set and a test set should be used, in this way the results achieved will be more reliable.

Seizure Detection Using Seizure Probability Estimation: Comparison of Features Used to Detect Seizures [32]

Authors: Levin Kuhlmann, Anthony N. Burkitt, Mark J. Cook, Karen Fuller, David B. Grayden, Linda Seiderer and Iven M. Y. Mareels.

Published: Annals of Biomedical Engineering, Vol. 37, No. 10, October 2009 (© 2009) pp. 2129–2145, received 6 February 2009; accepted 29 June 2009; published on-line 10 July 2009

Method: This method uses the framework developed by Saab and Gotman and analyses the impact of six additional features, in order to find out the best possible combinations of three features among the 84 possible.

Complexity: medium-high, a bayesian classifier is trained on combinations of features extracted from the EEG.

Specific/Generic: The method is based on Saab and Gotman algorithm, so it is generic as well.

Performance: (original Saab and Gotman/this paper alternative features)

Sensitivity: 79.0% / 81.0%,

FP/h: 0.62 / 0.60

Median detection delay: 21.3 s / 16.9 s

Data set: 525 h of scalp EEG, including 88 seizures in 21 patients (10-fold cross-validation). Type of Seizures used for training and testing is not specified precisely.

Considerations: Patients had different type of epilepsy and the 10-fold cross validation method assures high reliability of the results.

TABLE 4.1: Overview of the state of the art methods for seizure detection.

Article	Authors	Method	Sensitivity	FP/h	Delay(s)	Data set	Remarks
A Patient-Specific Algorithm for the Detection of Seizure Onset in Long-Term EEG Monitoring: Possible Use as a Warning Device	Hao and Gotman	Qu and Jean A modified nearest neighbour classifier is trained with a seizure EEG and with some non seizure EEG.	100%	0.02	9.35	scalp EEG recordings including 47 seizures in 12 patients	The data set is small and it only detects seizures similar to the template
Patient-Specific Seizure Onset Detection	Ali Shoeb et al.	Wavelet decomposition and support-vector machine classification algorithm	94%	0.22	8.0± 3.2	60 h of scalp EEG, including 139 seizures in 36 patients	No constraints regarding the types of seizure onsets, it has not been tested on long term EEG monitoring, patient specificity require more efforts
A system to detect the onset of epileptic seizures in scalp EEG	M.E. Saab and J. Gotman	Wavelet decomposition, feature extraction and data segmentation were employed to compute the a priori probabilities	77.9% / 76.0%	0.86 / 0.34	9.8 / 10.0	652 h of scalp EEG, including 126 seizures in 28 patients for training, 360 h, including 69 seizures in 16 patients for testing	The data set includes patients with different types of epilepsy and seizures. The algorithm is tested on data independent from the training one.
Comparison of Fractal Dimension Estimation Algorithms for Epileptic Seizure Onset Detection	Georgia E. Polchronaki et al.	Seizure onset detection is attempted by using a methodology based on fractal dimension	100 %	0.85	6.5	244.9 h of scalp EEG recording, 16 seizures in 3 patients	The data set is small and has only patients with MTL. A clear separation between training and test should have been employed.
Seizure Detection Using Seizure Probability Estimation: Comparison of Features Used to Detect Seizures	Levin Kuhlmann et al.	This method uses the framework developed by Saab and Gotman and analyses the impact of six additional features.	81%	0.60	16.9	525 h of scalp EEG, including 88 seizures in 21 patients.	Patients had different type of epilepsy and the 10-fold cross validation method assures high reliability of the results.

4.4 Choice of a Reference Method

The system developed by Georgia E. Polchronaki et al. [31] has been chosen as reference method because it is the algorithm which has shown the biggest development potential. The performance of the method are very good and even though the data set consist only of 3 patients, 249 hours of long term EEG have been analyzed. However the performance needs to be validated through a more reliable analysis: training data to tune the algorithm should be independent from test data. This study will be conducted in this thesis and particular care will be employed in reducing the FP rate. A novel algorithm will be designed for the detection of absence seizures, using as a starting point this method from Georgia E. Polchronaki et al., which was tuned and built for patients with refractory mesial temporal lobe epilepsy (MTLE).

Each one of the other methods analyzed also has its own advantages and drawbacks. The algorithm from Qu and Gotman [28] showed the best performance, but it could only detect seizures similar to the chosen template. Shoeb et al. [29] obtained the third best performance, anyway we have to consider it is a patient specific algorithm and that it has not been tested on long time EEG. Saab and Gotman [30] and Kuhlmann et al. [32] algorithm showed a low sensitivity with the advantage of being generic and not patient specific.

Chapter 5

Fractal Dimension

In this chapter the theoretical background to understand the approach of the algorithm in [31] is given. The intuitive and formal definition of fractal dimension is explained together with some examples to illustrate the theoretical concepts. The application to real world waveform through estimation algorithm is then discussed.

5.1 Intuitive Explanation

At first it is useful to define the concept of *topological dimension* as the minimum number of independent parameters necessary to define a set. It is always a natural number and for example if the set is a plane, it can be proved that its topological dimension is 2. [33]

This definition of topological dimension anyway does not behave properly in highly irregular set, such as fractals. A *fractal* is defined as “a rough or fragmented geometric shape that can be split into parts, each of which is (at least approximately) a reduced-size copy of the whole” [34]. In order to better characterize these type of sets, the definition of topological dimension needs an extension: the *fractal dimension*. This new dimension is not anymore a natural number but can be a real number in the interval $[0, +\infty]$. Roughly, the fractal dimension of a set can be defined when the following limit exists as a finite number:

$$\lim_{r \rightarrow 0} \frac{N(r)}{r^{\text{FD}}} \quad (5.1)$$

where FD is the fractal dimension and $N(r)$ is the number of balls of radius r necessary to cover the set.

From this definition it follows that for example a countable set has fractal dimension 0, while \mathbb{R}^n has dimension n .

5.2 Formal Definition

For the sake of precision in this section a more formal definition of fractal dimension is given. First we need to define the d -dimensional *Hausdorff content* of $S \subset X$, where X is a metric space, as the infimum of:

$$C_H^d(S) = \inf \left\{ \sum_i r_i^d \mid \exists \text{ a cover of } S \text{ by balls with radius } r_i > 0 \right\}, \quad (5.2)$$

where a ball of radius r and centered at a point p is defined by $B_r(p) \triangleq \{x \in M \mid \text{distance}(x, p) < r\}$.

Now we can define the *fractal dimension*(FD) (also known as *Hausdorff dimension* or *Hausdorff-Besicovitch dimension*) of X as [35]:

$$\text{FD}(X) = \inf \left\{ d \geq 0 \mid C_H^d(X) = 0 \right\} \quad (5.3)$$

5.3 Examples

In this section some popular fractals waveforms which will be very useful in our analysis are presented. The step by step proof of the calculation of the fractal dimension is not discussed but can be found in the corresponding references.

It must be noticed that the fractal dimension of a one dimensional function it holds [36]:

$$1 \leq \text{FD} \leq 2, \text{ for one dimensional functions.}$$

A straight line has a fractal dimension of 1.

5.3.1 Weierstrass Cosine Function (WCF)

In [37] WCF is defined as :

$$W_H(t) = \sum_{k=0}^{+\infty} \gamma^{-kH} \cos(2\pi\gamma^k t), \quad 0 < H < 1, \gamma > 1. \quad (5.4)$$

It can be proven that FD of this function is $FD = 2 - H$. In figure 5.1(a) a WCF with $FD = 1.5$ and $\gamma = 5$ is shown.

5.3.2 Weierstrass Mandelbrot Cosine Function (WMCF)

A modified version of the Weierstrass Cosine Function is later introduced by Mandelbrot [38] and is defined as:

$$W(t) = \sum_{k=-\infty}^{+\infty} \frac{1 - \cos(b^k t)}{b^{(2-D)k}}, \quad 1 < D < 2. \quad (5.5)$$

The corresponding fractal dimension is $FD = D$. In figure 5.1(b) a WMCF with $FD = 1.5$ and $b = 1.5$ is displayed.

5.3.3 Takagi Function (TF)

The Takagi function is defined in [39] as:

$$K(t) = \sum_{k=0}^{+\infty} a^k \phi(b^k t), \quad (5.6)$$

where $\phi(t) = |bt - \text{round}(bt)|$, $a \in [0, 1]$, $a \in \mathbb{R}$, $b \in \mathbb{Z}$. With some calculations it can be proven that its fractal dimension is $FD = \log(4a)/\log(b)$. An example with $a = 1$ and $b = 2$ is shown in figure 5.1(c).

5.3.4 Fractional Brownian motion (FBM)

FBM can be modeled as a non stationary stochastic process. A waveform of the desired FD and can be synthesized with a wavelet based approach as explained in [40]. An example with $FD = 1.5$ is shown in figure 5.1(d).

In figure 5.2 three FBM of 1000 samples with increasing values of FD are plotted. It can be noticed how to a higher value of FD corresponds a more irregular curve.

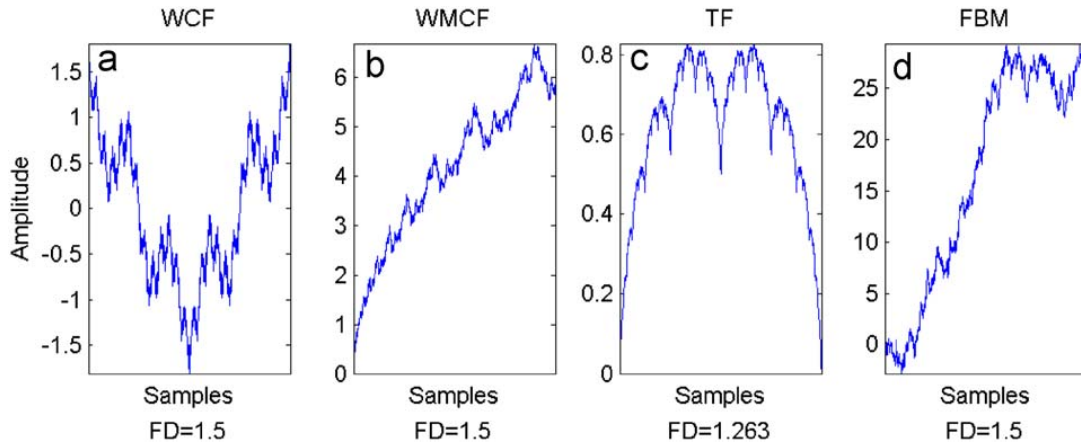


FIGURE 5.1: Synthetic fractal waveforms using, (a) Weierstrass-cosine function, (b) Weierstrass-Mandelbrot cosine function, (c) Takagi function, (d) Fractional Brownian motion. The length of the waveforms is $N = 1024$ samples. From [36].

5.4 Fractal Dimension of Biomedical Waveforms

In all the examples described until now it was possible to calculate the exact fractal dimension of the waveforms considered. When it comes to real world data, such as EEG or other biomedical waveforms, it is not possible to compute analytically the FD, which

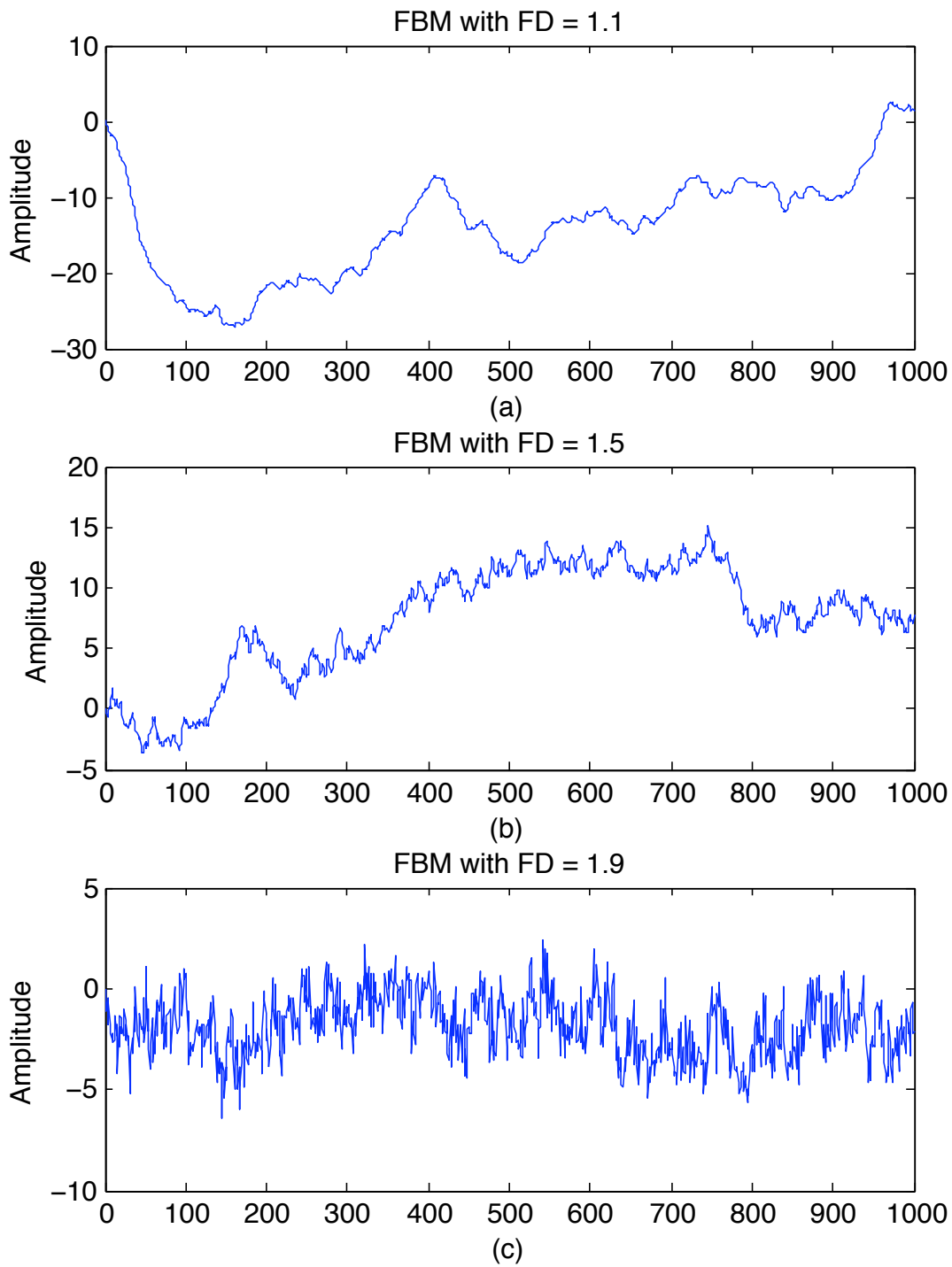


FIGURE 5.2: Synthetic fractal waveforms using Fractional Brownian motion with (a) $FD = 1.1$, (b) $FD = 1.5$, (c) $FD = 1.9$. The length of the waveforms is $N = 1000$ samples.

therefore must be estimated. Various algorithm for fractal dimension estimation exists but the most used ones are Katz's and Higuchi's method, which are described in the following.

5.4.1 Katz's Method

In [41] Katz defined a waveform as collection of points pairs (x, y) where the x values increase monotonically. He notices that real world waveforms can never become convoluted enough to fill a plane therefore their fractal dimension is usually confined between 1 and 1.5. Based on his considerations he proposed the following empirical estimate of fractal dimension:

$$FD = \frac{\log(n)}{\log(n) + \log(d/L)} \quad (5.7)$$

where $n = N - 1$, N is the number of point pairs, d is the diameter of the waveform and L is the length of the curve.

5.4.2 Higuchi's Method

Higuchi in [42] proposed an alternative method of FD estimation. In a waveform consider the second coordinate of an epoch of N samples, $y(1), \dots, y(N)$ and divide it in k sub-epochs of length $M = \lfloor (N - 1)/k \rfloor$:

$$y_k^m = \{y(m), y(m + k), y(m + 2k), \dots, y(m + Mk)\}, \quad m = 1, 2, \dots, k, \quad (5.8)$$

where m and k are integers indicating the initial time and the interval time, respectively. The length of the curve represented by each sub-epoch $L_m(k)$ is then computed as:

$$L_m(k) = \frac{\left(\sum_{i=1}^M |y(m + ik) - y(m + (i - 1)k)| \right) \frac{N-1}{Mk}}{k} \quad (5.9)$$

where $(N - 1)/Mk$ represents a normalization factor. The length of the curve for the specified time interval k is therefore defined as:

$$L(k) = \sum_{m=1}^k L_m(k) \quad (5.10)$$

If $L(k) \propto k^{-D}$, then the curve has fractal dimension $FD = D$. Therefore, if the waveform is a fractal, by plotting k and the corresponding $L(k)$ on a double logarithmic scale a straight line should be obtained. For real world data this is not the case and an estimation of FD is given by calculating the slope of the linear best fitting of these points.

5.4.3 Comparison

The performance of the two methods have been deeply analyzed on the fractals with known FD presented in the previous section [36]. The superiority of Higuchi estimation is clear. Higuchi outperforms Katz's method in several areas:

- **Precision of estimation:** In figure 5.3 Katz's and Higuchi's method performance are evaluated for four fractal curves with known FD. As it can be observed estimation using Higuchi's algorithm is much more accurate.
- **Amplitude independence:** Higuchi's method is independent on the amplitude of the waveform and gives an estimation only based on the shape of the curve. Katz's method instead is amplitude dependent, as shown in figure 5.4.
- **Sampling frequency dependence:** Higuchi's estimation is less sensitive than Katz's estimation to the sampling frequency of the waveforms considered, as pointed out in figure 5.5

Therefore Higuchi's method for estimation of fractal dimension will be employed in the seizure detection algorithm presented in this thesis.

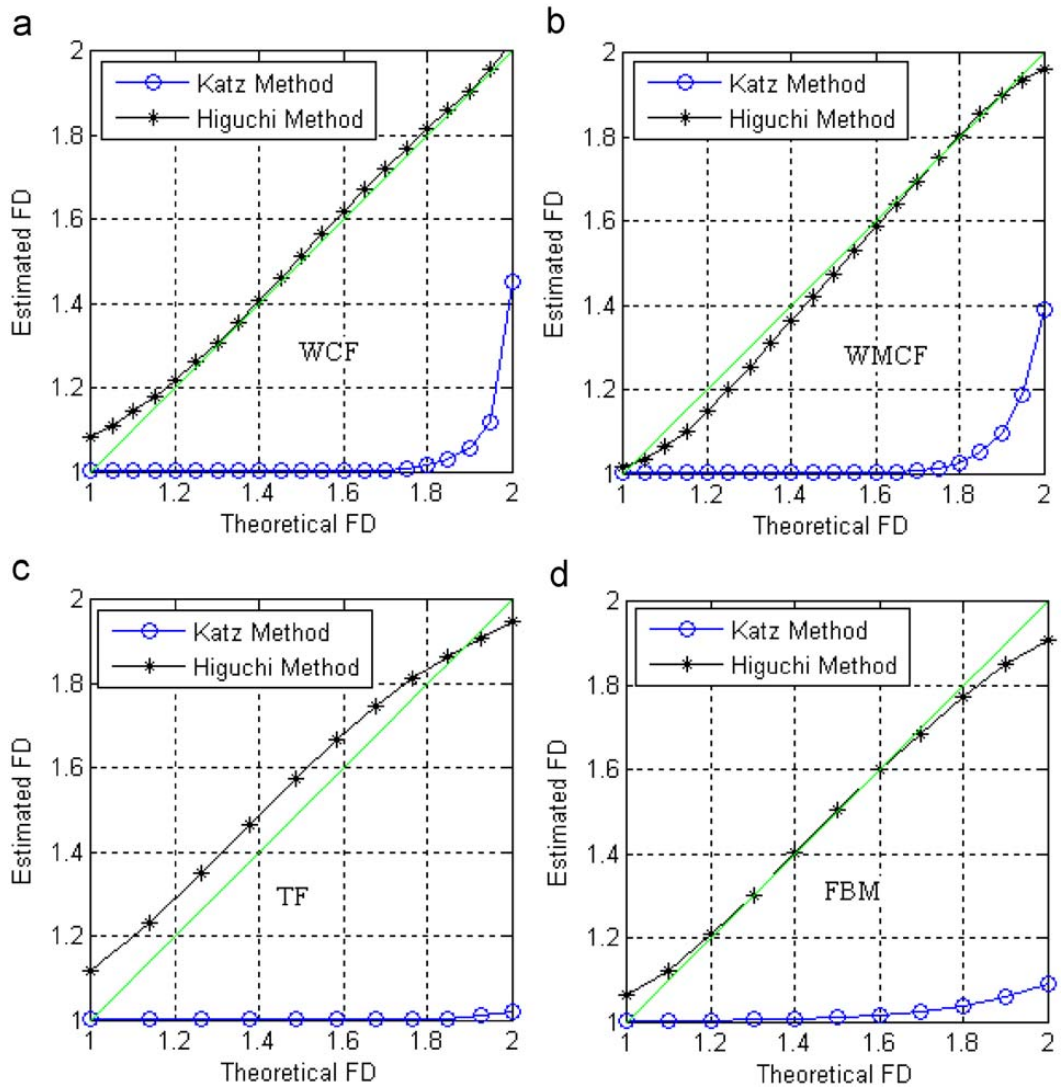


FIGURE 5.3: Theoretical fractal dimension (in green) and estimation using Higuchi's and Katz's algorithm for (a) Weierstrass-cosine function, (b) Weierstrass Mandelbrot cosine function, (c) Takagi function, (d) Fractional Brownian motion. From [36].

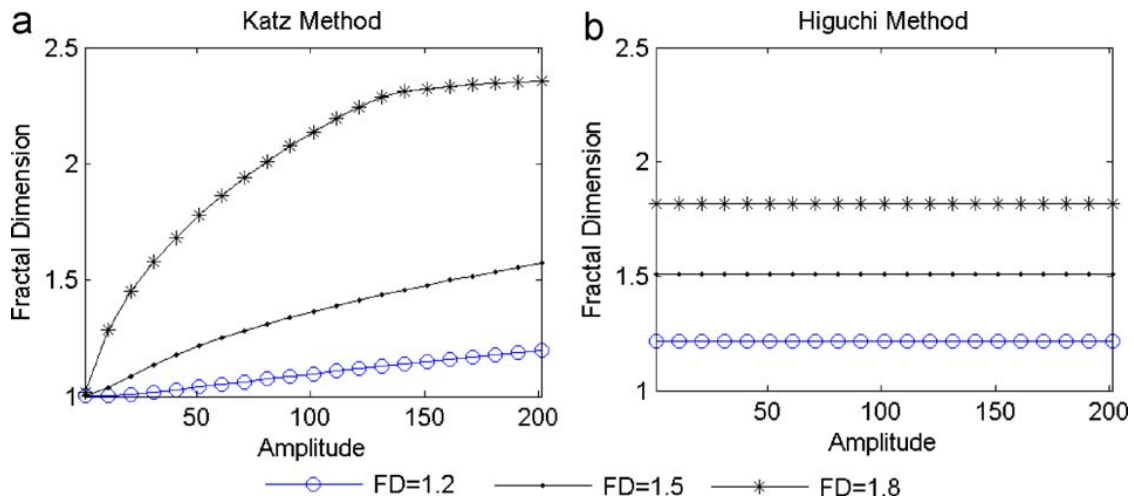


FIGURE 5.4: Dependence of the estimation of FD on the amplitude using (a) Katz's and (b) Higuchi's method. From [36].

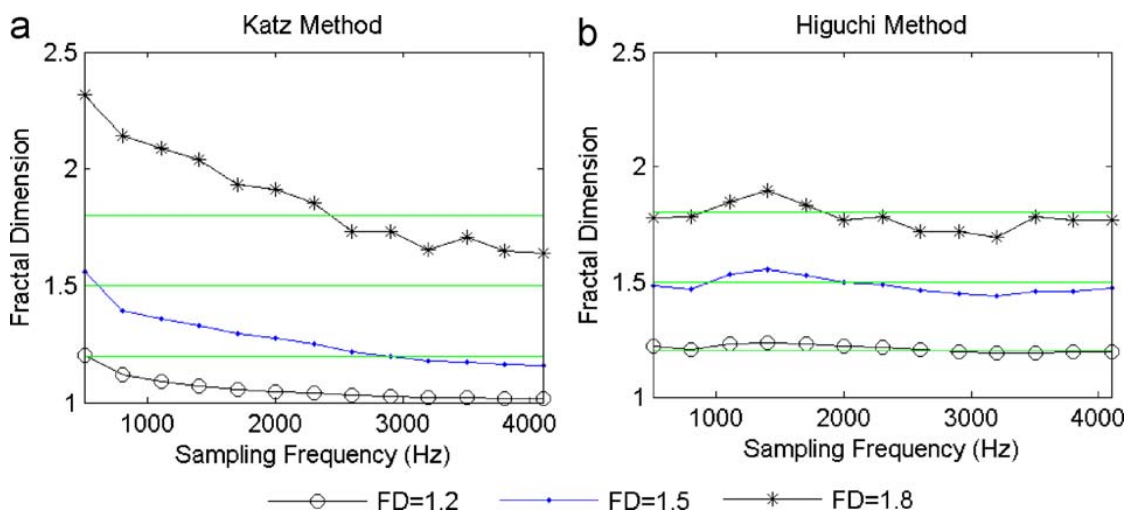


FIGURE 5.5: Dependence of the estimation of FD on the sampling frequency using (a) Katz's and (b) Higuchi's method. From [36].

Chapter 6

Absence Seizures Database

No publicly available database with absence seizures is available for current research, therefore part of the workload of this project has been collection and classification of data from patients with absence epilepsy. In the following the novel database is described in detail.

6.1 Collection and Classification of Data

Data from patients with known absences have been identified in the clinical NF database at Copenhagen University Hospital. The data were filtered with an analog bandpass filter from 0.56 Hz to 70 Hz and are sampled at 200 Hz. Most of the EEG recordings are in the proprietary data-format of Cadwell, some in the proprietary format of Stellate Harmonie. They were exported as European standard format (edf), through facilities available in both softwares, in an anonymized form. Then seizure onset was identified in collaboration with MD Troels Kjær.

Data from a total of 47 patients were collected. The EEG recordings are between 15 and 150 minutes long, with an average length of about half an hour. In figure 6.2 a sample recording is shown.

All the recordings consist of 19 channel, 18 EEG channels and one ECG channel. When exporting to the edf format the recordings were saved in *transversal montage*, in order to preserve the topographic information needed to achieve one of the main objective of this thesis. In figure 6.1 is shown a visualization of the transversal montage and in figure 6.2 an 18 channel sample EEG is shown.

6.2 Patients Selection and Database Description

After consultation with MD Troels Kjær, seizures shorter than 4 seconds were removed from the database, since these seizures were considered a minor impairment to the health of the patients. The patients has then been selected depending on the number of seizures

TABLE 6.1: Overview of the absence seizures database created for this project. In this table only the patients with at least 4 seizures are shown. The numbering of the patients refers to the complete database. This database consist of 17 patients for a total of 103 seizures in 12 hours of EEG recording.

Patient n.	Sex	Age	Diagnosis	n. Seizures
8	M	46	Juvenile Myoclonic Epilepsy (JME)	5
9	M	41	Periodic Short Interval Diffuse Discharges (PSIDDs)	5
11	F	17	Juvenile Absence epilepsy (JAE)	6
13	M	10	Childhood Absence epilepsy (CAE)	7
14	M	14	Juvenile Absence epilepsy (JAE)	5
16	F	7	Childhood Absence epilepsy (CAE)	7
17	M	5	Childhood Absence epilepsy (CAE)	7
18	M	9	Childhood Absence epilepsy (CAE)	6
19	F	10	Childhood Absence epilepsy (CAE)	5
20	F	10	Dystrophia Musculorum Congenita	6
23	M	9	Childhood Absence epilepsy (CAE)	6
25	M	10	Childhood Absence epilepsy (CAE)	8
36	M	14	Juvenile Myoclonic Epilepsy (JME)	4
42	F	7	Childhood Absence epilepsy (CAE)	11
43	M	17	Juvenile Myoclonic Epilepsy (JME)	4
46	F	15	Juvenile Myoclonic Epilepsy (JME)	6
51	M	13	Juvenile Absence Epilepsy (JAE)	5

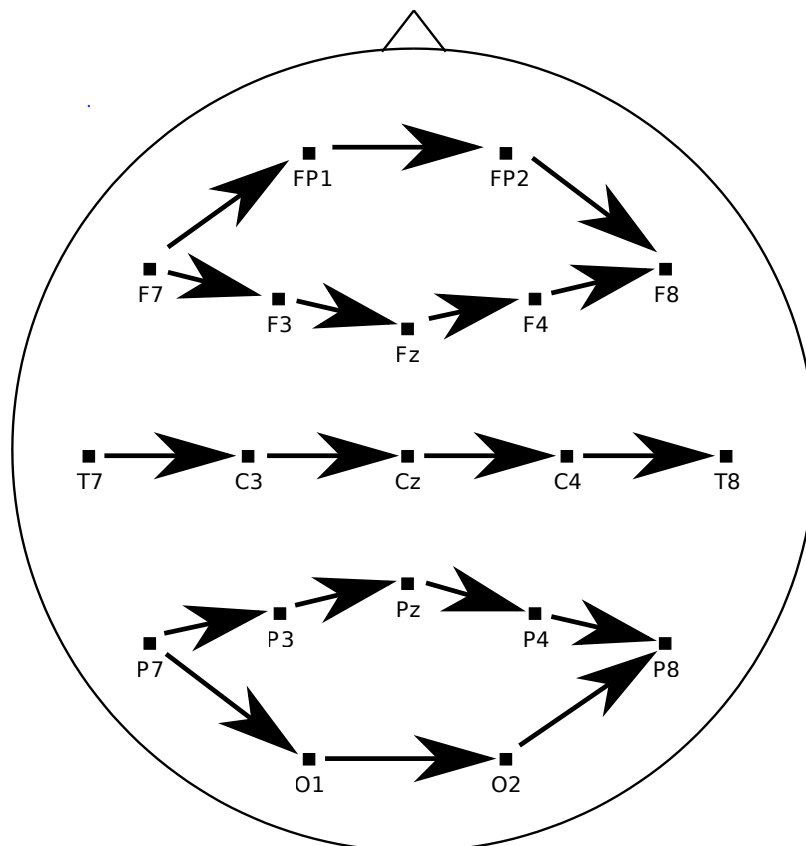


FIGURE 6.1: Visualization of the transversal montage. For each pair of electrodes of the montage an arrow pointing at first electrode and ending in the second electrode is shown.

in their recording. The algorithm for seizure detection is going to be patient specific, therefore only patients with at least 4 seizures have been considered, in order to provide the algorithm enough data for training. After the selection 18 patients are compatible with the chosen criteria and their clinical informations are available in table 6.1. This database consist of a total of 107 seizures in 12 hours of EEG recording. Both cases of idiopathic (CAE, JAE, JME) and symptomatic epilepsy (others) are present.



FIGURE 6.2: EEG recording in EDF format. An absence seizure is clearly recognizable in the recording. On the left pairs of electrodes corresponding to the transversal montage are visible.

Chapter 7

Implementation of an Absence Seizure Onset Detection Algorithm

In this chapter the concept of fractal dimension is exploited to develop an algorithm for absence seizure onset detection. Inspiration is taken from [31], but in this work several modifications are introduced and summarized in the end of the chapter.

7.1 Overview

A clear drop of fractal dimension of an EEG epoch during a seizure was already noticed in [43], where intracranial EEG recordings were taken into examination. In [31] this concept has been applied to scalp EEG. Using this work as a starting point a novel detection algorithm optimized for absence seizure detection is implemented.

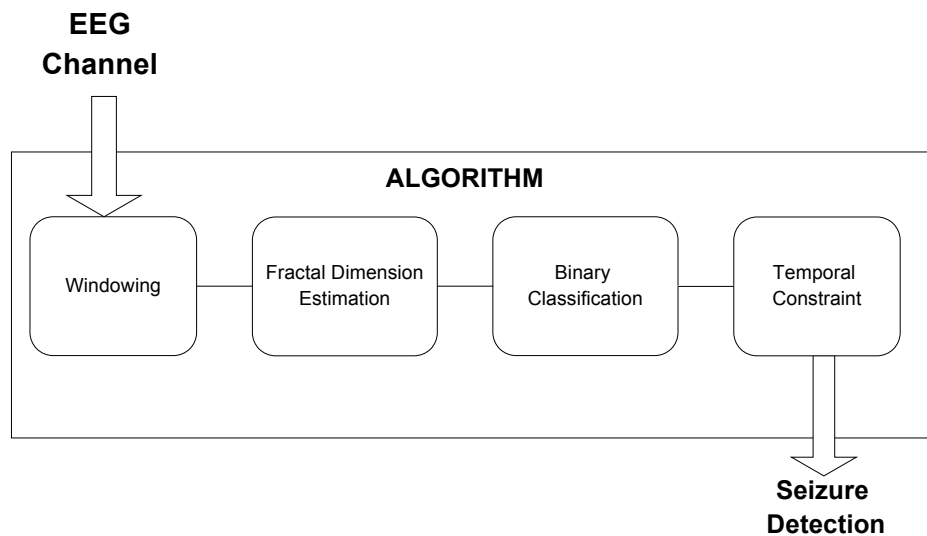


FIGURE 7.1: Architecture of seizure detection algorithm. For each epoch fractal dimension is estimated. A seizure onset is declared if FD is below a threshold for a fixed number epochs.

An overview of the architecture of the algorithm is shown in figure 7.1. After dividing the EEG in epochs, fractal dimension is estimated for each one of them. When FD is below a threshold for a fixed number of epochs, a seizure onset is declared. This concept is illustrated in figure 7.2.

7.2 Algorithm Input and Channel Constraint

Data used for analysis are scalp EEG recordings from the absence seizure database described in chapter 6. For each of the patients 18 EEG channels in transversal montage are available. These channels were already filtered with an analog bandpass filter between 0.5 Hz and 70 Hz embedded in the EEG recording machine. The goal of the bandpass filter is to remove baseline wandering and other high frequency artifacts. A digital notch filter has then been applied by the author to the EEG signal, in order to remove potential power line interference.

The algorithm is designed for the *Hypo-Safe A/S* device, which will operate with only *one* subcutaneously implanted electrode. This impose a constraint on the design of the algorithm. Seizure detection must be attempted using each EEG channel separately and not combining the information from the 18 channels, as all of the algorithms analyzed in chapter 4 do.

7.3 Epoching

In the database seizures shorter than 4 seconds were removed after consultation with MD Troels Kjær, since they constitute a minor impairment to the health of the patient. The algorithm has therefore to detect only seizures longer than 4 seconds and the length of EEG epochs must take into account this fact.

The EEG recordings are segmented into 2 seconds 50% overlapping epochs, which are long enough to capture the EEG characteristics needed to calculate FD and short enough to permit detection of 4 seconds seizures. A detection will be triggered when at least 3 epochs has a detected seizure status, as shown in figure 7.2. Overlapping of the epochs is 50 %, therefore the minimum total seizure time needed for a detection is 4 seconds, that is exactly the length of the shortest seizure in the database.

7.4 Fractal Dimension Estimation

Fractal dimension is estimated in each one of the epochs with Higuchi's method, which present several advantages over Katz's method, as already discussed in chapter 5. Higuchi's method when applied to real biomedical waveforms is not amplitude independent as for exactly fractal curves. Therefore, before estimating FD, each epoch was divided by its

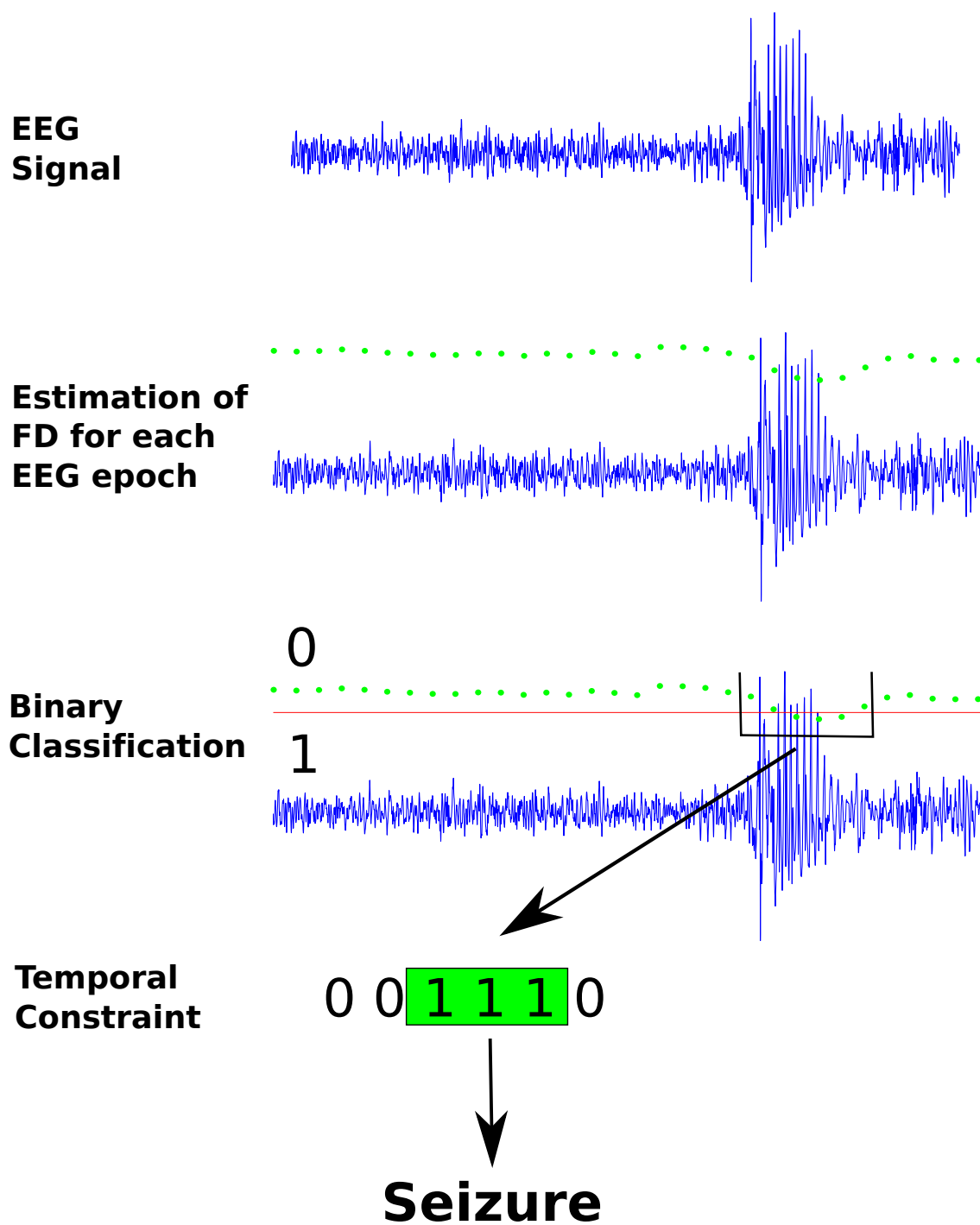


FIGURE 7.2: The three main steps of the seizure onset detector consisting of a FD estimator, a binary classifier and temporal constraint. FD is calculated for each 2 seconds epoch and it is displayed as green dots at the end of the corresponding epoch. Red line represents the threshold of the binary classifier. A seizure onset is declared after three consecutive seizure classified epochs.

variance in order to reduce the epoch amplitude when a seizure occurs. This procedure permits to lower further more FD of high amplitude seizures and simplify seizures detection.

7.4.1 Parameter Selection

There is one free parameter in Higuchi FD estimation, the interval time parameter k (see chapter 5.4.2). The approach presented in [36] is followed in this thesis, therefore \mathbf{k} is chosen as:

$$\mathbf{k} = \{k_1, k_2, \dots, k_N\}; \quad k_i = \begin{cases} i & k \leq 4 \\ \lceil 2^{\frac{(i-1)}{4}} \rceil & k > 4 \end{cases}$$

where N is the length of \mathbf{k} , which is set to 20.

7.5 Binary classification

Only one EEG channel at a time is used to perform classification and subsequent seizure detection. Therefore binary classification is performed by selecting a threshold for fractal dimension in a patient specific way. Values of FD under this threshold are considered indicators of a seizures activity. When N epochs in a row are classified in a seizure status, a detection is triggered. N was chosen equal to 3, in order to detect seizure of at least 4 seconds, as already explained earlier in the chapter.

Since the algorithm is patient specific, only seizures from the same patient can be used for training and testing. In some cases only 4 seizures are available per patient. In order to assure an accurate evaluation of the performance of the seizure detection algorithm also in these cases, *leave-one-out cross validation* method was employed for training and testing. Data for each patient are split into as many segments as the number of seizures for that patient. Each segment must contain a seizure and some non ictal EEG activity. For this project the splitting points are chosen as the the middle points between two seizures. The algorithm is now trained in all the segments excepts one, which is used for testing. The process is then repeated until all segments have been used both for training and testing. The overall performance is evaluated as the average of all the single run performance. A graphic illustration of the principle is available in figure 7.3.

Selection of the optimal threshold for each training set was performed by maximizing an objective function, which for a specific threshold value is defined as:

$$f = c_1 * N_{L<10} + c_2 * N_{L>10} - c_3 * N_{FP} \quad (7.1)$$

where $N_{L<10}$ and $N_{L>10}$ are the number of seizures longer and shorter than 10 seconds respectively, N_{FP} is the number of false positives and c_1, c_2, c_3 are the weight coefficients. After consultation with MD Troels Kjær on the *Hypo-Safe* device requirements, the

coefficients were chosen as:

$$c_1 = 1, \quad c_2 = 2, \quad c_3 = 0.5.$$

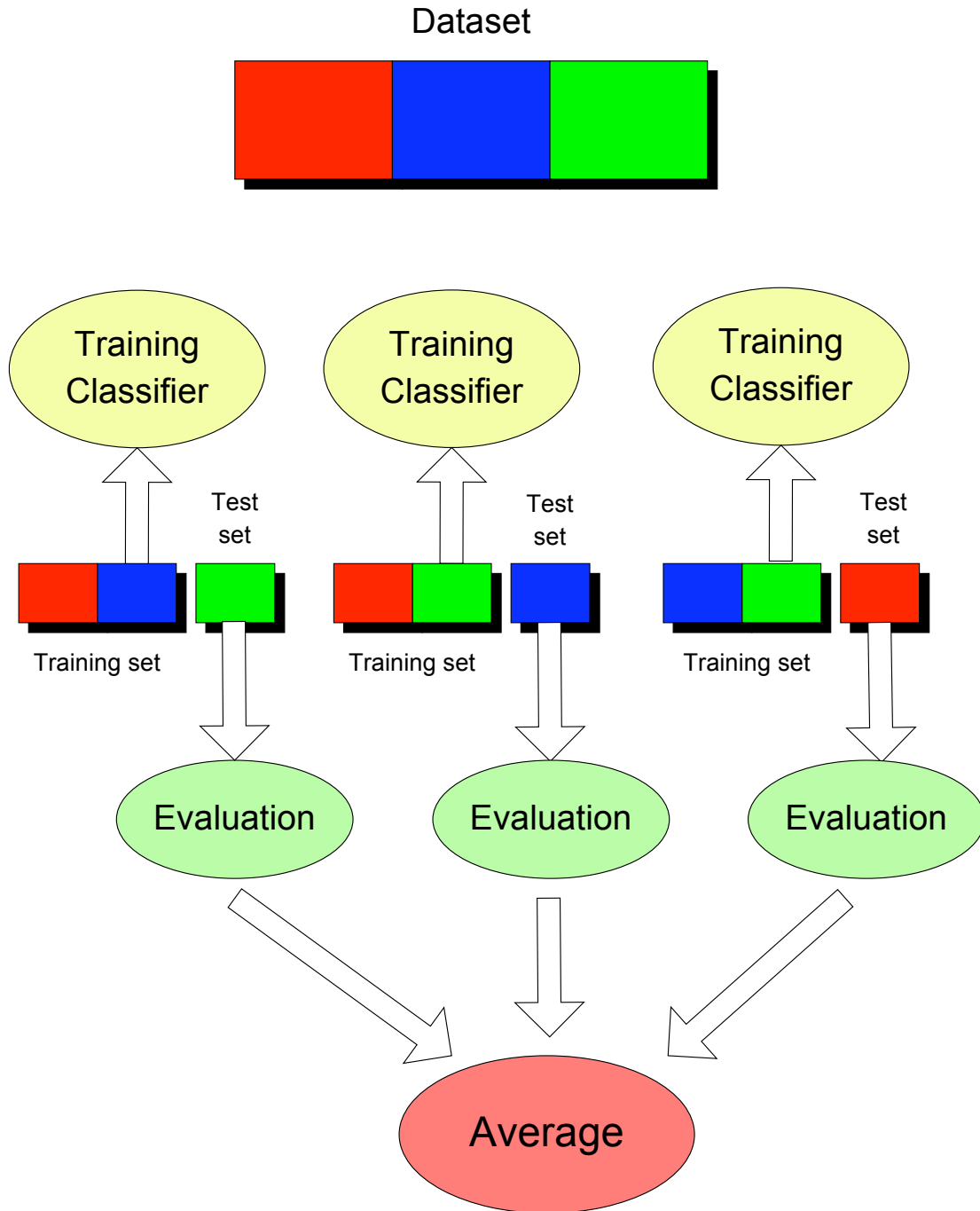


FIGURE 7.3: Illustration of the leave-one-out cross-validation principle in a patient with three seizures. Each block (red, blue and green) in the dataset contains one seizure and some non ictal EEG activity. In the first run, the algorithm is trained on the first two seizures (red and blue), and tested on data corresponding to the third seizure (green). This is repeated other two times and the overall performance is evaluated as the average of all three test runs.

7.6 Matlab Implementation

The algorithm has been completely implemented in Matlab by the author. A commented version of the matlab code can be found in appendix B.

7.7 Deviation from Georgia E. Polchronaki et al.

The algorithm and testing procedure presented in this chapter present several modifications compared to the ones proposed in [31]:

- **Patient specificity:** The implemented algorithm is patient specific. A patient-specific detector learns the specific features characterizing a particular patient's seizure onsets.
- **Single EEG channel:** Only one EEG channel is used to attempt seizure detection. This is due to the constraint imposed by the *Hypo-Safe* device, which operates with only one electrode. That is also one of the reasons why a patient specific approach was chosen.
- **FD Estimation:** An accurate and stable FD estimation is achieved through Higuchi's method. In chapter 5 it was proven to be a much more reliable tool than Katz's method.
- **Threshold selection:** An objective function was created to select the most appropriate threshold.
- **Proper training and testing:** In [31] the algorithm was trained and tested on the same data, giving biased performance results. In this thesis instead, as described in section 7.5, an accurate and statistically reliable leave-one-out cross validation method was employed.

7.8 Summary of algorithm parameters

As a conclusion of the chapter a summary of the parameters used for the seizure detection algorithm is given in table 7.1.

TABLE 7.1: Summary of the parameters used in the seizure detection algorithm.

	Paramter	Setting
Input	Data Type	sEEG
	Sampling frequency	200 Hz
	N. electrodes	18
	Montage	Transversal
Segmentation	Epoch length	2 s
	Overlapping	50 %
	Window	Rectangular
FD estimation	$\mathbf{k} = \{k_1, k_2, \dots, k_N\}$	$k_i = \begin{cases} i & k \leq 4 \\ \lceil 2^{\frac{(i-1)}{4}} \rceil & k > 4 \end{cases}$
Classification	N. Epochs before detection	$N = 3$
	First coefficient	$c_1 = 1$
	Second coefficient	$c_2 = 2$
	Third coefficient	$c_3 = 0.5$

Chapter 8

Results and Discussion

Objective of this chapter is to give an overview of topographic distribution of absence seizures. Therefore results of the seizure detection algorithm for each EEG channel are presented and discussed under different angles and a novel visualization method is introduced. At first performance across all patients in the database are evaluated, then results are segmented considering the various type of epilepsy that can cause absence seizures. Along with the discussion a recommendation on the placement of the *Hypo-Safe* device is given.

8.1 Visualization Method

In order to present Sensitivity (SE) and False Positive Rate (FPR) for each EEG channel in an effective way a new visualization method is introduced. Consider a map containing all electrodes positions of a transversal montage. A circle is positioned between every two electrodes that constitutes a valid pair in the transversal montage (see figure 6.1). Color of the circles are related to corresponding FPR, according to the colorbar on the right. FPR greater than 2 FP/h are merged in one color (white). Size of the circles are exponentially proportional to sensitivity, in order to emphasize graphically differences in SE. On the top left a sample circle is visualized: red zone indicate a SE lower than 50 %, yellow zone a SE between 50 % and 90 %, green zone a SE greater than 90 %. A sample "head plot" is shown in appendix in figure A.0.

In appendix A performance of the algorithm for each of the 16 patients in the database are presented using the visualization method described above.

8.2 Overall Performance

Average performance of the algorithm across all patients are visible in figure 8.1 and in table 8.1. The best performance are found in channels F3-FZ and F4-F8, where a SE

TABLE 8.1: Average performance across all patients. For each channel average Sensitivity (SE), False Positive Rate (FPR) and their standard deviation σ is reported.

Channel	N_{patients}	N_{seizures}	$SE_{\text{TOT}}(\%)$	σ_{SE}	FPR(FP/h)	σ_{FPR}
F7-FP1	17	103	84.1	34.0	0.46	0.71
FP1-FP2	17	103	77.4	37.3	0.66	0.57
FP2-F8	17	103	79.7	38.4	0.55	0.64
F7-F3	17	103	85.0	32.5	0.24	0.25
F3-FZ	17	103	85.6	32.5	0.22	0.20
FZ-F4	17	103	83.8	33.7	0.24	0.29
F4-F8	17 </td <td>103</td> <td>85.6</td> <td>32.6</td> <td>0.18</td> <td>0.21</td>	103	85.6	32.6	0.18	0.21
T7-C3	17	103	83.8	32.1	0.35	0.38
C3-CZ	17	103	78.3	37.8	0.53	0.91
CZ-C4	17	103	80.8	34.6	0.32	0.72
C4-T8	17	103	83.6	32.7	0.29	0.35
P7-P3	17	103	84.4	32.3	0.19	0.27
P3-PZ	17	103	77.4	37.9	0.69	0.92
PZ-P4	17	103	76.0	39.4	0.49	0.88
P4-P8	17	103	84.1	32.8	0.26	0.26
P7-O1	17	103	83.4	32.6	0.47	0.58
O1-O2	17	103	52.6	39.4	0.90	1.12
O2-P8	17	103	84.3	32.4	0.39	0.43

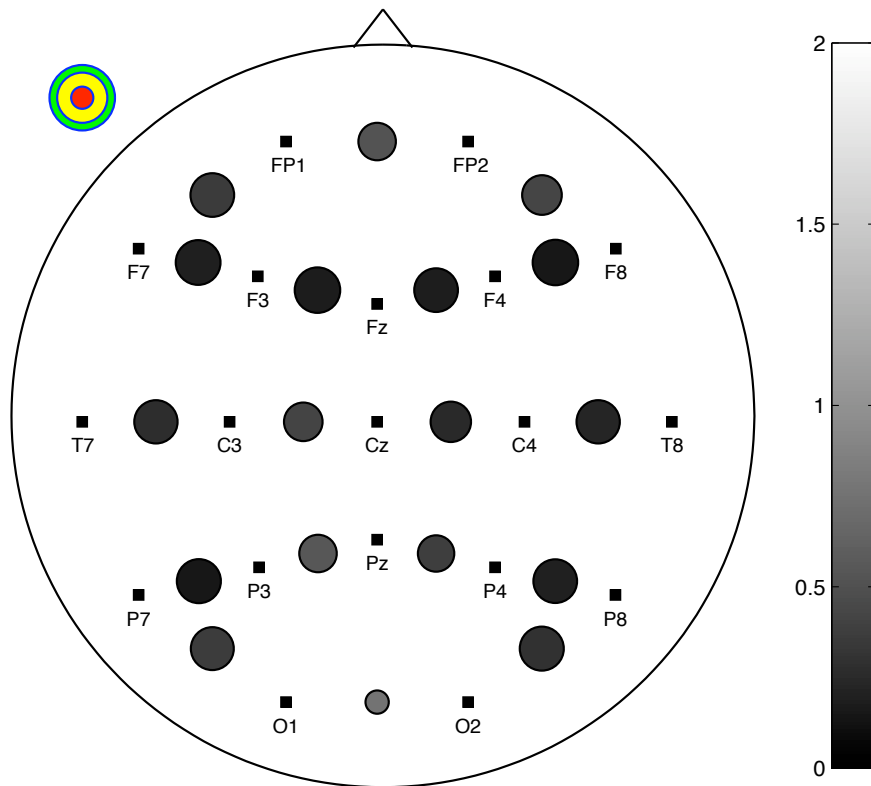


FIGURE 8.1: Visualization of average performance across all patients. For each channel average Sensitivity (SE), False Positive Rate (FPR) is visible.

of 85.65 % and 85.63 % respectively is reached, together with a FPR of 0.22 FP/h and 0.18 FP/h. Standard deviation of SE is very high in all the channels and this makes choosing a placement for *Hypo-Safe* device very hard due to this high uncertainty. However it must be noticed that , out of 17 patients analyzed by the author's algorithm, 3 patients are affected by symptomatic epilepsy with atypical absences (patient n 8,9, 20 of table 6.1) that heavily affects the average performance and standard deviation. Therefore in the following sections performances are analyzed by type of epilepsy.

Median delay in seconds between the automatically detected seizure onset and the one marked by the neurologist is an other usual performance measure. For this study average latency across all channels and patients is 6.1 seconds. It is given just for information purposes, since it is not a relevant parameter for the *Hyposafe* device and it will not taken into account anymore.

8.3 Performance by type of Epilepsy

In this section patients are grouped according to their type of epilepsy:

- Childhood Absence Epilepsy (CAE)
- Juvenile Absence Epilepsy (JAE)
- Juvenile Myoclonic Epilepsy (JME)
- Symptomatic Epilepsy with Absence Seizures

Performance of the algorithm are evaluated for each one of these groups.

For CAE and JAE patients (table 8.2 and 8.3) SE is in most of the channel above 90 % with a peak of 98.9% for CAE and 100 %, with a FPR of 0.15 FP/h and 0.18 FP/h respectively. Standard deviation dropped heavily touching a minimum of 3.2% in channels F4-F8 and C4-T8 for CAE patients. In JAE patients a standard deviation of 0% is reached in some of the channels, but since JAE patients are only 3, this result is not as significant as the 3.2% with the 8 CAE patients. In JME patients (table 8.4)) performance are comparable but a general increase in the FPR and its standard deviation across all channels can be noticed. A consistent drop from 50 to 70 % in the SE accompanied by a huge rise in its standard deviation, is observed in patients with absence seizures affected by a symptomatic type of epilepsy (8.5). This is due to atypical absences present in these patients.

8.3.1 Performance in Patients with CAE

TABLE 8.2: Average performance across patients with CAE. For each channel average Sensitivity (SE), False Positive Rate (FPR) and their standard deviation σ is reported.

Channel	N_{patients}	N_{seizures}	$SE_{\text{TOT}}(\%)$	σ_{SE}	FPR(FP/h)	σ_{FPR}
F7-FP1	8	55	91.3	18.1	0.26	0.32
FP1-FP2	8	55	81.0	33.4	0.63	0.61
FP2-F8	8	55	86.4	35.0	0.34	0.23
F7-F3	8	55	97.5	7.1	0.22	0.32
F3-FZ	8	55	98.9	3.2	0.17	0.22
FZ-F4	8	55	94.6	15.2	0.18	0.23
F4-F8	8	55	98.9	3.2	0.15	0.17
T7-C3	8	55	97.1	5.6	0.41	0.49
C3-CZ	8	55	93.4	9.2	0.42	0.64
CZ-C4	8	55	94.8	10.2	0.12	0.19
C4-T8	8	55	98.9	3.2	0.28	0.43
P7-P3	8	55	96.4	7.3	0.24	0.34
P3-PZ	8	55	83.4	34.5	0.58	0.69
PZ-P4	8	55	86.4	29.6	0.27	0.65
P4-P8	8	55	97.7	6.4	0.22	0.36
P7-O1	8	55	92.1	11.5	0.45	0.67
O1-O2	8	55	49.1	40.5	0.84	1.40
O2-P8	8	55	98.2	5.1	0.20	0.28

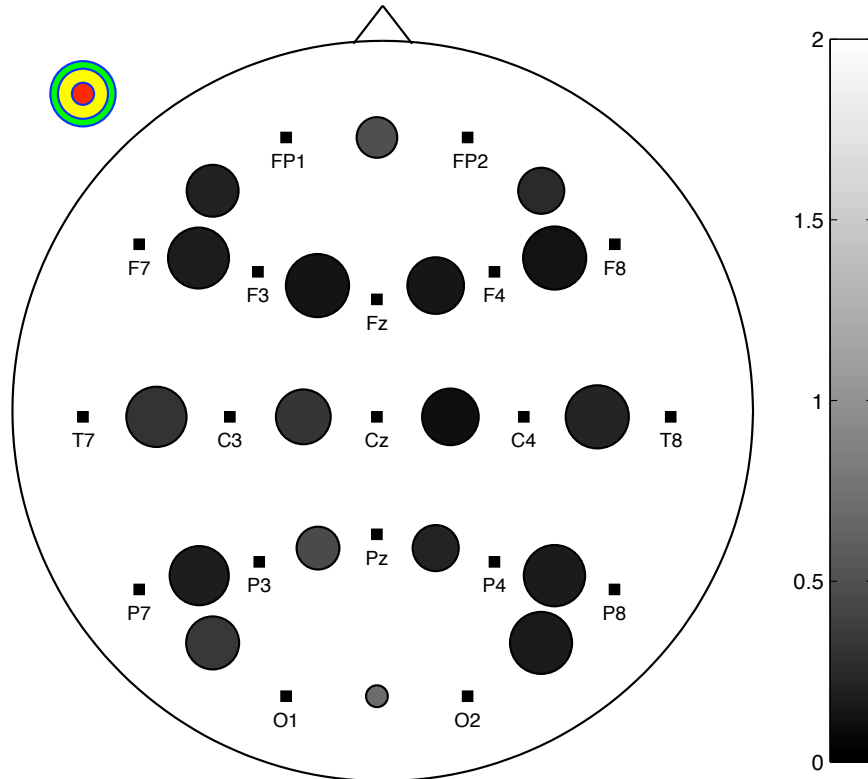


FIGURE 8.2: Visualization of average performance across patients with CAE. For each channel average Sensitivity (SE), False Positive Rate (FPR) is visible.

8.3.2 Performance in Patients with JAE

TABLE 8.3: Average performance across patients with JAE. For each channel average Sensitivity (SE), False Positive Rate (FPR) and their standard deviation σ is reported.

Channel	N_{patients}	N_{seizures}	$SE_{\text{TOT}}(\%)$	σ_{SE}	FPR(FP/h)	σ_{FPR}
F7-FP1	3	17	100.0	0.0	0.43	0.22
FP1-FP2	3	17	100.0	0.0	0.77	0.73
FP2-F8	3	17	93.3	11.5	0.48	0.42
F7-F3	3	17	93.3	11.5	0.29	0.13
F3-FZ	3	17	93.3	11.5	0.29	0.13
FZ-F4	3	17	100.0	0.0	0.14	0.17
F4-F8	3	17	93.3	11.5	0.16	0.20
T7-C3	3	17	93.3	11.5	0.43	0.30
C3-CZ	3	17	100.0	0.0	0.18	0.17
CZ-C4	3	17	93.3	11.5	0.14	0.17
C4-T8	3	17	93.3	11.5	0.14	0.17
P7-P3	3	17	93.3	11.5	0.08	0.14
P3-PZ	3	17	93.3	11.5	0.16	0.17
PZ-P4	3	17	100.0	0.0	0.19	0.17
P4-P8	3	17	93.3	11.5	0.35	0.03
P7-O1	3	17	93.3	11.5	0.18	0.17
O1-O2	3	17	86.7	23.1	0.91	1.22
O2-P8	3	17	93.3	11.5	0.18	0.19

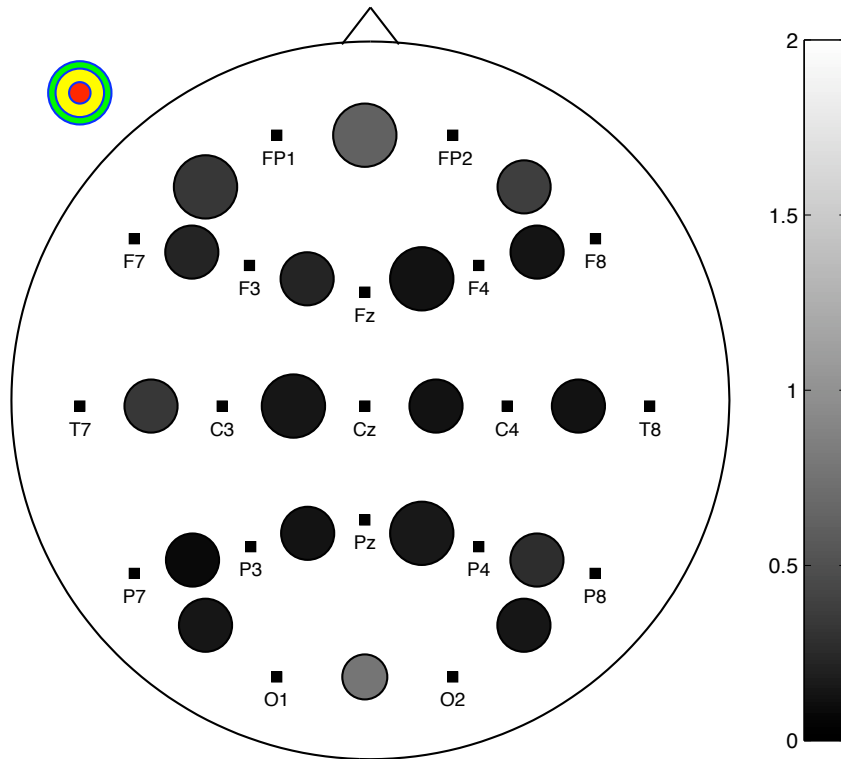


FIGURE 8.3: Visualization of average performance across patients with JAE. For each channel average Sensitivity (SE), False Positive Rate (FPR) is visible.

8.3.3 Performance in Patients with JME

TABLE 8.4: Average performance across patients with JME. For each channel average Sensitivity (SE), False Positive Rate (FPR) and their standard deviation σ is reported.

Channel	N_{patients}	N_{seizures}	$SE_{\text{TOT}}(\%)$	σ_{SE}	FPR(FP/h)	σ_{FPR}
F7-FP1	3	14	100.0	0.0	0.28	0.25
FP1-FP2	3	14	94.4	9.6	0.56	0.50
FP2-F8	3	14	94.4	9.6	0.61	0.11
F7-F3	3	14	100.0	0.0	0.12	0.20
F3-FZ	3	14	100.0	0.0	0.22	0.25
FZ-F4	3	14	88.8	19.2	0.49	0.57
F4-F8	3	14	100.0	0.0	0.12	0.20
T7-C3	3	14	94.4	9.6	0.12	0.20
C3-CZ	3	14	66.6	57.7	1.29	1.94
CZ-C4	3	14	77.7	38.5	1.13	1.67
C4-T8	3	14	94.4	9.6	0.28	0.25
P7-P3	3	14	100.0	0.0	0.28	0.25
P3-PZ	3	14	88.8	19.2	1.81	1.56
PZ-P4	3	14	72.2	48.1	1.40	1.70
P4-P8	3	14	100.0	0.0	0.33	0.17
P7-O1	3	14	100.0	0.0	0.91	0.74
O1-O2	3	14	63.8	37.6	1.47	0.87
O2-P8	3	14	94.4	9.6	1.04	0.37

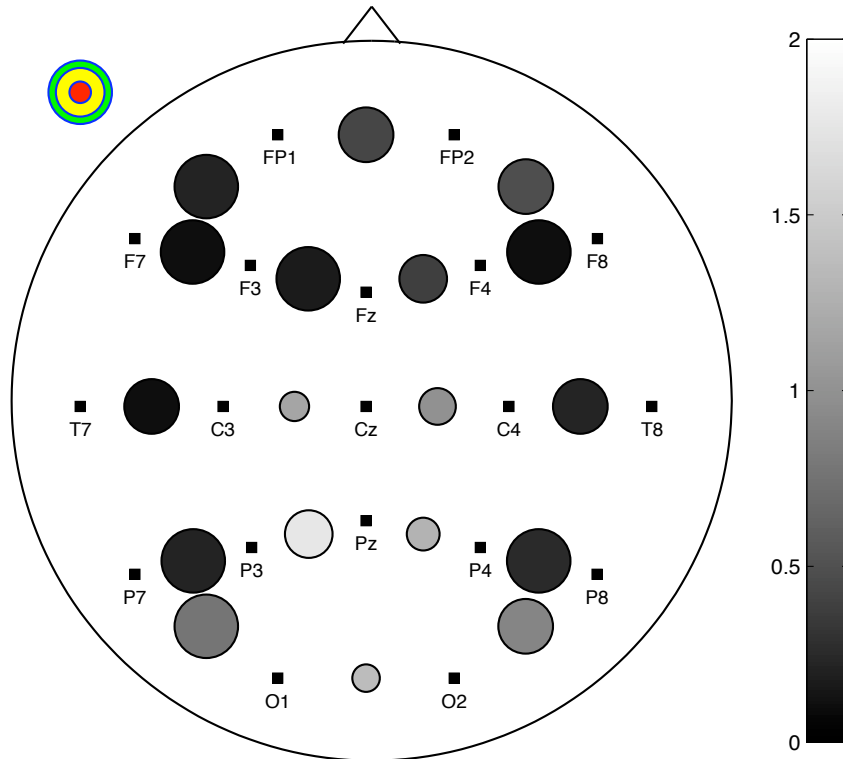


FIGURE 8.4: Visualization of average performance across patients with JME. For each channel average Sensitivity (SE), False Positive Rate (FPR) is visible.

8.3.4 Performance in patients with Symptomatic Epilepsy

TABLE 8.5: Average performance across patients with symptomatic epilepsy. For each channel average Sensitivity (SE), False Positive Rate (FPR) and their standard deviation σ is reported.

Channel	N_{patients}	N_{seizures}	$SE_{\text{TOT}}(\%)$	σ_{SE}	FPR(FP/h)	σ_{FPR}
F7-FP1	3	17	33.6	57.5	1.22	1.57
FP1-FP2	3	17	28.4	47.6	0.73	0.67
FP2-F8	3	17	33.6	57.5	1.11	1.50
F7-F3	3	17	28.4	47.6	0.37	0.19
F3-FZ	3	17	28.4	47.6	0.30	0.19
FZ-F4	3	17	33.9	57.3	0.23	0.14
F4-F8	3	17	28.2	47.7	0.35	0.35
T7-C3	3	17	28.4	47.6	0.35	0.20
C3-CZ	3	17	28.4	47.6	0.42	0.46
CZ-C4	3	17	33.9	57.2	0.22	0.14
C4-T8	3	17	22.7	38.1	0.47	0.41
P7-P3	3	17	28.3	47.7	0.07	0.13
P3-PZ	3	17	34.0	57.2	0.38	0.34
PZ-P4	3	17	28.2	47.7	0.44	0.44
P4-P8	3	17	22.8	38.0	0.18	0.19
P7-O1	3	17	33.6	57.5	0.40	0.38
O1-O2	3	17	16.8	28.8	0.47	0.41
O2-P8	3	17	28.0	47.9	0.45	0.40

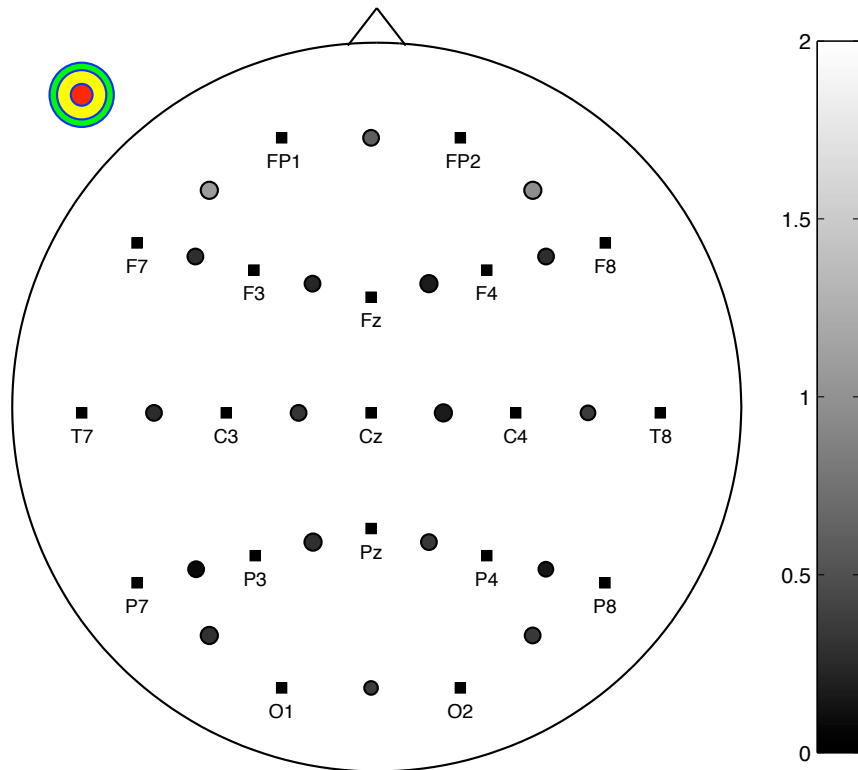


FIGURE 8.5: Visualization of average performance across patients with symptomatic epilepsy. For each channel average Sensitivity (SE), False Positive Rate (FPR) is visible.

8.4 Performance Excluding Patients with Symptomatic Epilepsy

After examination of the results of the algorithm for each type of epilepsy, it is clear that symptomatic epilepsy represents a special case to take into account when performing seizure detection. Therefore it is wise to evaluate performance excluding from the database patients with symptomatic epilepsy (patient n. 8,9,20). Comparing the results of table 8.6 to table 8.1 an average rise of 10% in sensitivity is noticeable, together with a consistent drop in SE standard deviation. Best performance, considering SE, FPR and their standard deviation, are reached in channel F4-F8 where $SE = 97.9 \pm 5.7 \%$ and $FPR = 0.15 \pm 0.17 \text{ FP/h}$.

8.5 Performance Excluding Patients with Symptomatic Epilepsy and JME

Also JME represents a particular type of epilepsy with absence seizures, since also generalized tonic clonic seizures and myoclonic jerks are present. Comparing performance in patients with JAE, CAE and JME, it is noticeable that in patients with Juvenile Myoclonic Epilepsy an higher FPR across all the channels is present. In table 8.7 performance are evaluated excluding patients with symptomatic epilepsy and JME. Taking as a reference table 8.6, a slightly decrease in FPR can be observed.

8.6 Discussion and Positioning of *Hypo-Safe* Device Electrode

Results are not directly comparable with other studies for two main reasons. Since this project is focusing on topographic distribution of absence seizures only one channel is used to achieve seizure detection, while in all other studies all EEG channels are exploited in order to increase performance. On the other hand only absence seizures were analyzed by the presented algorithm. For the sake of completeness a comparison is anyway attempted. Performance of the algorithm developed in [31] cannot be used as a reference, since they were calculated without separating training and test. However, as a point of reference, performance of a patient specific algorithm like Shoeb et al. [29] can be used. In his paper he claimed a sensitivity of 94 % and a FPR of 0.22 FP/h using all EEG channels.

In this paper considering all patients in some EEG channels is reached a SE higher than 85% and a FPR lower than 0.22 FP/h (table 8.1). Although good, SE and FPR has a too high variability(standard deviation) across all patients, therefore it is difficult to make a recommendation on the placement of the subcutaneous electrode of the *Hypo-Safe* device taking into account only these data.

TABLE 8.6: Average performance excluding patients with symptomatic epilepsy. For each channel average Sensitivity (SE), False Positive Rate (FPR) and their standard deviation σ is reported.

Channel	N_{patients}	N_{seizures}	$SE_{\text{TOT}}(\%)$	σ_{SE}	FPR(FP/h)	σ_{FPR}
F7-FP1	14	86	95.0	14.0	0.30	0.28
FP1-FP2	14	86	88.0	26.2	0.64	0.57
FP2-F8	14	86	89.6	26.7	0.43	0.27
F7-F3	14	86	97.1	7.3	0.22	0.26
F3-FZ	14	86	97.9	5.7	0.20	0.20
FZ-F4	14	86	94.6	14.0	0.24	0.32
F4-F8	14	86	97.9	5.7	0.15	0.17
T7-C3	14	86	95.7	7.4	0.35	0.41
C3-CZ	14	86	89.1	26.7	0.55	0.99
CZ-C4	14	86	90.8	18.8	0.34	0.80
C4-T8	14	86	96.7	6.9	0.25	0.34
P7-P3	14	86	96.5	7.4	0.21	0.28
P3-PZ	14	86	86.7	27.1	0.75	0.99
PZ-P4	14	86	86.3	30.3	0.50	0.96
P4-P8	14	86	97.3	6.9	0.27	0.28
P7-O1	14	86	94.1	10.1	0.49	0.63
O1-O2	14	86	60.3	37.7	0.99	1.21
O2-P8	14	86	96.4	7.3	0.38	0.45

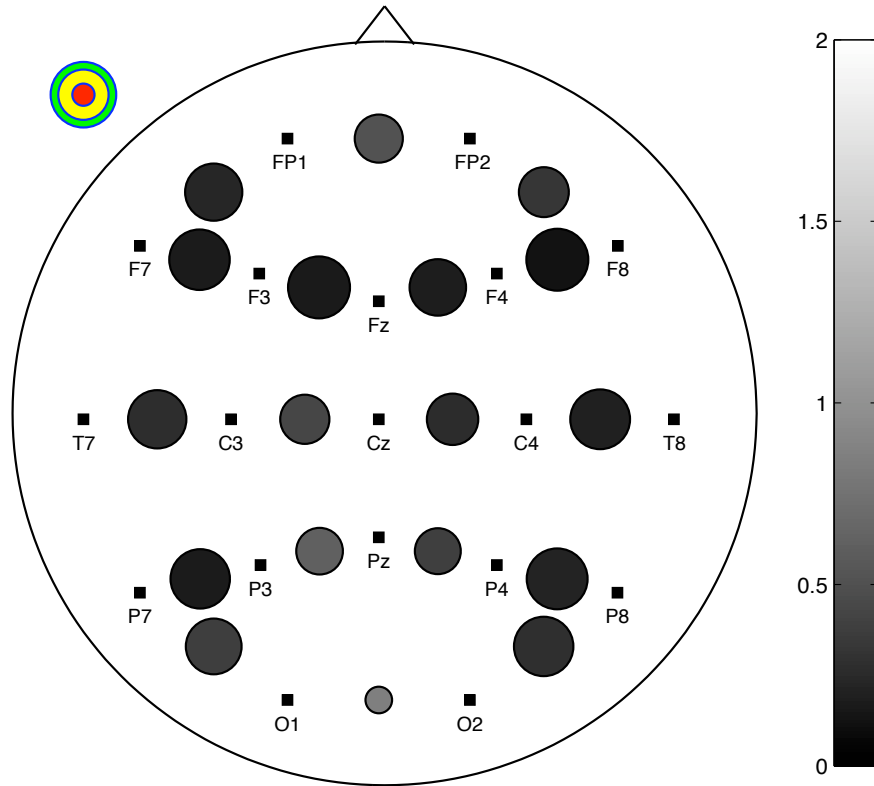


FIGURE 8.6: Visualization of average performance excluding patients with symptomatic epilepsy. For each channel average Sensitivity (SE), False Positive Rate (FPR) is visible.

TABLE 8.7: Average performance excluding patients with symptomatic epilepsy and JME. For each channel average Sensitivity (SE), False Positive Rate (FPR) and their standard deviation σ is reported.

Channel	N_{patients}	N_{seizures}	$SE_{\text{TOT}}(\%)$	σ_{SE}	FPR(FP/h)	σ_{FPR}
F7-FP1	11	72	93.6	15.7	0.31	0.30
FP1-FP2	11	72	86.2	29.3	0.67	0.61
FP2-F8	11	72	88.3	29.9	0.38	0.28
F7-F3	11	72	96.4	8.1	0.24	0.28
F3-FZ	11	72	97.4	6.4	0.20	0.20
FZ-F4	11	72	96.1	12.9	0.17	0.21
F4-F8	11	72	97.4	6.4	0.15	0.17
T7-C3	11	72	96.1	7.2	0.42	0.43
C3-CZ	11	72	95.2	8.3	0.35	0.55
CZ-C4	11	72	94.4	10.0	0.13	0.17
C4-T8	11	72	97.4	6.4	0.24	0.37
P7-P3	11	72	95.5	8.1	0.19	0.30
P3-PZ	11	72	86.1	29.7	0.47	0.61
PZ-P4	11	72	90.1	25.6	0.25	0.55
P4-P8	11	72	96.5	7.7	0.26	0.31
P7-O1	11	72	92.5	10.9	0.37	0.58
O1-O2	11	72	59.4	39.5	0.86	1.29
O2-P8	11	72	96.9	7.1	0.20	0.25

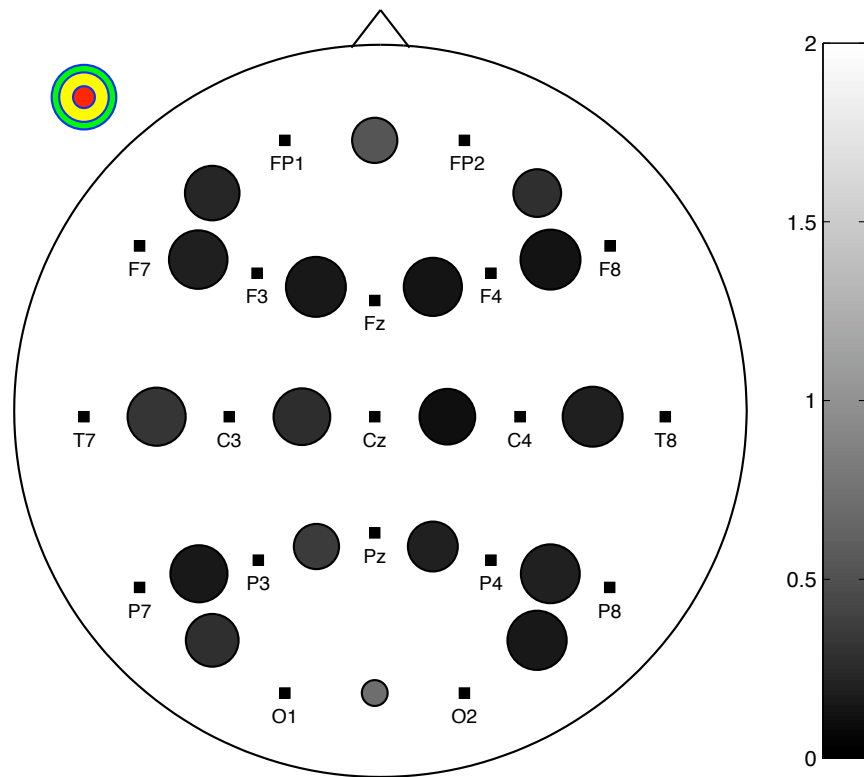


FIGURE 8.7: Visualization of average performance excluding patients with symptomatic epilepsy and JME across all patients. For each channel average Sensitivity (SE), False Positive Rate (FPR) is visible.

From performance segmentation by different type of epilepsy it has emerged that a huge increase in SE, FPR can be achieved by excluding patients with symptomatic epilepsy. From table 8.6 it is clear that the best channel for SE, FDR and standard deviation is F4-F8 ($SE = 97.9 \pm 5.7 \%$ and $FPR = 0.15 \pm 0.17 \text{ FP/h.}$), therefore, considering our data, the best placement of the *Hypo-Safe* device electrode is certainly in this area. Channels C4-T8 and P7-P3 constitutes a valid alternative with similar performance and standard deviation. If CAE patients are considered alone, suggestions for the placement of the electrode remains the same, channel F4-F8 still has the best performance. Analogous consideration cannot be done for JAE or JME patients alone, since only three patients are available for each type of epilepsy. More hours of EEG recording and more patients would be necessary to give a recommendation based on JAE and JME patients alone.

In patients with symptomatic epilepsy is still possible to find an optimal location for the *Hypo-Safe* device electrode, but they must be assessed individually and the location will vary from patient to patient. For example in patient n.8, although many channel with low performance are present, in channel T7-C3 a SE of 100 % with FDR of 0.56 Fp/h was achieved (see table A.15). For patient n.9 a good suggestion with perfect performance would be channel P4-P8 (see table A.16) while channel FZ-F4 is a good location for patient n.20 (see table A.17).

Chapter 9

Conclusion

A patient-specific absence seizure onset detection algorithm has been designed, implemented and tested together with a topographic evaluation of seizure patterns. This analysis permitted to formulate a suggestion on possible locations of the subcutaneously implanted electrode of *Hypo-Safe* device for absence seizures monitoring.

The first step involved a precise state of the art literature study, in which the article in [31] was taken as reference and the algorithm redesigned for absence seizures. A background on type of epilepsies presenting absence seizures and EEG was given as an introduction to the project. It was followed by theoretical and practical explanation of the concept of fractal dimension, which is the main mathematical concept on which the seizure detection algorithm relies upon. A scalp EEG database was appositely created by the author for this thesis and since the main objective is topographic distribution of absence seizures patterns, a transversal EEG montage was employed to preserve topographic information. *Hypo-Safe* device will operate with only one EEG channel through a subcutaneously implanted electrode, so the same constraint had to be respected when designing the algorithm for seizure detection. After describing the core structure of the algorithm, a detailed performance evaluation was finally conducted. Only scalp EEG was considered in this analysis since this is the most similar type of EEG to the one *Hypo-Safe* device is working with.

At first overall performance for each EEG channel across all the patients were evaluated. Although obtaining in most of the channels an average SE higher than 80% and FDR as low as 0.22 FP/h, their standard deviation was really high due to the performance variation of the algorithm across patients with different types of epilepsy. Given this high variability of the results from patient to patient, it was not feasible to formulate a suggestion for the location of the electrode of the *Hypo-Safe* device. SE and FDR were then evaluated for each type of epilepsy with absence seizures. From this segmentation it has emerged that excluding from the analysis patients with symptomatic epilepsy it was possible to achieve a SE of 97% and a FDR of 0.15 with a much lower standard deviation on channel F4-F8. Similar performance could also be achieved in a few neighboring channels. Therefore for patients with CAE, JAE and JME this area represents a very good location for placing the *Hypo-Safe* subcutaneous electrode. In patients with

symptomatic epilepsy it is still possible to find a good location, but they must be assessed individually and the optimal position will change from patient to patient.

At last, it must be noticed that, although it has been formulated a suggestion for the location of the electrode of the *Hypo-Safe* device, before implementation for clinical use more testing is required. For this study EEG recordings, in most cases, shorter than an hour were used to evaluate the algorithm performance. The ideal database for this project would consist of long term EEG recordings of at least one day, where true capabilities of the algorithm in term of SE and FPR could be evaluated.

Bibliography

- [1] W. Blume , H. Lüders, E. Mizrahi, C. Tassinari, W. van Emde Boas, J. Engel, Glossary of descriptive terminology for ictal semiology: report of the ILAE task force on classification and terminology, *Epilepsia*, 42(9):1212-1218, 2001.
- [2] G.D. Cascino, Epilepsy: contemporary perspectives on evaluation and treatment, *Mayo Clinic Proc*, 69:1199-1211, 1994.
- [3] F.A. Gibbs, H. Davis, W.G. Lennox, The EEG in epilepsy and in conditions of impaired consciousness, *Arch Neurol Psychiat*, 34:1134-1148, 1935.
- [4] W.A. Hauser, J.F. Annegers, L.T. Kurland, Prevalence of epilepsy in Rochester, Minnesota, *Epilepsia*, 32:429-45, 1991.
- [5] R.S. Fisher, W. van Emde Boas, W. Blume, C. Elger, P. Genton, P. Lee and J. Engel, Epileptic Seizures and Epilepsy: Definitions Proposed by the International League Against Epilepsy (ILAE) and the International Bureau for Epilepsy (IBE) , *Epilepsia*, 46(4):470-472, 2005
- [6] Proposal for revised clinical and electroencephalographic classification of epileptic seizures. From the Commission on Classification and Terminology of the International League Against Epilepsy, *Epilepsia*, 22(4):489-501, 1981
- [7] J. Engel, Report of the ILAE classification core group, *Epilepsia*, 47(9):1558-1668, 2006.
- [8] O. Temkin, The Falling Sickness, *Johns Hopkins Press*, Baltimore, MD, page 250, 1971.
- [9] J. Engel, T.A. Pedley, Epilepsy: a comprehensive textbook, *Lippincott, William and Wilkins*, 2397–2411, 2007.
- [10] J. Roger, M. Bureau, et al, Epileptic syndromes in infancy, childhood and adolescence, *John Libbey*, 2nd ed. London, England, 1985.
- [11] E. Wyllie, A. Gupta, D.K. Lachhwani, The Treatment of Epilepsy. Principles and Practice. *Lippincott, Williams and Wilkins*, 4th ed. Philadelphia, 305-315, 2006.
- [12] A.T. Berg, S.F. Berkovic, M.J. Brodie, J. Buchhalter, J.H. Cross, W. van Emde Boas, Revised terminology and concepts for organization of seizures and epilepsies: Report of the ILAE Commission on Classification and Terminology, *Epilepsia*, 51(4):676-685, February 26th 2010.

- [13] T.R. Browne, J.K. Penry, R.J. Proter, F.E. Dreifuss, Responsiveness before, during, and after spike-wave paroxysms, *Neurology*, 24(7):659-665, July 1974.
- [14] J.K. Penry, R.J. Porter, R.E. Dreifuss, Simultaneous recording of absence seizures with video tape and electroencephalography. A study of 374 seizures in 48 patients, *Brain*, 98(3):427-440, September 1975.
- [15] P.L. Nunez, Electric Fields of the Brain: The Neurophysics of EEG, *Oxford University Press*, New York, page 484, 1981.
- [16] E. Niedermeyer, F. Lopes da Silva, Electroencephalography: Basic Principles, Clinical Applications, and Related Fields, *Lippincot Williams and Wilkins*, page 140, 2004.
- [17] T.J. Nowak and A.G. Handford, Pathophysiology: Concepts and Applications for Health Care Professionals, *McGraw-Hill Higher Education*, Boston, 3rd edition, 2004.
- [18] D. Zumsteg, H.G. Wieser, Presurgical Evaluation: Current Role of Invasive EEG, *Epilepsia*, 41(3):S55-S58, 2000.
- [19] V.L. Towle, J. Bolaños, D. Suarez, K. Tan, R. Grzeszczuk, D.N. Levin, R. Cakmur, S.A. Frank, J.P. Spire, The spatial location of EEG electrodes: locating the best-fitting sphere relative to cortical anatomy, *Neurophysiol*, 86(1):1-6, 1993.
- [20] H. Aurlen, I.O. Gjerde, J.H. Aarseth, B. Karlsen, H. Skeidsvoll, N.E. Gilhus EEG background activity described by a large computerized database, *Clinical Neurophysiology*, 115(3):665-673, March 2004.
- [21] P.L. Nunez, K.L. Pilgreen, The spline-Laplacian in clinical neurophysiology: a method to improve EEG spatial resolution, *Clinical Neurophysiology*, 8(4):397-413, 1991.
- [22] R. Cooper, J.W. Osselton, J.C. Shaw, EEG Technology, *Butterworths*, 2nd ed., London, page 275, 1969.
- [23] Blumhardt LD, Barrett G, Halliday AM, Kriss A The asymmetrical visual evoked potential to pattern reversal in one half field and its significance for the analysis of visual field effects, *Br. J. Ophthalmol*, 61:454:461, 1977.
- [24] F. Sharbrough, G.E. Chatrian, R.P. Lesser, H. Lüders, M. Nuwer, T.M. Picton, American Electroencephalographic Society Guidelines for Standard Electrode Position Nomenclature, *J. Clin. Neurophysiol*, 8:200-202, 1991.
- [25] J. Malmivuo, R. Plonsey, Bioelectromagnetism - Principles and Applications of Bioelectric and Biomagnetic Fields, *Oxford University Press*, New York, chapter 13, 1995.
- [26] R.M. Rangayyan Biomedical Signal Analysis - A Case-Study Approach, *John Wiley and Sons, Inc*, pages 28-30, 2002.

- [27] T. Jung, S. Makeig, C. Humphries, T. Lee, M.J. McKeown, V.I.T.J. Sejnowski Removing electroencephalographic artifacts by blind source separation, *Psychophysiology*, 37(2):163-289, 19 March 2003.
- [28] H. Qu, J. Gotman. A patient-specific algorithm for the detection of seizure onset in long-term EEG monitoring: possible use as a warning device, *IEEE Transactions on Biomedical Engineering*, 44(2):115-122, 1997.
- [29] A. Shoeb, H. Edwards, J. Connolly, B. Bourgeois, S. Ted Treves, and J. Guttag, Patient-specific seizure onset detection, *Epilepsy and Behavior*, 5(4):483-498, 2004.
- [30] M.E. Saab, J. Gotman, A system to detect the onset of epileptic seizures in scalp EEG, *Clinical Neurophysiology*, 116:427-442, 2005.
- [31] G.E. Polchronaki, P. Ktonas, S. Gatzonis, A. Siatouni, H. Tsekou, D. Sakas. K.S. Nikita, A system to detect the onset of epileptic seizures in scalp EEG, *IEEE transaction*, July 5th, 2008.
- [32] L. Kuhlmann, A.N. Burkitt, M.J. Cook, K. Fuller, D.B. Grayden, L. Seiderer, I.M.Y. Mareels, Seizure Detection Using Seizure Probability Estimation: Comparison of Features Used to Detect Seizures, *Annals of Biomedical Engineering*, 37(10):2129- 2145, 10th July 2009.
- [33] A.R. Pears, Dimension Theory of General Spaces, *Cambridge University Press*, 1975.
- [34] B.B. Mandelbrot, The Fractal Geometry of Nature, *W.H. Freeman and Company*, 1982.
- [35] M.M. Dodson, S. Kristensen, Hausdorff Dimension and Diophantine Approximation, *Proceeding of Symposia in Pure Mathematics*, pages 1-6, 12th June 2003.
- [36] B.S. Raghavendra, D.N. Dutt, A note on fractal dimensions of biomedical waveforms, *Computers in Biology and Medicine*, 39:1006-1012, 2009.
- [37] R. Esteller, G. Vachtsevanos, J. Echauz, B. Litt, A comparison of waveform fractal dimension algorithms, *IEEE Trans. Biomed. Eng.*, 48(2):177-183. 2001.
- [38] J. Feder, A comparison of waveform fractal dimension algorithms, *Plenum Press*, New York, 1988.
- [39] B. Dubuc, S. Dubuc, Error bounds on the estimation of fractal dimension, *J. Numer. Anal*, 33(2):602-626, 1996.
- [40] P. Flandrin, Wavelet analysis and synthesis of fractional Brownian motion, *IEEE Trans. Info. Theor.*, 38(2):910-917, 1992.
- [41] M.J. Katz, Fractals and analysis of waveforms, *Comput. Bid. Med.*, 18(3):145-156, 1988.
- [42] T. Higuchi, Approach to an irregular time series on the basis of the fractal theory, *Physica D.*, 31(2):277-283, 1988.

- [43] R. Esteller, J. Echauz, T. Tcheng, B. Litt, B. Pless, Line Length: An efficient feature for seizure onset detection, *Proceeding of the 23rd Annual EMBS International Conference*, Istanbul, Turkey, 1707-1710, 2001.

Appendix A

Algorithm Results across all the Patients

In this Appendix results of the seizure detection algorithm are presented. For each patient a performance table with numeric results is given, together with a visual representation of the same results (see figure A.0 for an explanation of the visualization method).

Patients are ordered by type of epilepsy:

- Childhood Absence Epilepsy (CAE)
- Juvenile Absence Epilepsy (JAE)
- Juvenile Myoclonic Epilepsy (JME)
- Symptomatic Epilepsy with Absence Seizures

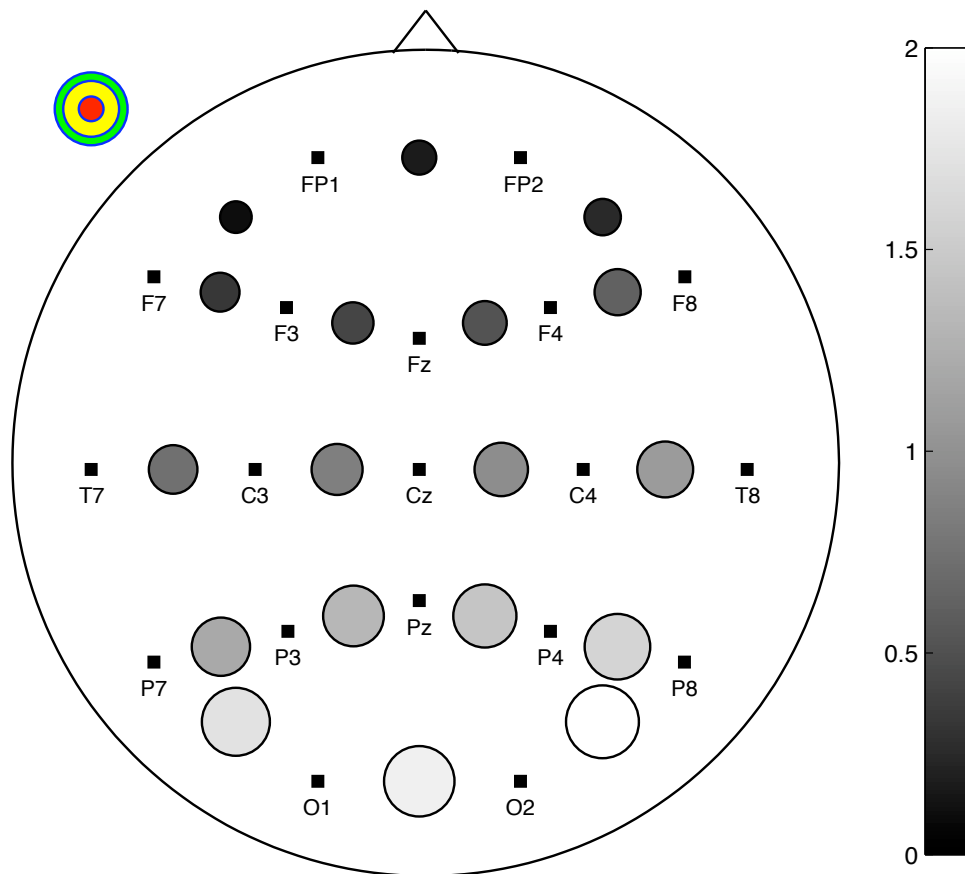


FIGURE A.0: Illustration of the the visualization method used. Positions of the circles represents the EEG channel, e.g, a circle between FP7 and FP1 indicate channel FP7-FP1. Color of the circles are related to corresponding FPR, according to the colorbar on the right. FPR greater than 2 FP/h are merged in one color (white). Size of the circles are exponentially proportional to SE. On the top left a sample circle is visualized: red zone indicate a SE lower than 50 %, yellow zone a SE between 50 % and 90 %, green zone a SE greater than 90 %. Data used in this figure are just for illustration purposes.

Patients with Childhood Absence Epilepsy (CAE)

TABLE A.1: Performance of the seizure detection algorithm on patient n. 13.

Channel	n. Seizures			Overall Performance		$SE_{L<10}(\%)$	$SE_{L>10}(\%)$
	N_{TOT}	$N_{L<10}$	$N_{L>10}$	$SE_{TOT}(\%)$	FPR(FP/h)		
F7-FP1	7	7	0	100.0	0.00	100.0	n.a.
FP1-FP2	7	7	0	85.7	0.00	85.7	n.a.
FP2-F8	7	7	0	100.0	0.00	100.0	n.a.
F7-F3	7	7	0	100.0	0.00	100.0	n.a.
F3-FZ	7	7	0	100.0	0.00	100.0	n.a.
FZ-F4	7	7	0	100.0	0.00	100.0	n.a.
F4-F8	7	7	0	100.0	0.00	100.0	n.a.
T7-C3	7	7	0	100.0	0.00	100.0	n.a.
C3-CZ	7	7	0	100.0	0.00	100.0	n.a.
CZ-C4	7	7	0	100.0	0.00	100.0	n.a.
C4-T8	7	7	0	100.0	0.00	100.0	n.a.
P7-P3	7	7	0	100.0	0.00	100.0	n.a.
P3-PZ	7	7	0	85.7	0.29	85.7	n.a.
PZ-P4	7	7	0	100.0	0.00	100.0	n.a.
P4-P8	7	7	0	100.0	0.00	100.0	n.a.
P7-O1	7	7	0	100.0	0.00	100.0	n.a.
O1-O2	7	7	0	85.7	0.00	85.7	n.a.
O2-P8	7	7	0	100.0	0.00	100.0	n.a.

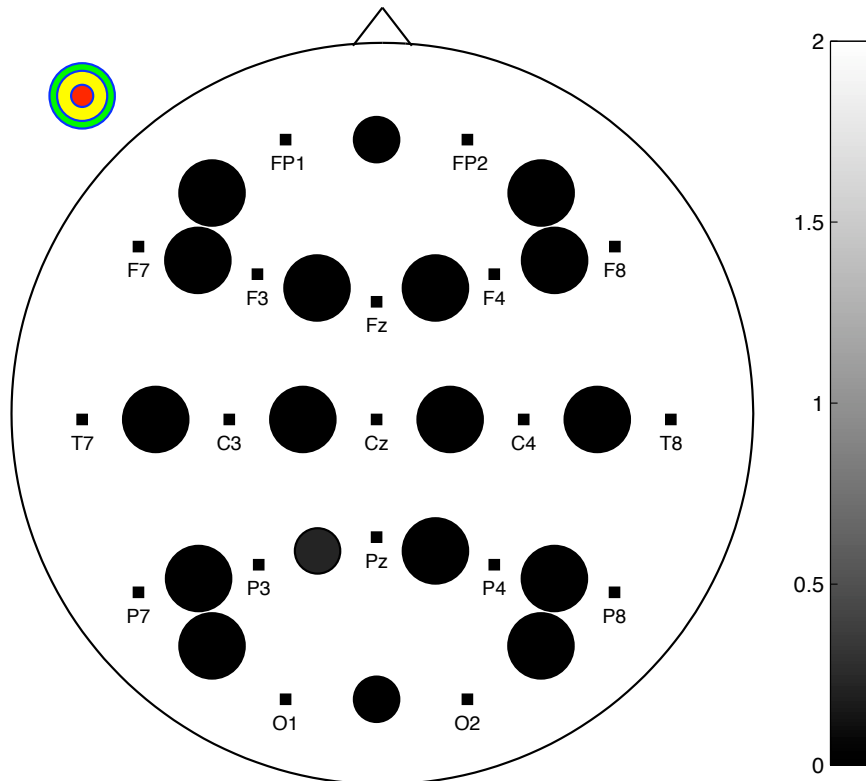


FIGURE A.1: Performance on patient n. 13

TABLE A.2: Performance of the seizure detection algorithm on patient n. 16.

Channel	n. Seizures			Overall Performance			
	N_{TOT}	$N_{L<10}$	$N_{L>10}$	$SE_{TOT}(\%)$	FPR(FP/h)	$SE_{L<10}(\%)$	$SE_{L>10}(\%)$
F7-FP1	7	7	0	100.0	0.82	100.0	n.a.
FP1-FP2	7	7	0	85.7	0.63	85.7	n.a.
FP2-F8	7	7	0	100.0	0.41	100.0	n.a.
F7-F3	7	7	0	100.0	0.21	100.0	n.a.
F3-FZ	7	7	0	100.0	0.21	100.0	n.a.
FZ-F4	7	7	0	57.1	0.62	57.1	n.a.
F4-F8	7	7	0	100.0	0.41	100.0	n.a.
T7-C3	7	7	0	85.7	0.41	85.7	n.a.
C3-CZ	7	7	0	100.0	0.41	100.0	n.a.
CZ-C4	7	7	0	85.7	0.21	85.7	n.a.
C4-T8	7	7	0	100.0	0.21	100.0	n.a.
P7-P3	7	7	0	100.0	0.82	100.0	n.a.
P3-PZ	7	7	0	0.0	1.85	0.0	n.a.
PZ-P4	7	7	0	14.2	1.85	14.2	n.a.
P4-P8	7	7	0	100.0	0.21	100.0	n.a.
P7-O1	7	7	0	71.4	1.85	71.4	n.a.
O1-O2	7	7	0	14.2	0.62	14.2	n.a.
O2-P8	7	7	0	85.7	0.62	85.7	n.a.

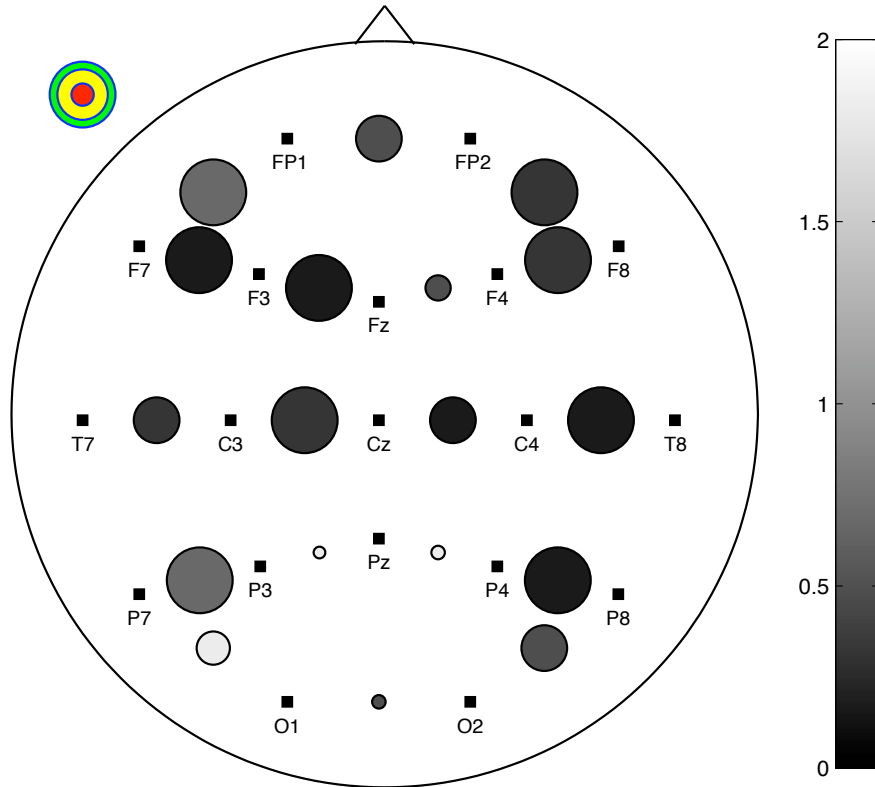


FIGURE A.2: Performance on patient n. 16

TABLE A.3: Performance of the seizure detection algorithm on patient n. 17.

Channel	n. Seizures			Overall Performance		SE _{L<10} (%)	SE _{L>10} (%)
	N _{TOT}	N _{L<10}	N _{L>10}	SE _{TOT} (%)	FPR(FP/h)		
F7-FP1	7	0	7	100.0	0.00	n.a.	100.0
FP1-FP2	7	0	7	85.7	0.00	n.a.	85.7
FP2-F8	7	0	7	100.0	0.32	n.a.	100.0
F7-F3	7	0	7	100.0	0.00	n.a.	100.0
F3-FZ	7	0	7	100.0	0.00	n.a.	100.0
FZ-F4	7	0	7	100.0	0.00	n.a.	100.0
F4-F8	7	0	7	100.0	0.32	n.a.	100.0
T7-C3	7	0	7	100.0	0.00	n.a.	100.0
C3-CZ	7	0	7	85.7	0.32	n.a.	85.7
CZ-C4	7	0	7	100.0	0.32	n.a.	100.0
C4-T8	7	0	7	100.0	0.00	n.a.	100.0
P7-P3	7	0	7	100.0	0.00	n.a.	100.0
P3-PZ	7	0	7	100.0	0.00	n.a.	100.0
PZ-P4	7	0	7	85.7	0.00	n.a.	85.7
P4-P8	7	0	7	100.0	0.00	n.a.	100.0
P7-O1	7	0	7	85.7	0.65	n.a.	85.7
O1-O2	7	0	7	42.8	4.19	n.a.	42.8
O2-P8	7	0	7	100.0	0.00	n.a.	100.0

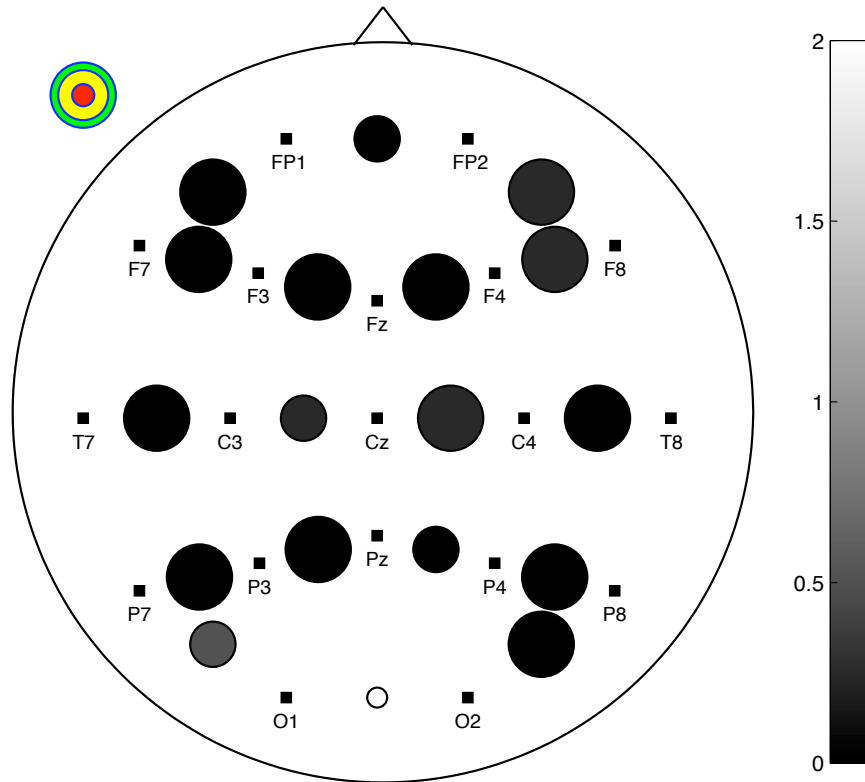


FIGURE A.3: Performance on patient n. 17

TABLE A.4: Performance of the seizure detection algorithm on patient n. 18.

Channel	n. Seizures			Overall Performance		$SE_{L<10}(\%)$	$SE_{L>10}(\%)$
	N_{TOT}	$N_{L<10}$	$N_{L>10}$	$SE_{TOT}(\%)$	FPR(FP/h)		
F7-FP1	6	0	6	100.0	0.00	n.a.	100.0
FP1-FP2	6	0	6	100.0	0.00	n.a.	100.0
FP2-F8	6	0	6	100.0	0.00	n.a.	100.0
F7-F3	6	0	6	100.0	0.00	n.a.	100.0
F3-FZ	6	0	6	100.0	0.00	n.a.	100.0
FZ-F4	6	0	6	100.0	0.00	n.a.	100.0
F4-F8	6	0	6	100.0	0.00	n.a.	100.0
T7-C3	6	0	6	100.0	0.00	n.a.	100.0
C3-CZ	6	0	6	100.0	0.00	n.a.	100.0
CZ-C4	6	0	6	100.0	0.00	n.a.	100.0
C4-T8	6	0	6	100.0	0.00	n.a.	100.0
P7-P3	6	0	6	100.0	0.00	n.a.	100.0
P3-PZ	6	0	6	100.0	0.00	n.a.	100.0
PZ-P4	6	0	6	100.0	0.00	n.a.	100.0
P4-P8	6	0	6	100.0	0.00	n.a.	100.0
P7-O1	6	0	6	100.0	0.00	n.a.	100.0
O1-O2	6	0	6	100.0	0.00	n.a.	100.0
O2-P8	6	0	6	100.0	0.00	n.a.	100.0

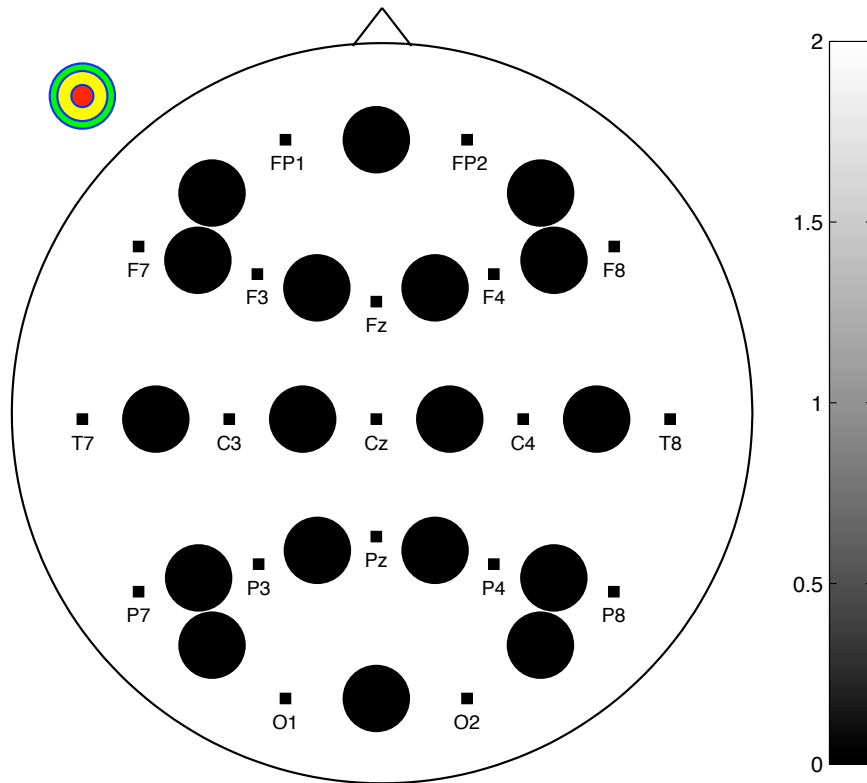


FIGURE A.4: Performance on patient n. 18

TABLE A.5: Performance of the seizure detection algorithm on patient n. 19.

Channel	n. Seizures			Overall Performance		SE _{L<10} (%)	SE _{L>10} (%)
	N _{TOT}	N _{L<10}	N _{L>10}	SE _{TOT} (%)	FPR(FP/h)		
F7-FP1	5	0	5	80.0	0.35	n.a.	80.0
FP1-FP2	5	0	5	100.0	1.06	n.a.	100.0
FP2-F8	5	0	5	100.0	0.35	n.a.	100.0
F7-F3	5	0	5	80.0	0.35	n.a.	80.0
F3-FZ	5	0	5	100.0	0.35	n.a.	100.0
FZ-F4	5	0	5	100.0	0.35	n.a.	100.0
F4-F8	5	0	5	100.0	0.00	n.a.	100.0
T7-C3	5	0	5	100.0	1.06	n.a.	100.0
C3-CZ	5	0	5	80.0	0.00	n.a.	80.0
CZ-C4	5	0	5	100.0	0.00	n.a.	100.0
C4-T8	5	0	5	100.0	0.35	n.a.	100.0
P7-P3	5	0	5	80.0	0.00	n.a.	80.0
P3-PZ	5	0	5	100.0	0.35	n.a.	100.0
PZ-P4	5	0	5	100.0	0.35	n.a.	100.0
P4-P8	5	0	5	100.0	0.00	n.a.	100.0
P7-O1	5	0	5	80.0	0.00	n.a.	80.0
O1-O2	5	0	5	0.0	0.00	0.0	
O2-P8	5	0	5	100.0	0.00	n.a.	100.0

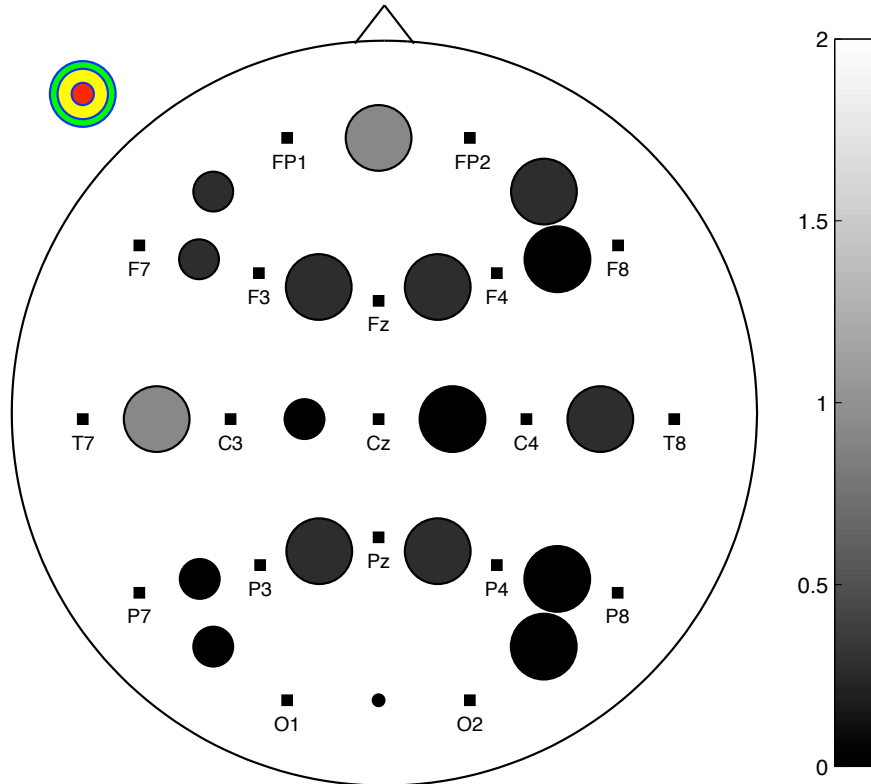


FIGURE A.5: Performance on patient n. 19

TABLE A.6: Performance of the seizure detection algorithm on patient n. 23.

Channel	n. Seizures			Overall Performance		$SE_{L<10}(\%)$	$SE_{L>10}(\%)$
	N_{TOT}	$N_{L<10}$	$N_{L>10}$	$SE_{TOT}(\%)$	FPR(FP/h)		
F7-FP1	6	0	6	100.0	0.62	100.0	n.a.
FP1-FP2	6	0	6	100.0	0.62	100.0	n.a.
FP2-F8	6	0	6	100.0	0.62	100.0	n.a.
F7-F3	6	0	6	100.0	0.92	100.0	n.a.
F3-FZ	6	0	6	100.0	0.62	100.0	n.a.
FZ-F4	6	0	6	100.0	0.31	100.0	n.a.
F4-F8	6	0	6	100.0	0.31	100.0	n.a.
T7-C3	6	0	6	100.0	1.23	100.0	n.a.
C3-CZ	6	0	6	100.0	1.85	100.0	n.a.
CZ-C4	6	0	6	100.0	0.00	100.0	n.a.
C4-T8	6	0	6	100.0	1.23	100.0	n.a.
P7-P3	6	0	6	100.0	0.62	100.0	n.a.
P3-PZ	6	0	6	100.0	1.23	100.0	n.a.
PZ-P4	6	0	6	100.0	0.00	100.0	n.a.
P4-P8	6	0	6	100.0	0.92	100.0	n.a.
P7-O1	6	0	6	100.0	0.92	100.0	n.a.
O1-O2	6	0	6	66.6	0.92	66.6	n.a.
O2-P8	6	0	6	100.0	0.00	100.0	n.a.

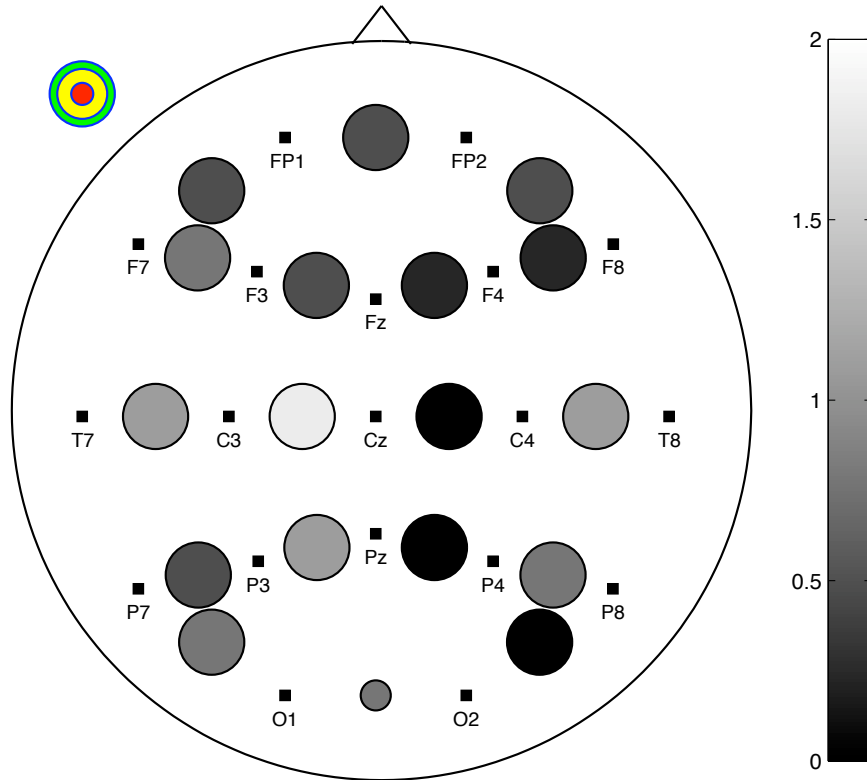


FIGURE A.6: Performance on patient n. 23

TABLE A.7: Performance of the seizure detection algorithm on patient n. 25.

Channel	n. Seizures			Overall Performance		SE _{L<10} (%)	SE _{L>10} (%)
	N _{TOT}	N _{L<10}	N _{L>10}	SE _{TOT} (%)	FPR(FP/h)		
F7-FP1	8	0	8	50.0	0.00	n.a.	50.0
FP1-FP2	8	0	8	0.0	0.00	n.a.	0.0
FP2-F8	8	0	8	0.0	0.00	n.a.	0.0
F7-F3	8	0	8	100.0	0.00	n.a.	100.0
F3-FZ	8	0	8	100.0	0.00	n.a.	100.0
FZ-F4	8	0	8	100.0	0.00	n.a.	100.0
F4-F8	8	0	8	100.0	0.00	n.a.	100.0
T7-C3	8	0	8	100.0	0.10	n.a.	100.0
C3-CZ	8	0	8	100.0	0.00	n.a.	100.0
CZ-C4	8	0	8	100.0	0.00	n.a.	100.0
C4-T8	8	0	8	100.0	0.00	n.a.	100.0
P7-P3	8	0	8	100.0	0.00	n.a.	100.0
P3-PZ	8	0	8	100.0	0.00	n.a.	100.0
PZ-P4	8	0	8	100.0	0.00	n.a.	100.0
P4-P8	8	0	8	100.0	0.00	n.a.	100.0
P7-O1	8	0	8	100.0	0.00	n.a.	100.0
O1-O2	8	0	8	0.0	0.00	n.a.	0.0
O2-P8	8	0	8	100.0	0.00	n.a.	100.0

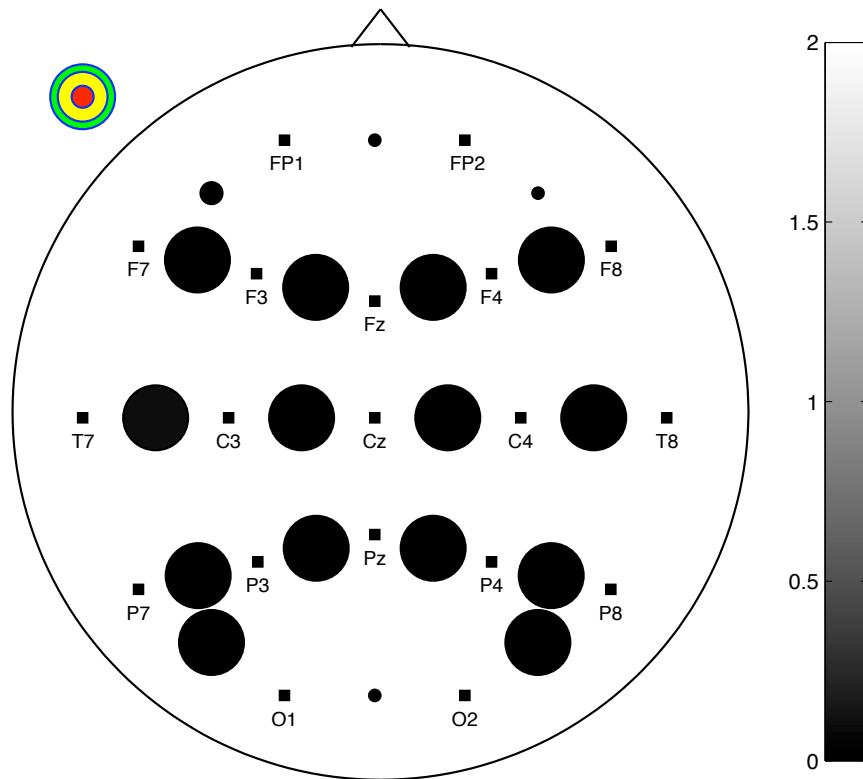


FIGURE A.7: Performance on patient n. 25

TABLE A.8: Performance of the seizure detection algorithm on patient n. 42.

Channel	n. Seizures			Overall Performance		$SE_{L<10}(\%)$	$SE_{L>10}(\%)$
	N_{TOT}	$N_{L<10}$	$N_{L>10}$	$SE_{TOT}(\%)$	FPR(FP/h)		
F7-FP1	11	0	11	100.0	0.31	100.0	n.a.
FP1-FP2	11	0	11	90.9	1.09	90.9	n.a.
FP2-F8	11	0	11	90.9	0.47	90.9	n.a.
F7-F3	11	0	11	100.0	0.31	100.0	n.a.
F3-FZ	11	0	11	90.9	0.16	90.9	n.a.
FZ-F4	11	0	11	100.0	0.16	100.0	n.a.
F4-F8	11	0	11	90.9	0.16	90.9	n.a.
T7-C3	11	0	11	90.9	0.47	90.9	n.a.
C3-CZ	11	0	11	81.8	0.78	81.8	n.a.
CZ-C4	11	0	11	72.7	0.47	72.7	n.a.
C4-T8	11	0	11	90.9	0.47	90.9	n.a.
P7-P3	11	0	11	90.9	0.47	90.9	n.a.
P3-PZ	11	0	11	81.8	0.93	81.8	n.a.
PZ-P4	11	0	11	90.9	0.00	90.9	n.a.
P4-P8	11	0	11	81.8	0.62	81.8	n.a.
P7-O1	11	0	11	100.0	0.16	100.0	n.a.
O1-O2	11	0	11	100.0	0.47	100.0	n.a.
O2-P8	11	0	11	100.0	0.47	100.0	n.a.

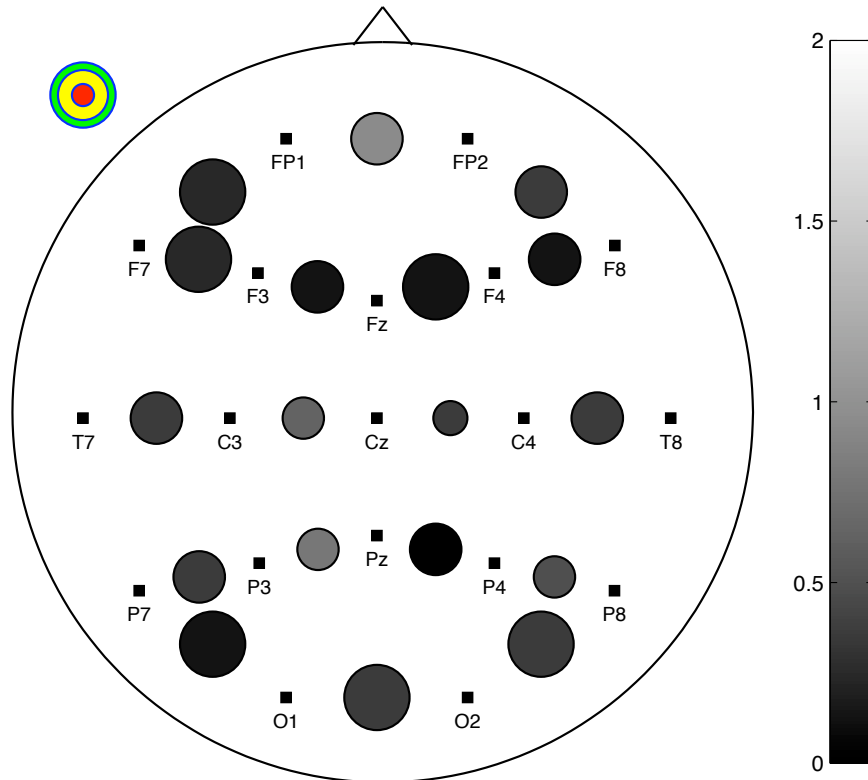


FIGURE A.8: Performance on patient n. 42

Patients with Juvenile Absence Epilepsy (JAE)

TABLE A.9: Performance of the seizure detection algorithm on patient n. 11.

Channel	n. Seizures			Overall Performance		SE _{L<10} (%)	SE _{L>10} (%)
	N _{TOT}	N _{L<10}	N _{L>10}	SE _{TOT} (%)	FPR(FP/h)		
F7-FP1	7	0	7	100.0	0.34	n.a.	100.0
FP1-FP2	7	0	7	100.0	0.34	n.a.	100.0
FP2-F8	7	0	7	100.0	0.00	n.a.	100.0
F7-F3	7	0	7	100.0	0.34	n.a.	100.0
F3-FZ	7	0	7	100.0	0.34	n.a.	100.0
FZ-F4	7	0	7	83.3	0.34	n.a.	83.3
F4-F8	7	0	7	100.0	0.34	n.a.	100.0
T7-C3	7	0	7	100.0	0.34	n.a.	100.0
C3-CZ	7	0	7	100.0	0.00	n.a.	100.0
CZ-C4	7	0	7	100.0	0.00	n.a.	100.0
C4-T8	7	0	7	100.0	0.00	n.a.	100.0
P7-P3	7	0	7	100.0	0.00	n.a.	100.0
P3-PZ	7	0	7	100.0	0.00	n.a.	100.0
PZ-P4	7	0	7	100.0	0.00	n.a.	100.0
P4-P8	7	0	7	100.0	0.00	n.a.	100.0
P7-O1	7	0	7	100.0	0.00	n.a.	100.0
O1-O2	7	0	7	100.0	0.00	n.a.	100.0
O2-P8	7	0	7	100.0	0.00	n.a.	100.0

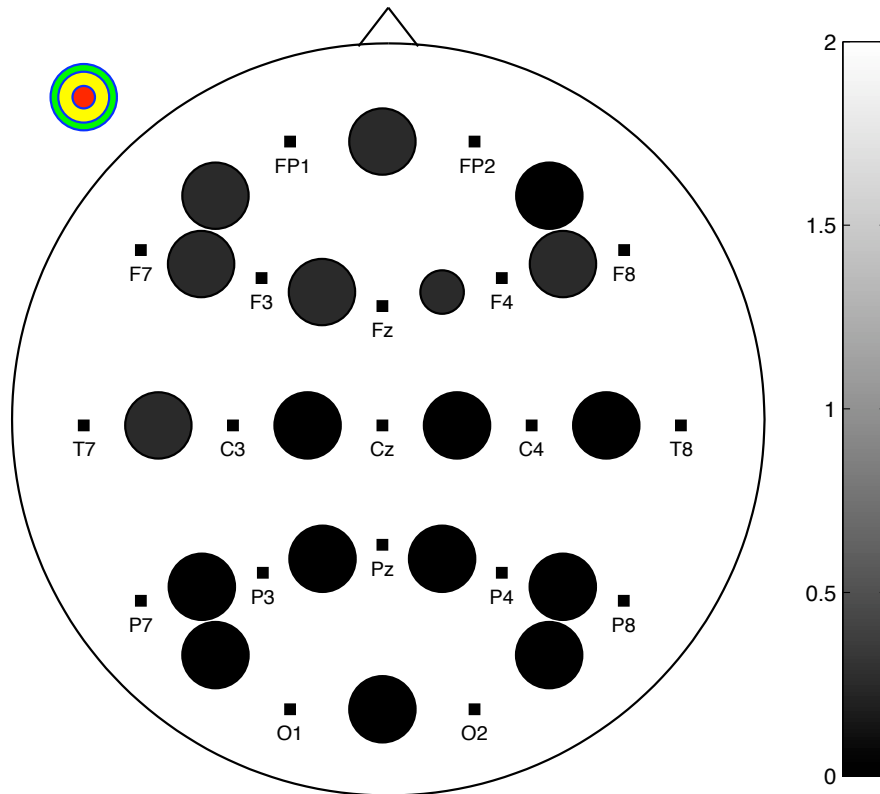


FIGURE A.9: Performance on patient n. 11

TABLE A.10: Performance of the seizure detection algorithm on patient n. 14.

Channel	n. Seizures			Overall Performance		$SE_{L<10}(\%)$	$SE_{L>10}(\%)$
	N_{TOT}	$N_{L<10}$	$N_{L>10}$	$SE_{TOT}(\%)$	FPR(FP/h)		
F7-FP1	5	0	5	100.0	0.39	n.a.	100.0
FP1-FP2	5	0	5	100.0	1.54	n.a.	100.0
FP2-F8	5	0	5	80.0	0.77	n.a.	80.0
F7-F3	5	0	5	100.0	0.39	n.a.	100.0
F3-FZ	5	0	5	100.0	0.39	n.a.	100.0
FZ-F4	5	0	5	100.0	0.00	n.a.	100.0
F4-F8	5	0	5	80.0	0.39	n.a.	80.0
T7-C3	5	0	5	100.0	0.77	n.a.	100.0
C3-CZ	5	0	5	100.0	0.00	n.a.	100.0
CZ-C4	5	0	5	100.0	0.00	n.a.	100.0
C4-T8	5	0	5	100.0	0.00	n.a.	100.0
P7-P3	5	0	5	100.0	0.00	n.a.	100.0
P3-PZ	5	0	5	100.0	0.00	n.a.	100.0
PZ-P4	5	0	5	100.0	0.00	n.a.	100.0
P4-P8	5	0	5	80.0	0.39	n.a.	80.0
P7-O1	5	0	5	100.0	0.00	n.a.	100.0
O1-O2	5	0	5	60.0	2.31	n.a.	60.0
O2-P8	5	0	5	100.0	0.39	n.a.	100.0

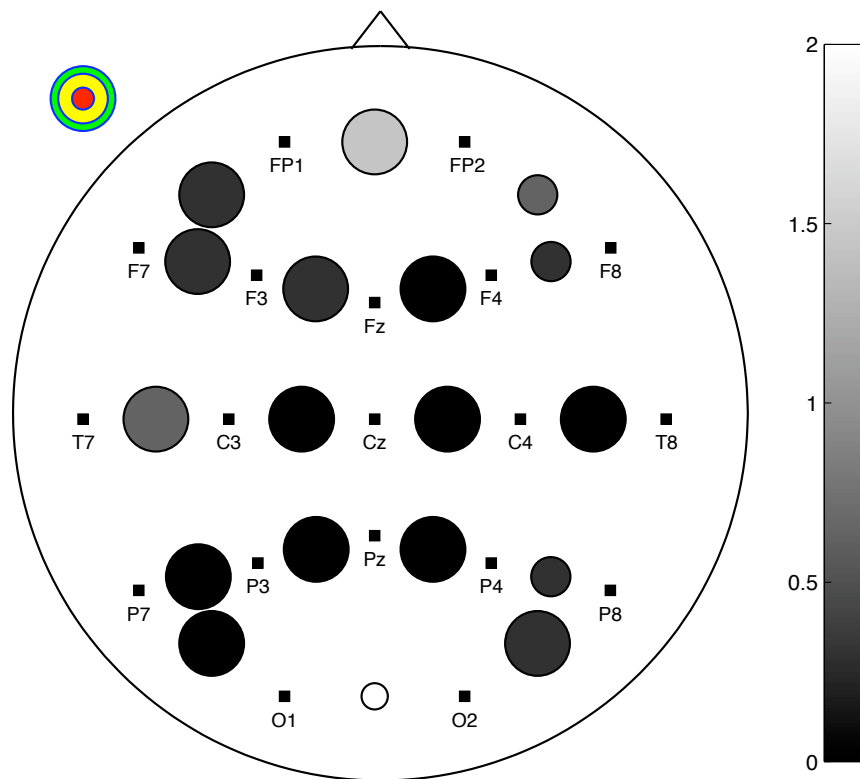


FIGURE A.10: Performance on patient n. 14

TABLE A.11: Performance of the seizure detection algorithm on patient n. 51.

Channel	n. Seizures			Overall Performance		SE _{L<10} (%)	SE _{L>10} (%)
	N _{TOT}	N _{L<10}	N _{L>10}	SE _{TOT} (%)	FPR(FP/h)		
F7-FP1	5	0	5	100.0	0.24	n.a.	100.0
FP1-FP2	5	0	5	100.0	0.10	n.a.	100.0
FP2-F8	5	0	5	100.0	0.00	n.a.	100.0
F7-F3	5	0	5	80.0	0.14	n.a.	80.0
F3-FZ	5	0	5	80.0	0.14	n.a.	80.0
FZ-F4	5	0	5	100.0	0.10	n.a.	100.0
F4-F8	5	0	5	100.0	0.10	n.a.	100.0
T7-C3	5	0	5	80.0	0.19	n.a.	80.0
C3-CZ	5	0	5	100.0	0.19	n.a.	100.0
CZ-C4	5	0	5	80.0	0.10	n.a.	80.0
C4-T8	5	0	5	80.0	0.10	n.a.	80.0
P7-P3	5	0	5	80.0	0.24	n.a.	80.0
P3-PZ	5	0	5	80.0	0.14	n.a.	80.0
PZ-P4	5	0	5	100.0	0.24	n.a.	100.0
P4-P8	5	0	5	100.0	0.33	n.a.	100.0
P7-O1	5	0	5	80.0	0.19	n.a.	80.0
O1-O2	5	0	5	100.0	0.10	n.a.	100.0
O2-P8	5	0	5	80.0	0.14	n.a.	80.0

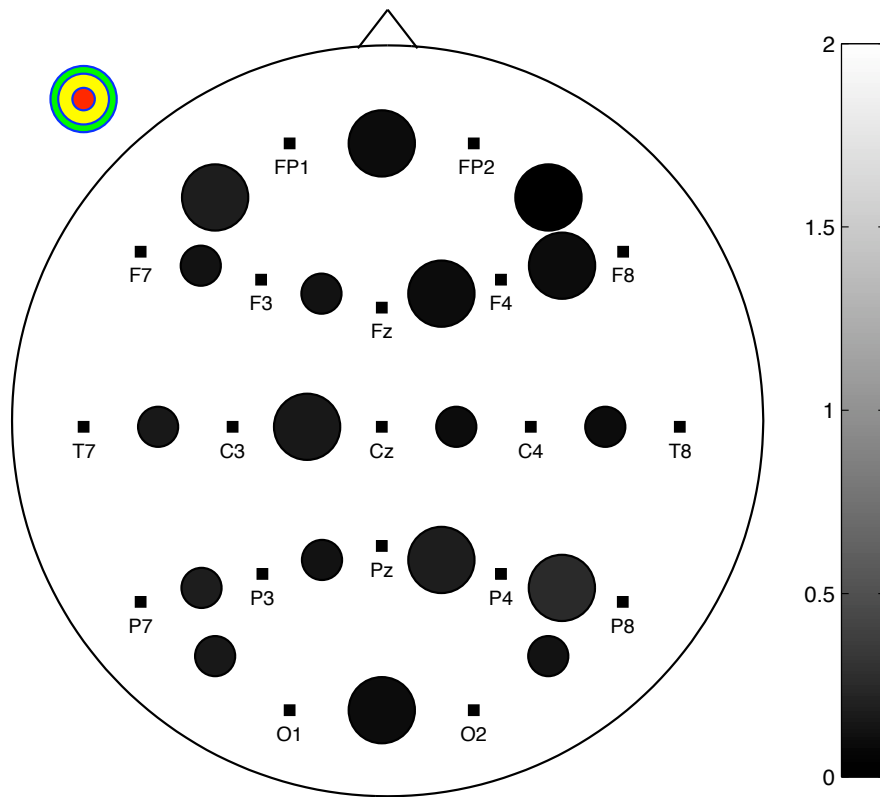


FIGURE A.11: Performance on patient n. 51

Patients with Juvenile Myoclonic Epilepsy (JME)

TABLE A.12: Performance of the seizure detection algorithm on patient n. 36.

Channel	n. Seizures			Overall Performance		$SE_{L<10}(\%)$	$SE_{L>10}(\%)$
	N_{TOT}	$N_{L<10}$	$N_{L>10}$	$SE_{TOT}(\%)$	FPR(FP/h)		
F7-FP1	4	0	4	100.0	0.00	100.0	n.a.
FP1-FP2	4	0	4	100.0	0.00	100.0	n.a.
FP2-F8	4	0	4	100.0	0.49	100.0	n.a.
F7-F3	4	0	4	100.0	0.00	100.0	n.a.
F3-FZ	4	0	4	100.0	0.49	100.0	n.a.
FZ-F4	4	0	4	100.0	0.00	100.0	n.a.
F4-F8	4	0	4	100.0	0.00	100.0	n.a.
T7-C3	4	0	4	100.0	0.00	100.0	n.a.
C3-CZ	4	0	4	100.0	0.00	100.0	n.a.
CZ-C4	4	0	4	100.0	0.00	100.0	n.a.
C4-T8	4	0	4	100.0	0.49	100.0	n.a.
P7-P3	4	0	4	100.0	0.00	100.0	n.a.
P3-PZ	4	0	4	100.0	0.49	100.0	n.a.
PZ-P4	4	0	4	100.0	0.49	100.0	n.a.
P4-P8	4	0	4	100.0	0.49	100.0	n.a.
P7-O1	4	0	4	100.0	0.49	100.0	n.a.
O1-O2	4	0	4	100.0	0.98	100.0	n.a.
O2-P8	4	0	4	100.0	0.98	100.0	n.a.

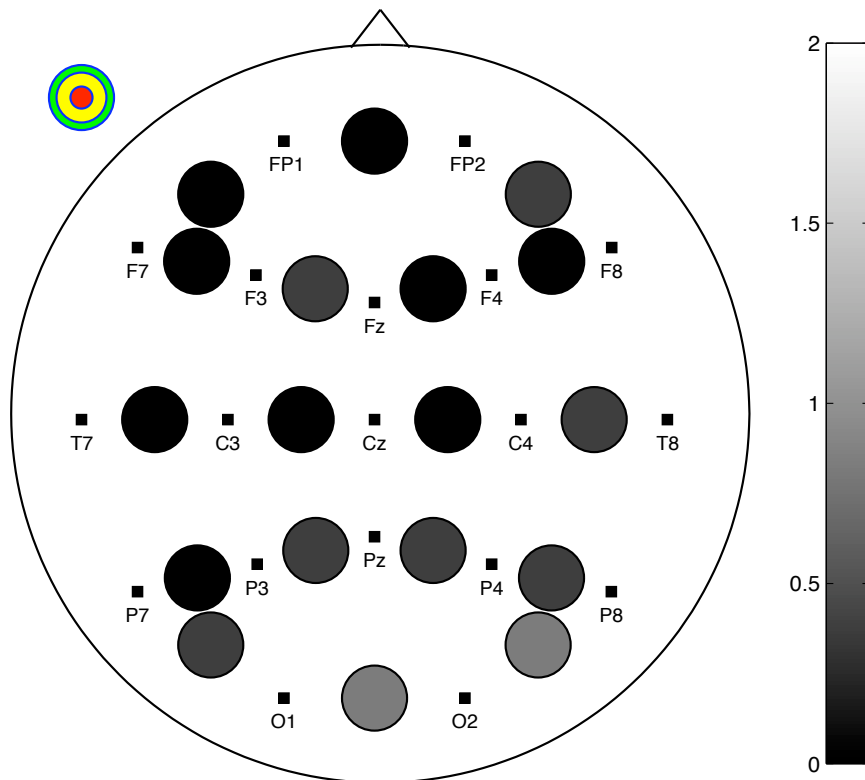


FIGURE A.12: Performance on patient n. 36

TABLE A.13: Performance of the seizure detection algorithm on patient n. 43.

Channel	n. Seizures			Overall Performance		SE _{L<10} (%)	SE _{L>10} (%)
	N _{TOT}	N _{L<10}	N _{L>10}	SE _{TOT} (%)	FPR(FP/h)		
F7-FP1	4	0	4	100.0	0.35	n.a.	100.0
FP1-FP2	4	0	4	100.0	0.71	n.a.	100.0
FP2-F8	4	0	4	100.0	0.71	n.a.	100.0
F7-F3	4	0	4	100.0	0.35	n.a.	100.0
F3-FZ	4	0	4	100.0	0.00	n.a.	100.0
FZ-F4	4	0	4	100.0	0.35	n.a.	100.0
F4-F8	4	0	4	100.0	0.35	n.a.	100.0
T7-C3	4	0	4	100.0	0.35	n.a.	100.0
C3-CZ	4	0	4	100.0	0.35	n.a.	100.0
CZ-C4	4	0	4	100.0	0.35	n.a.	100.0
C4-T8	4	0	4	100.0	0.35	n.a.	100.0
P7-P3	4	0	4	100.0	0.35	n.a.	100.0
P3-PZ	4	0	4	100.0	1.41	n.a.	100.0
PZ-P4	4	0	4	100.0	0.35	n.a.	100.0
P4-P8	4	0	4	100.0	0.35	n.a.	100.0
P7-O1	4	0	4	100.0	1.77	n.a.	100.0
O1-O2	4	0	4	25.0	2.47	n.a.	25.0
O2-P8	4	0	4	100.0	0.71	n.a.	100.0

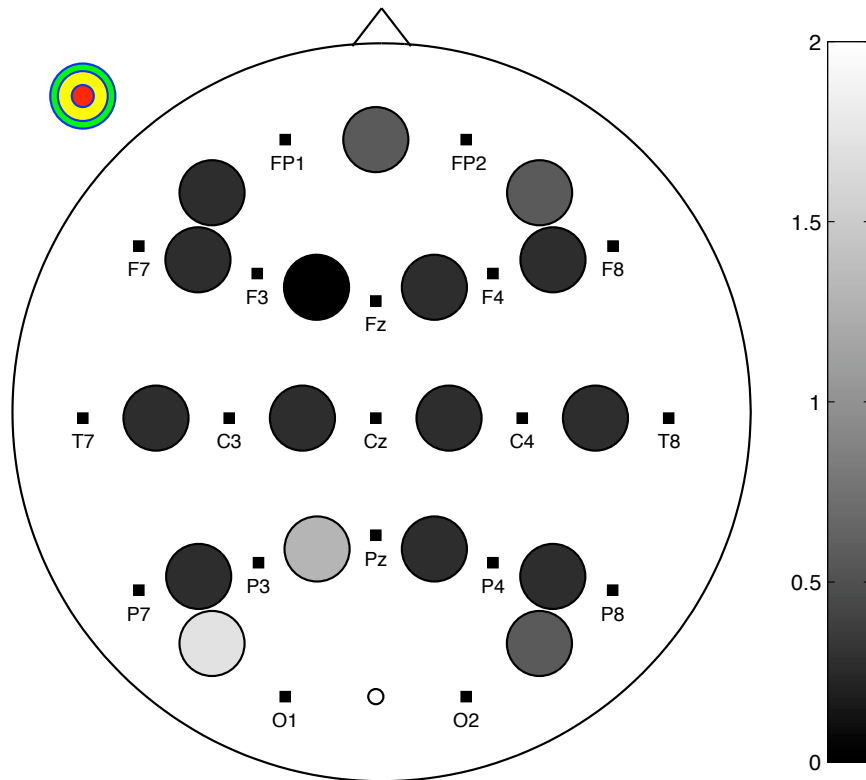


FIGURE A.13: Performance on patient n. 43

TABLE A.14: Performance of the seizure detection algorithm on patient n. 46.

Channel	n. Seizures			Overall Performance		$SE_{L<10}(\%)$	$SE_{L>10}(\%)$
	N_{TOT}	$N_{L<10}$	$N_{L>10}$	$SE_{TOT}(\%)$	FPR(FP/h)		
F7-FP1	6	0	6	100.0	0.48	n.a.	100.0
FP1-FP2	6	0	6	83.3	0.96	n.a.	83.3
FP2-F8	6	0	6	83.3	0.64	n.a.	83.3
F7-F3	6	0	6	100.0	0.00	n.a.	100.0
F3-FZ	6	0	6	100.0	0.16	n.a.	100.0
FZ-F4	6	0	6	66.6	1.12	n.a.	66.6
F4-F8	6	0	6	100.0	0.00	n.a.	100.0
T7-C3	6	0	6	83.3	0.00	n.a.	83.3
C3-CZ	6	0	6	0.0	3.53	n.a.	0.0
CZ-C4	6	0	6	33.3	3.05	n.a.	33.3
C4-T8	6	0	6	83.3	0.00	n.a.	83.3
P7-P3	6	0	6	100.0	0.48	n.a.	100.0
P3-PZ	6	0	6	66.6	3.53	n.a.	66.6
PZ-P4	6	0	6	16.6	3.37	n.a.	16.6
P4-P8	6	0	6	100.0	0.16	n.a.	100.0
P7-O1	6	0	6	100.0	0.48	n.a.	100.0
O1-O2	6	0	6	66.6	0.96	n.a.	66.6
O2-P8	6	0	6	83.3	1.44	n.a.	83.3

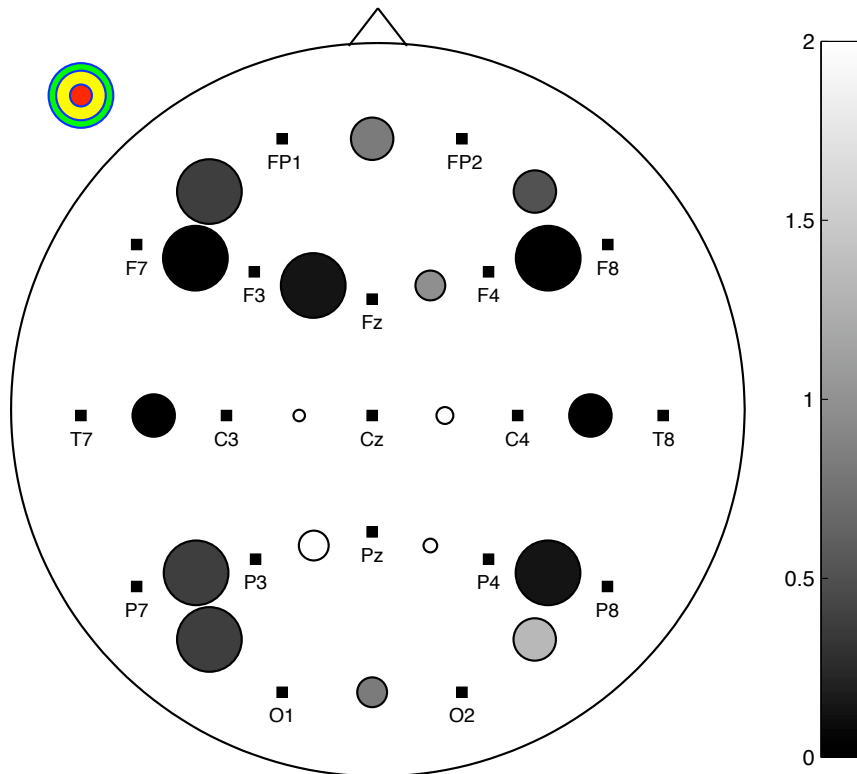


FIGURE A.14: Performance on patient n. 46

Patients with Symptomatic Epilepsy Presenting Absence Seizures

TABLE A.15: Performance of the seizure detection algorithm on patient n. 8.

Channel	n. Seizures			Overall Performance		SE _{L<10} (%)	SE _{L>10} (%)
	N _{TOT}	N _{L<10}	N _{L>10}	SE _{TOT} (%)	FPR(FP/h)		
F7-FP1	5	5	0	0.0	3.00	0.0	n.a.
FP1-FP2	5	5	0	80.0	1.31	80.0	n.a.
FP2-F8	5	5	0	0.0	2.81	0.0	n.a.
F7-F3	5	5	0	100.0	0.56	100.0	n.a.
F3-FZ	5	5	0	80.0	0.37	80.0	n.a.
FZ-F4	5	5	0	80.0	0.37	80.0	n.a.
F4-F8	5	5	0	40.0	0.75	40.0	n.a.
T7-C3	5	5	0	100.0	0.56	100.0	n.a.
C3-CZ	5	5	0	80.0	0.94	80.0	n.a.
CZ-C4	5	5	0	80.0	0.19	80.0	n.a.
C4-T8	5	5	0	60.0	0.94	60.0	n.a.
P7-P3	5	5	0	80.0	0.00	80.0	n.a.
P3-PZ	5	5	0	100.0	0.75	100.0	n.a.
PZ-P4	5	5	0	40.0	0.94	40.0	n.a.
P4-P8	5	5	0	80.0	0.00	80.0	n.a.
P7-O1	5	5	0	80.0	0.75	80.0	n.a.
O1-O2	5	5	0	40.0	0.75	40.0	n.a.
O2-P8	5	5	0	80.0	0.75	80.0	n.a.

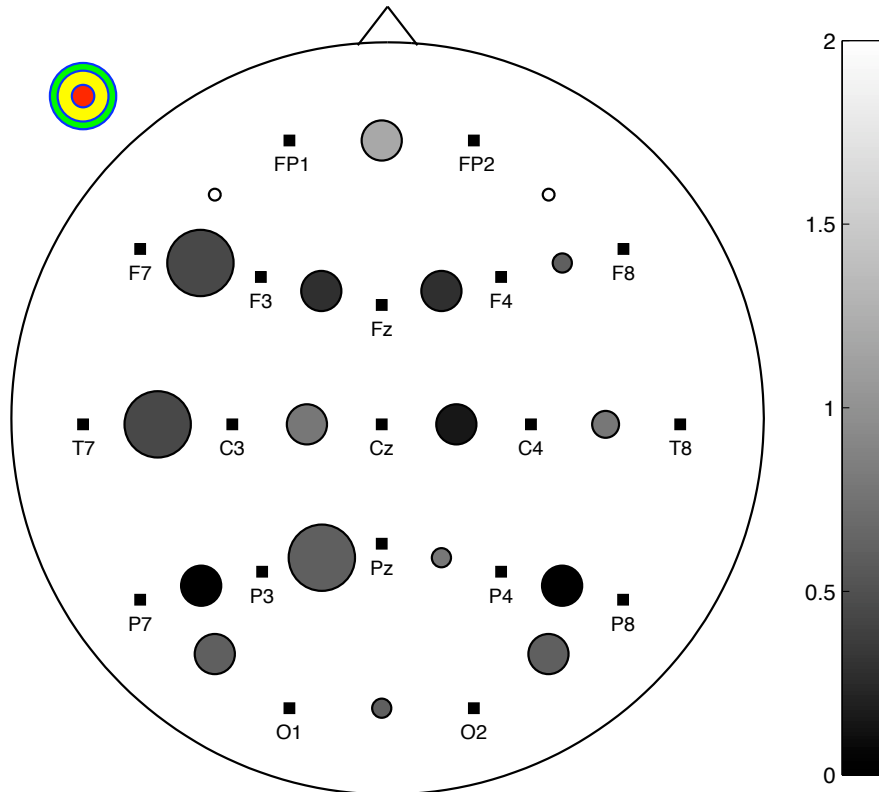


FIGURE A.15: Performance on patient n. 8

TABLE A.16: Performance of the seizure detection algorithm on patient n. 9.

Channel	n. Seizures			Overall Performance		$SE_{L<10}(\%)$	$SE_{L>10}(\%)$
	N_{TOT}	$N_{L<10}$	$N_{L>10}$	$SE_{TOT}(\%)$	FPR(FP/h)		
F7-FP1	6	0	6	80.0	3.00	n.a.	80.0
FP1-FP2	6	0	6	100.0	1.31	n.a.	100.0
FP2-F8	6	0	6	80.0	2.81	n.a.	80.0
F7-F3	6	0	6	80.0	0.56	n.a.	80.0
F3-FZ	6	0	6	100.0	0.37	n.a.	100.0
FZ-F4	6	0	6	80.0	0.37	n.a.	80.0
F4-F8	6	0	6	100.0	0.75	n.a.	100.0
T7-C3	6	0	6	80.0	0.56	n.a.	80.0
C3-CZ	6	0	6	100.0	0.94	n.a.	100.0
CZ-C4	6	0	6	100.0	0.19	n.a.	100.0
C4-T8	6	0	6	80.0	0.94	n.a.	80.0
P7-P3	6	0	6	80.0	0.00	n.a.	80.0
P3-PZ	6	0	6	100.0	0.75	n.a.	100.0
PZ-P4	6	0	6	100.0	0.94	n.a.	100.0
P4-P8	6	0	6	100.0	0.00	n.a.	100.0
P7-O1	6	0	6	0.0	0.75	n.a.	0.0
O1-O2	6	0	6	0.0	0.75	n.a.	0.0
O2-P8	6	0	6	0.0	0.75	n.a.	0.0

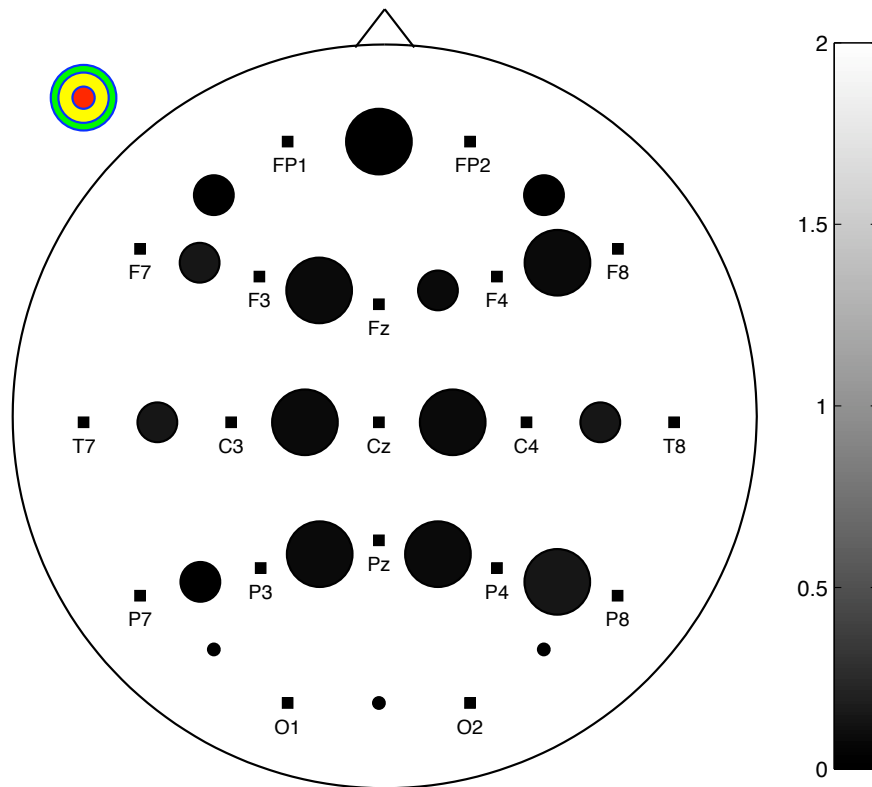


FIGURE A.16: Performance on patient n. 9

TABLE A.17: Performance of the seizure detection algorithm on patient n. 20.

Channel	n. Seizures			Overall Performance		$SE_{L<10}(\%)$	$SE_{L>10}(\%)$
	N_{TOT}	$N_{L<10}$	$N_{L>10}$	$SE_{TOT}(\%)$	FPR(FP/h)		
F7-FP1	6	0	6	100.0	0.67	100.0	n.a.
FP1-FP2	6	0	6	83.3	0.89	83.3	n.a.
FP2-F8	6	0	6	100.0	0.52	100.0	n.a.
F7-F3	6	0	6	83.3	0.37	83.3	n.a.
F3-FZ	6	0	6	83.3	0.45	83.3	n.a.
FZ-F4	6	0	6	100.0	0.22	100.0	n.a.
F4-F8	6	0	6	83.3	0.22	83.3	n.a.
T7-C3	6	0	6	83.3	0.3	83.3	n.a.
C3-CZ	6	0	6	83.3	0.22	83.3	n.a.
CZ-C4	6	0	6	100.0	0.37	100.0	n.a.
C4-T8	6	0	6	66.6	0.3	6.6	n.a.
P7-P3	6	0	6	83.3	0.22	83.3	n.a.
P3-PZ	6	0	6	100.0	0.3	100.0	n.a.
PZ-P4	6	0	6	83.3	0.3	83.3	n.a.
P4-P8	6	0	6	66.6	0.37	66.6	n.a.
P7-O1	6	0	6	100.0	0.45	100.0	n.a.
O1-O2	6	0	6	50.0	0.67	50.0	n.a.
O2-P8	6	0	6	83.3	0.6	83.3	n.a.

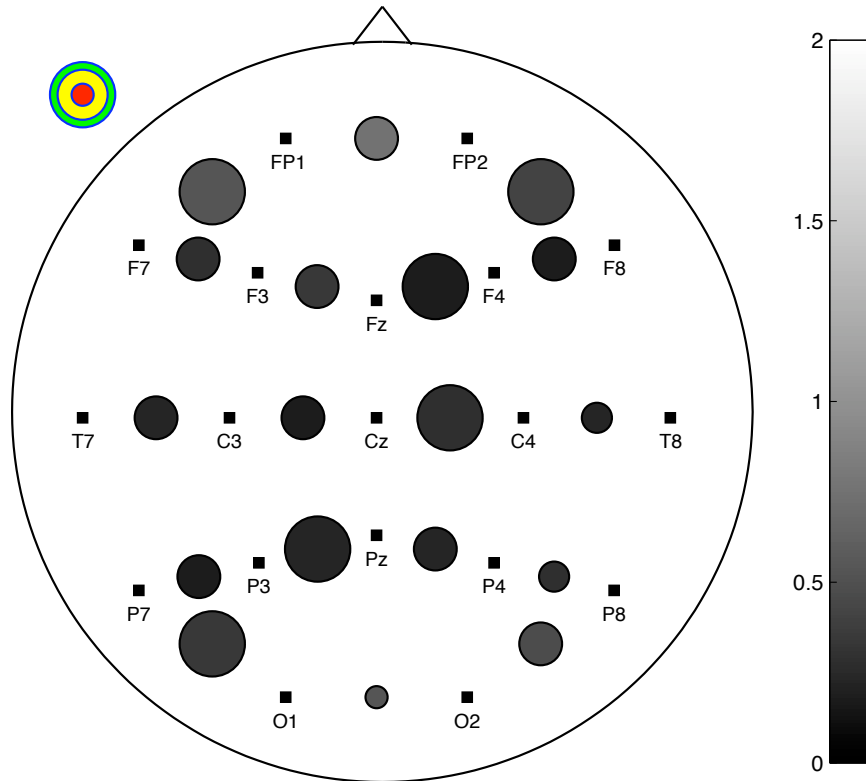


FIGURE A.17: Performance on patient n. 20

Appendix B

Matlab Code

This part of the appendix includes part of the MATLAB code written by this author. The full source code is included in the enclosed DVD

main.m

```
1 % MAIN tests the performance of the algorithm. The output
2 % is a struct containing performance measures (sensitivity, false positive
3 % rate) for each patient.
4 %
5 % Author: Andrea Mazzaretto, s081182, Technical University of Denmark
6 % Date/Version: August 2010
7
8
9 close all
10 clear all
11 clc;
12
13
14 % Sampling rate
15 Fs = 200;
16
17 % Load Seizure Boundaries
18 getboundaries()
19
20 % Selecting a patient
21 filename = 'pt25';
22 ptp = pt25;
23 ptpend = pt25end;
24
25 % Loading Data from the selected patient
26 EDF = sdfopen([filename '.rec'],'r');
27 [S,EDF] = sdfread(EDF, Inf);
28
29 % Number of EEG channels
30 NEEG = 18;
31
32 % Minimum Length of a seizure in seconds
33 MIN_LENGTH = 4;
34
35
36 % Window dimension
```

```

37 N = 400;
38
39 % Overlapping
40 overlap = floor(0.5*N);
41
42 % Temporal Constraint, minimum number of epochs with a seizure status in
43 % order to trigger a detection
44 Nwindow = 3;
45
46
47 %% Performing Seizure Detection
48 testresults = seizuredetection(S,NEEG,ptp,ptpend,N,overlap,Nwindow, 1,2,0.5);
49
50
51 %% Visualizing the results graphically
52 visualization(mtestresults);

```

calculateFD.m

```

1 function FD = calculateFD(waveform,method)
2 % Calculate the fractal dimension of the 1-D signal waveform, with the
3 % method specified in the method variable.
4 % Input:
5 %     waveform: input 1-D signal
6 %     method: method to apply to calculate the fractal dimension.
7 %     Choose between 'Katz', 'KNN' or 'Higuchi'
8 % Output:
9 %     FD: estimated fractal dimension of waveform
10 % Author: Andrea Mazzaretto, s081182, Technical University of Denmark
11 % Date/Version: August 2010
12
13
14 x = waveform(1,:);
15 y = waveform(2,:);
16 N = length(x);
17
18 if strcmp(method,'Katz') == 1
19     %% Katz's estimate
20     n = N - 1;
21
22     % Calculating the length L of the waveform
23     L = 0;
24     for i = 1:N-1
25         distance = sqrt( (x(i+1)-x(i))^2 + (y(i+1)-y(i))^2 );
26         L = L + distance;
27     end
28
29     % Calculating the diameter d of the waveform
30     d = 0;
31     for j = 2:N
32         diameter = sqrt( (x(j)-x(1))^2 + (y(j)-y(1))^2 );
33         if diameter > d
34             d = diameter;
35         end
36     end
37
38     D = log10(n)/(log10(n) + log10(d/L));
39
40 elseif strcmp(method,'KNN') == 1
41     %% K-th nearest neighbour estimation
42     kmin = 2;

```

```

43     kmax = 130;
44     % kmax should be at most N-1
45     if N < kmax
46         kmax = N-1;
47     end
48     gamma = 1.5;
49     threshold = 10e-5;
50     maxiterations = 4;
51
52     K = kmin:kmax;
53
54     % Calculating the Euclidean distance from each point to all the others
55     r = zeros(N,N);
56     for i = 1:N
57         for j = 1:N
58             r(i,j) = sqrt( (x(j)-x(i))^2 + (y(j)-y(i))^2 );
59         end
60     end
61
62     % Estimating fractal dimension in at most maxiterations
63     rk = sort(r,2);
64     rk = rk(:,2:N);
65     xpoints(1:(kmax-kmin+1)) = log(K/N);
66     iterations = 0;
67     quantity = threshold + 1;
68     while (iterations < maxiterations) && (quantity > threshold)
69         ypoints = zeros(1,length(xpoints));
70         iterations = iterations + 1;
71         for k = K
72             rki = mean(rk(:,k),2);
73             avgrk = mean(rki.^gamma);
74             ypoints(k-kmin+1) = log(avgrk);
75         end
76         s = polyfit(xpoints,ypoints,1);
77         prevgamma = gamma;
78         gamma = prevgamma/s(1);
79         quantity = abs((gamma-prevgamma)/(0.5*(gamma-prevgamma)));
80     end
81
82     D = gamma;
83
84 elseif strcmp(method,'Higuchi') == 1
85     %% Higuchi estimation
86     % Set the maximum value of the interval time k
87     Nk = 20;
88
89     % Creating the vector interval time vector
90     K = zeros(1,Nk);
91     K(1:4) = 1:4;
92     for j = 11:Nk+11-5
93         K(j-6) = floor(2^((j-1)/4));
94     end
95
96     % Calculating the average length L(k)
97     xpoints(K) = log(1./K);
98     for k = K
99         ypoints = zeros(1,k);
100        L = 0;
101        for m = 1:k
102            M = floor((N-m)/k);
103            distance = 0;
104            for i = 2:M
105                distance = distance + abs(y(m+i*k)-y(m+(i-1)*k));
106            end
107            Lm = 1/k * ((N-1)/M*k * distance);

```

```

108         L = L + Lm;
109     end
110     ypoints(k) = log(L);
111 end
112
113     % Estimating the fractal dimension D of the waveform
114     s = polyfit(xpoints, ypoints, 1);
115     D = -s(1);
116
117 else
118     error(strcat('Undefined method ', method, '. Choose between ' + ...
119         'Katz', 'KNN' or 'Higuchi'))
120 end
121 FD = D;
122
123 end

```

seizuredetection.m

```

1 function mttestresults = seizuredetection(S, NEEG, ptp, ptpend, N, ...
2 overlap, Nwindow, c1, c2, c3)
3 % Perform seizure detection thorough FD estimation. For each EEG channel an
4 % output SE and FPR is given
5 %
6 % Input
7 %     S: EEG signal to analyze
8 %     NEEG: Number of EEG channels
9 %     ptp, ptpend: Seizure Boundaries in S
10 %     N: Size of window used for FD estimation
11 %     overlap: percentage of overlapping of FD estimation window
12 %     Nwindow: Temporal Constraint, number of EEG epochs with seizure
13 %               status necessary to trigger a detection
14 %     c1, c2, c3: Coefficient of the objective function
15 % Output
16 %     mttestresults
17 %
18 % Author: Andrea Mazzaretto, s081182, Technical University of Denmark
19 % Date/Version: August 2010
20
21
22
23 % Remove from the Seizure Boundaries Seizures shorter than 4 seconds
24 pt = [];
25 ptpend = [];
26 lseizures = [];
27 for i = 1 : length(ptp)
28     if ((ptpend(i) - ptp(i))/Fs >= MINLENGTH && ptpend(i) <= length(S))
29         pt = [pt ptp(i)];
30         ptpend = [ptpend ptpend(i)];
31         lseizures = [lseizures (ptpend(i) - ptp(i))/Fs];
32     end
33 end;
34
35
36
37 cost = [];
38 % Weighting each seizure
39 for i = 1 : length(lseizures)
40     if lseizures < 10
41         cost(i) = c1;
42     else

```

```

43         cost(i) = c2;
44     end
45 end
46
47 mtestresults = [];
48 for n = 1:NEEG
49
50     trainresults = [];
51     testresults = [];
52
53     % Selecting EEG signal for the analysis
54     signal = S(:,n)';
55
56     % Notch Filtering of the EEG channel
57     load NotchFilter.mat;
58     order = 999;
59     delay = floor(order/2);
60     signal = filter(Num,1,[signal signal(end-delay+1:end)]);
61     signal = signal(delay + 1:end);
62     L = length(signal);
63
64
65     % Estimating FD for each epoch
66     FD = zeros(1,1);
67     i = 0;
68     j = 0;
69     while i+N < L
70         j = j + 1;
71         FD(j) = calculateFD([i:1/Fs:(i+N/Fs-1/Fs); ...
72             signal(i+1:i+N)/var(signal(i+1:i+N)) ], 'Higuchi ');
73         i = i + N - overlap;
74     end
75
76
77
78     % Storing in sstartv and sendv the epoch where each seizure starts and
79     % end respectively
80     index = 1:N-overlap:(j)*(N-overlap);
81     sstartv = [];
82     ssendv = [];
83     seizure = zeros(length(FD),1);
84     for i = 1:length(pt)
85         sstart = find(pt(i) >= index, 1, 'last')-1;
86         send = find(ptend(i) >= index, 1, 'last')+1;
87         if i == 1 || sstart ~= ssendv(end)
88             sstartv = [sstartv sstart ];
89             ssendv = [ssendv send];
90         else
91             ssendv(end) = send;
92         end
93         if send < length(FD)
94             seizure(sstart:send) = 1;
95         else
96             seizure(sstart:end) = 1;
97         end
98     end
99
100
101
102
103     %% Leave One Out Cross Validation
104
105     % Splitting EEG signal in as many segments as the number of seizures.
106     % The splitting point is the middle point between two seizures.
107     Nsplits = length(pt);

```

```

108
109 % Keeping track of the total and detected seizures depending on their
110 % length
111 nts410 = 0;
112 nts1020 = 0;
113 nds410 = 0;
114 nds1020 = 0;
115
116 % Training and Testing the algorithm for each split
117 for loo = 1:Nsplits
118
119     % Defining indexes of the training and test set
120     if loo == 1
121         testset = 1:round((ssendv(loo) + sstartv(loo+1))/2);
122         trainingset = (round((ssendv(loo) + ...
123             sstartv(loo+1))/2)+1):length(FD);
124         costindex = 2:length(pt);
125
126     elseif loo == Nsplits
127         testset = round((ssendv(loo-1) + sstartv(loo))/2):length(FD);
128         trainingset = 1:round((ssendv(loo-1) + sstartv(loo))/2)-1;
129         costindex = 1:length(pt)-1;
130     else
131         testset = round((ssendv(loo-1) + ...
132             sstartv(loo))/2):round((ssendv(loo) + sstartv(loo+1))/2);
133         trainingset = [1:round((ssendv(loo-1) + sstartv(loo))/2)-1 ...
134             (round((ssendv(loo) + sstartv(loo+1))/2)+1):length(FD)];
135         costindex = [1:loo-1 loo+1:length(pt)];
136
137     end
138
139     % Selecting the best threshold by evaluating the objective function
140     % on the training set
141
142     bthreshold = 0;
143     bperf = -100000;
144     indext = linspace( min(FD(trainingset)), mean(FD(trainingset)) ...
145         - 0.8 * std(FD(trainingset)), 50);
146     bndst = 0;
147     bnfpt = 0;
148     bnmst = 0;
149     for threshold = indext
150         seizureretrainclassified = zeros(length(FD(trainingset)),1);
151         seizureretrainclassified(FD(trainingset) < threshold) = 1;
152         seizureretrain = seizure(trainingset);
153         dvect = [];
154         cvect = [];
155         ndst = 0;
156         nfpt = 0;
157         nmst = 0;
158         ntst = 0;
159         i = 1;
160         while i < length(FD(trainingset))
161             if seizureretrain(i) == 1
162                 endseizure = false;
163
164                 maxa = 0;
165                 a = 0;
166                 while (seizureretrainclassified(i) == 1 || ...
167                     seizureretrain(i) == 1) &&...
168                     (i < length(FD(trainingset)))
169                     if seizureretrain(i) == 0
170                         endseizure = true;
171                     end
172

```

```

173
174         if ( (seizuretrain(i) == 1) && (endseizure == true))
175             break;
176         end
177
178         if ((seizuretrainclassified(i) == 1))
179             a = a + 1;
180         else
181             if a > maxa
182                 maxa = a;
183             end
184             a = 0;
185         end
186
187
188         i = i + 1;
189
190     end
191     if a > maxa
192         maxa = a;
193     end
194     ntst = ntst + 1;
195     dvect(ntst) = 0;
196     cvect(ntst) = i;
197     if maxa >= Nwindow
198         ndst = ndst + 1;
199         dvect(ntst) = 1;
200         i = i+3;
201     else
202         nmst = nmst + 1;
203         i = i + 1;
204     end
205     elseif (seizuretrainclassified(i) == 1 ...
206             && seizuretrain(i) == 0)
207         f = 0;
208         while (seizuretrainclassified(i) == 1 && ...
209               seizuretrain(i) == 0) && ...
210               (i < length(FD(trainingset)))
211             i = i + 1;
212             f = f + 1;
213         end
214         if f >= Nwindow
215             nfpt = nfpt + 1;
216         end
217     else
218         i = i + 1;
219     end
220 end
221
222
223     perf = cost(costindex) * dvect' - nfpt * c3;
224     if perf >= bperf
225         bthreshold = threshold;
226         bndst = ndst;
227         bnfpt = nfpt;
228         bnmst = nmst;
229         bperf = perf;
230     end
231
232
233
234 end;
235
236 % Using the best threshold calculated in the training phase to
237 % evaluate the test set

```

```

238     threshold = bthreshold;
239     seizuretestclassified = zeros(length(FD(testset)),1);
240     seizuretestclassified(FD(testset) < threshold) = 1;
241     seizuretest = seizure(testset);
242     dvec= [];
243     nds = 0;
244     nfp = 0;
245     nms = 0;
246     nts = 0;
247     i = 1;
248     while i < length(FD(testset))
249         if seizuretest(i) == 1
250             maxa = 0;
251             a = 0;
252             while (seizuretestclassified(i) == 1 || ...
253                 seizuretest(i) == 1) && (i < length(FD(testset)))
254                 if seizuretestclassified(i) == 1
255                     a = a + 1;
256                 else
257                     if a > maxa
258                         maxa = a;
259                     end
260                     a = 0;
261                 end
262                 i = i + 1;
263             end
264             if a > maxa
265                 maxa = a;
266             end
267             nts = nts + 1;
268             dvec(nts) = 0;
269             if maxa >= Nwindow
270                 nds = nds + 1;
271                 dvec(nts) = 1;
272                 i = i+3;
273             else
274                 nms = nms + 1;
275                 i = i + 1;
276             end
277             elseif (seizuretestclassified(i) == 1 && seizuretest(i) == 0)
278                 f = 0;
279                 while (seizuretestclassified(i) == 1 && ...
280                     seizuretest(i) == 0) && (i < length(FD(testset)))
281                     i = i + 1;
282                     f = f+1;
283                 end
284                 if f >= Nwindow
285                     nfp = nfp + 1;
286                 end
287             else
288                 i = i + 1;
289             end
290     end
291
292     if cost(loo) == c1
293         nts410 = nts410 + 1;
294         nds410 = nds410 + nds;
295     elseif cost(loo) == c2
296         nts1020 = nts1020 + 1;
297         nds1020 = nds1020 + nds;
298     end
299
300     LengthRec = length(signal)/(Fs*3600);
301
302     trainresults = [trainresults; ntst bndst bnfpt];

```

```

303     testresults = [testresults; nds nfp/LengthRec ];
304     end
305     % End Leave one out cross validation
306
307
308     mtest = mean(testresults);
309     mtestresults =[mtestresults2; [mtest nds410/nts410 nds1020/nts1020 ]];
310
311 end
312
313 end

```

visualization.m

```

1  function visualization(mtestresults)
2  % This function visualize graphically the results contained in the matrix
3  % mtestresults, which contains SE and FPR for all the EEG channel of a
4  % transversal montage
5  % Input
6  %     mtestresults: matrix containing SE and FPR for all the EEG channel
7  %     of a transversal montage
8  % Output
9  %     Visualization of the results through a "head" plot.
10 %
11 % Author: Andrea Mazzaretto, s081182, Technical University of Denmark
12 % Date/Version: August 2010
13
14 % Size in points of the biggest circle in the visualization
15 MAXsize = 30;
16
17 % Label of the electrodes
18 label = [
19     ' FP1 ';
20     ' FP2 ';
21     ' F7  ';
22     ' F3  ';
23     ' Fz  ';
24     ' F4  ';
25     ' F8  ';
26     ' T7  ';
27     ' C3  ';
28     ' Cz  ';
29     ' C4  ';
30     ' T8  ';
31     ' P7  ';
32     ' P3  ';
33     ' Pz  ';
34     ' P4  ';
35     ' P8  ';
36     ' O1  ';
37     ' O2  ';
38     ];
39
40 % X coordinates of the electrodes
41 x = [
42     -0.3090;
43     0.3090;
44     -0.8090;
45     -0.4045
46     0.0000;
47     0.4;

```

```
48     0.81;
49     -1.0000;
50     -0.5000;
51     0.0000;
52     0.5;
53     1.0000;
54     -0.8090;
55     -0.4;
56     0.0000;
57     0.4;
58     0.8090;
59     -0.3090;
60     0.3090;
61     ];
62
63 % Y coordinates of the electrodes
64 y = [
65     0.9511;
66     0.9511;
67     0.5878;
68     0.4939;
69     0.4;
70     0.4939;
71     0.5878;
72     0.0000;
73     0.0000;
74     0.0000;
75     0.0000;
76     0.0000;
77     -0.5878;
78     -0.4939;
79     -0.4;
80     -0.4939;
81     -0.5878;
82     -0.9511;
83     -0.9511;
84     ];
85
86 % Pair of electrodes constituting Transversal montage (number refers to
87 % the label previously defined)
88 Transversal = [
89     3     1;
90     1     2;
91     2     7;
92     3     4;
93     4     5;
94     5     6;
95     6     7;
96     8     9;
97     9    10;
98    10    11;
99    11    12;
100    13    14;
101    14    15;
102    15    16;
103    16    17;
104    13    18;
105    18    19;
106    19    17;
107     ];
108
109 %% Drawing the head
110 scrsz = get(0, 'ScreenSize');
111 x = x/2 + 0.5;
112 y = y/2 + 0.5;
```

```

113 h = figure('Position',[1 scrsz(4), scrsz(3)/1.65 scrsz(4)]);
114 axis off;
115 co = gray(200);
116 colormap gray(200)
117 colorbar('Location','East','YTickLabel',...
118         {'0','0.5','1','1.5','2'},'Ytick', 1:50:201');
119 nElec = length(x);
120 nTran = length(Transversal);
121 set(gcf,'Name',sprintf('Absences longer than 4 seconds'),...
122      'NumberTitle','off')
123 m = 100;
124 t = 0:pi/100:2*pi;
125 r = 1.25*m/2 + 0.5;
126 nosel = [sin(pi/2-pi/32)*r + m/2+1; cos(pi/2-pi/32)*r + m/2+1]' - m/2;
127 noser = [sin(pi/2-pi/32)*r + m/2+1; cos(pi/2-pi/32)*r + m/2+1]' - m/2;
128 nosec = [sin(pi/2)*r + m/2+1; cos(pi/2-pi/32)*r + m/2+1+0.1*r]' - m/2;
129 head = [sin(t)*r + m/2+1; cos(t)*r + m/2+1]' - m/2;
130 scrsz = get(0,'ScreenSize');
131 d = min(scrsz(3:4)) / 2;
132 whitebg('w');
133 axes('position',[0 0 1 1]);
134 set(gca,'Visible','off');
135 axis square
136 line(head(:,1),head(:,2),'Color','k','LineWidth',1);
137
138 mark = '.sk';
139 hold on;
140 for e = 1:nElec
141     plot(x(e)*m - m/2,y(e)*m - m/2,'-sk','MarkerSize',6,...
142         'MarkerEdgeColor','k','MarkerFaceColor','k');
143     text(x(e)*m - m/2, ...
144         y(e)*m - m/2 - 4*m/100, ...
145         label(e,:), ...
146         'FontSize',9, ...
147         'VerticalAlignment','middle', ...
148         'HorizontalAlignment','center');
149 end
150
151
152 %% Drawing the electrodes and the circles
153 for e = 1:nTran
154     if mtestresults(e,3) >= 2
155         color = co(200,:);
156     else
157         color = co(ceil((mtestresults(e,2) + 0.0000001)*100),:);
158     end
159
160     if nts1020 ~= 0 && nts410 ~= 0
161         size420 = 1/exp(exp((1))) * (exp(exp(mtestresults(e,1))))*MAXsize;
162     elseif nts1020 == 0 && nts410 == 0
163         size420 = MAXsize;
164     elseif nts410 == 0
165         size420 = 1/exp(exp((1))) * (exp(exp(mtestresults(e,4))))*MAXsize;
166     elseif nts1020 == 0
167         size420 = MAXsize /exp(exp((1))) * (exp(exp(mtestresults(e,3))));
168     end
169
170     plot((x(Transversal(e,1)) + x(Transversal(e,2)))/2*m - m/2,...
171         (y(Transversal(e,1)) + y(Transversal(e,2)))/2*m - m/2, 'o', ...
172         'LineWidth', 1, 'MarkerSize',size420, 'MarkerEdgeColor','k', ...
173         'MarkerFaceColor',color);
174 end
175
176 %% Plotting reference circle
177 plot(0/2*m - m/2,2.1/2*m - m/2, '—o','LineWidth', 1, 'MarkerSize', ...

```

```

178     MAXsize /exp(exp((1))) * exp(exp(1)), 'MarkerEdgeColor', 'b', ...
179     'MarkerFaceColor', 'g' );
180 plot(0/2*m - m/2, 2.1/2*m - m/2, '—o', 'LineWidth', 1, 'MarkerSize', ...
181     MAXsize /exp(exp((1))) * exp(exp(0.9)), 'MarkerEdgeColor', ...
182     'b', 'MarkerFaceColor', 'y' );
183 plot(0/2*m - m/2, 2.1/2*m - m/2, '—o', 'LineWidth', 1, 'MarkerSize', ...
184     MAXsize /exp(exp((1))) * exp(exp(0.5)), 'MarkerEdgeColor', ...
185     'b', 'MarkerFaceColor', 'r' );
186
187
188 plot([-4 1],[63.5 70], '-k', 'LineWidth', 1);
189 plot([6 1],[63.5 70], '-k', 'LineWidth', 1);
190 axis off;
191
192 % Saving the visualization in a pdf file
193 saveas(h,[filename 'Absences.pdf'])
194
195 end

```

getboundaries.m

```

1 function getboundaries()
2 % Loads into the workspace the seizure boundaries
3 % Author: Andrea Mazzaretto, s081182, Technical University of Denmark
4 % Date/Version: August 2010
5
6
7 pt08 = [ 1200      8100      33240      76400      85940      88080      93960      98420 ...
8         115660     131280     133720     142280     147320     149640     157680     161780 ...
9         164900     167120     170700];
10 pt08end = [ 1800      8500      33900      77100      86480      88520      95300 ...
11            99420     116720     131760     134200     143320     148000     150000     158200 ...
12            162680     165360     167480     170800];
13
14 pt09 = [10000     25700     27200     104740    114440    117800    143600    150320 ...
15         190760     212280     218620     219300     230400     256380     275200     309800 ...
16         311020     328200     328980     330640     339140     339620     349340     385860 ...
17         403500     404880     414420     420480     421160     439520     440260     454160 ...
18         461560     466220     472720     474360     500920     506640     540120     569740 ...
19         570800     571640     577560     659800     662080     664240];
20 pt09end = [10520     26420     27440     105080    114560    117920    143700 ...
21            150660     191080     212400     219080     219680     230680     257560     275380 ...
22            310000     311280     328540     329180     330860     339280     339840     351280 ...
23            387880     403640     405020     414540     420760     422680     439860     440480 ...
24            454480     462000     466880     472860     474500     501140     507000     540360 ...
25            582200     570960     571800     577840     660240     662600     664600];
26
27 pt11 = [82780     145820     286400     296400     302980     312400];
28 pt11end = [84680      149680     288840     297680     304920     314440];
29
30 pt13 = [36900     58040     87120     105540    115860    117700    133400    145160 ...
31         274480     306660     315200];
32 pt13end = [37080     59400     87320     106720    116240    118560    134360 ...
33         146320     275880     307620     315440];
34
35 pt16 = [14280     16300     39640     65720     71280     129480    147120    229740 ...
36         232560     254020];
37 pt16end = [15260     17600     41220     66560     72240     130060    148060 ...
38         230640     233300     254740];
39
40 pt17 = [83120     108340    131180    151060    171060    193780    196000    198760 ...

```

```

41     229620     231520  239220  308720];
42 pt17end = [88600     111020  136120  153600  174800  193920  196180 ...
43     198940     229800  233560  239340  311500];
44
45 pt18 = [800     24000  33000  61300  89880  93980  128420  178220];
46 pt18end = [5080  24400  40960  66400  90180  99260  131740  182640];
47
48 pt19 = [154660  211340  257740  352080  365940];
49 pt19end = [156320     213060  259200  353600  366780];
50
51 pt20 = [1920     5160  7620  12960  14760  17240  17960  18940 ...
52     22240     24940  29880  35880  38560  41720  45760  48400 ...
53     52020     54100  55580  59580  66620  69140  75460  77000 ...
54     83600     87180  90420  98480  100340  105100  110480  112180 ...
55     113500     117820  124740  127680  131040  133840  141500  148160 ...
56     155380     165400  168400  176280  179080  183100  187520  201080 ...
57     208300     211380  215360  222760  223560  225440  229640  244100 ...
58     253000     256660  262140  268860  279120  290480  314120  327380 ...
59     344060     347020];
60 pt20end = [2680     5340  8000  12920  15160  17280  18080  19720 ...
61     22620     25420  30160  36220  39060  42320  46040  48860 ...
62     52240     54240  55960  59980  67140  71280  75660  77800 ...
63     85600     87380  91600  98740  100700  105700  110920  112800 ...
64     113660     118180  125340  128560  131680  134080  142000  149000 ...
65     155920     166120  168600  176400  179320  183720  187760  201280 ...
66     208580     211560  215520  222960  224020  225860  229800  244280 ...
67     253100     256800  262440  269020  279300  290680  314400  316120 ...
68     344240     347580];
69
70 pt23 = [73160  84200  91260  118940  213900  373420];
71 pt23end = [74520     85640  92520  120360  215220  374800];
72
73 pt25 = [68640  413720  673800  767860  943080  1235720  1288140  1364480];
74 pt25end = [70440  415160  675760  769180  944400  1237260  1289760  1365480];
75
76 pt36 = [21460  35320  50220  74800  91660  100740  126620 ...
77     162140     214640];
78 pt36end = [22840     36600  50940  75560  92400  101240  127680 ...
79     162940     215380];
80
81 pt42 = [19960  31580  41420  49520  59820  88500  92500 ...
82     100880  109440  112880  148220  193820  194340  215240  227500 ...
83     237200  256020  274360  275160  292460  301480  292440  301480 ...
84     374600];
85 pt42end = [22800     34320  41580  52080  62240  88720  92720 ...
86     101080  109640  113040  149160  193940  195400  216260  227760 ...
87     238280  258080  274440  275920  292760  301480  292720  303080 ...
88     378400];
89
90 pt43 = [48760  96080  127920  189100  181740  253840  271960 ];
91 pt43end = [49960     96540  141400  190340  182100  254460 ...
92     273260     318840];
93
94 pt51 = [108180  156860  961340  1043320  1946780  1972460  2512720];
95 pt51end = [109160     156980  962080  1044300  1947800  1974860  2514000];
96
97
98 end

```